dc_1896_21

Characteristics of the T cell response in the neonate

Thesis

Doctorate of the Hungarian Academy of Sciences

Gergely Toldi

Budapest

2023

TABLE OF CONTENTS

ABBREVIATIONS

aEEG	amplitude-integrated electroencephalography
APB	adult peripheral blood
APC	antigen presenting cell
AR	adenosine receptor
AUC	area under the curve
BBB	blood brain barrier
BFA	brefeldin A
cAMP	cyclic adenosine monophosphate
CBMC	cord blood mononuclear cell
CNS	central nervous system
CSF	cerebrospinal fluid
CTLA-4	cytotoxic T lymphocyte antigen 4
DC	dendritic cell
DHE	dihidroethidium
DMSO	dimethyl sulfoxide
ER	endoplasmic reticulum
FBS	fetal bovine serum
G-CSF	granulocyte colony stimulating factor
GM-CSF	granulocyte-macrophage colony-stimulating factor
HIE	hypoxic ischaemic encephalopathy
HP	healthy pregnancy
HPLC	high-performance liquid chromatography
ICOS	inducible costimulator of T cells

IDO	indoleamine 2,3-dioxygenase
IFN-γ	interferon gamma
IL	interleukin
IP3	inositol trisphosphate
KYN	kynurenine
KYNA	kynurenic acid
LDA	linear discriminant analysis
LPS	lipopolysaccharide
mAb	monoclonal antibody
MCA	middle cerebral artery
MCP-1	monocyte chemoattractant protein 1
MFI	mean fluorescence intensity
MIP-1b	macrophage inflammatory protein 1b
MLR	mixed lymphocyte reaction
NAIS	neonatal arterial ischemic stroke
NFAT	nuclear factor of activated T cells
NIMA	non-inherited maternal antigen
NK	natural killer
NMDA	N-methyl-D-aspartate
NP	non-pregnant
OOB	out of bag
OTU	operational taxonomic unit
PBMC	peripheral blood mononuclear cell
PBS	phosphate buffered saline
PCA	principal component analysis

PD-1	programmed death 1 receptor
PDE	phosphodiesterase
PE	preeclampsia
PHA	phytohemagglutinin
PMA	phorbol 12-myristate 13-acetate
RF	random forest
ROC	receiver operating characteristic
ROS	reactive oxygen species
RyR	ryanodine receptor
SCFA	short chain fatty acid
SOCE	store-operated calcium entry
TCR	T cell receptor
TGF-β	transforming growth factor beta
TNF-α	tumor necrosis factor alpha
Treg	regulatory T cell
TRP	tryptophan
UCB	umbilical cord blood
VCAM-1	vascular cell adhesion molecule 1
VLA-4	very late antigen 4

1. INTRODUCTION

The neonatal immune system was regarded immature compared to its adult counterpart over decades. Indeed, neonates are the most susceptible age group to infection, and infection and sepsis are significant contributors to neonatal morbidity and mortality worldwide [1-3]. As a clinician, I experience the devastating effects of neonatal infections on a daily basis, making me aware that it is one of the greatest healthcare burdens in the field of neonatology. There is a clearly unmet medical need to better understand the development and the function of the neonatal immune system in order to improve clinical outcomes of infection and other immune-mediated complications in preterm and term neonates. These include some of the most common diseases of prematurity, such as necrotizing enterocolitis or bronchopulmonary dysplasia, as well as perinatal asphyxia, which more often affects term or post-term neonates. These pathologies are all driven by inflammatory reactions and can severely reduce quality of life or, in the worst case, can even be life limiting conditions.

Due to the restricted availability and quantity of human samples, most of our knowledge on the early development and function of the immune system arise from animal studies. However, these studies have several limitations in their direct applicability in human immunology.

Thanks to research efforts in the field over the recent years, the long held view of the neonatal immune system being immature has finally started to change. Studies in humans demonstrated that neonatal immune cells can function at levels seen in adults under in vitro conditions, and therefore, the neonatal immune system should be considered as differently regulated rather than immature [4-6]. This is in line with the recognition that the neonatal immune response developmentally needs to meet different requirements compared to its adult counterpart. However, details of this different regulation and how it increases susceptibility to infection are yet to be described.

Following my PhD studies in the field of immunology, mostly investigating adult autoimmune diseases, I started my clinical training as a paediatrician and neonatologist. In my simultaneous postdoctoral research, I decided to combine my clinical interest with my research interest in immunology, and contribute to the efforts of better understanding the architecture and function of the neonatal immune system, as well as the maternal immune regulation during healthy pregnancy and preeclampsia. For this, I collected human samples and employed my expertise in flow cytometry, often creating new methodological protocols, in order to extract as much information as possible from small amounts of blood.

In this thesis, I would like to highlight key aspects of my research activity after the completion of my PhD studies, related to the neonatal immune system and immune regulation during pregnancy. First, I describe how physiological costimulatory function during antigen presentation, an important regulatory mechanism in T cell activation, differs in healthy term neonates compared to adults, as well as in healthy pregnancy versus preeclampsia. Second, I provide an overview of the differences in regulatory T cell subsets between healthy pregnancy and preeclampsia. Third, I discuss how nutrition in the neonatal period, in particular breastfeeding, contributes to the development of immunity, with a specific focus on the regulatory T cell compartment. These findings received broad international media attention and were discussed as news items in several countries. In the fourth part, I present how commonly used medications in neonatology with well-known immunological effects (caffeine, milrinone and sildenafil) influence the neonatal immune function in healthy neonates. Finally, I describe how the inflammatory immune response contributes to disease progression in two pathologies mostly affecting term neonates, perinatal asphyxia and neonatal arterial ischaemic stroke.

2. BACKGROUND

2.1. The neonatal immune response

Exposure and adaptation to extra-uterine life represents a substantial homeostatic challenge for the cardiovascular and respiratory as well as the immune systems of neonates. Paramount amongst these are modifications within immune function which must facilitate acquisition of a symbiotic microbiome whilst protecting against pathogen challenge. Our current understanding of the functional capacity of the neonatal immune system in the first few weeks of life remains limited. Substantial differences are observed between neonatal and adult immune function [4,5]. For example, Interleukin-8 (IL-8) is the major effector chemokine of neonatal T cells whilst production of interferon gamma (IFN-γ) is markedly suppressed and a reduction in natural killer (NK) cell numbers is observed [4,6].

Elegant multi-dimensional analyses have recently revealed a significant increase or decrease in various immune cell subsets as well as plasma protein levels within the first week of life, initiating a stereotypic immune differentiation pathway. This profile is seen in both preterm and term infants and as such appears to represent a response to multiple environmental cues, predominantly microbial, that are received after birth [7]. Dynamic alterations in the interferon and complement pathways, as well as neutrophil-associated signalling, are also particularly prominent [8].

2.2. B7 costimulatory molecules

Antigen presentation and costimulation are the initial steps in adequate T cell function and play an important role in the coordination of downstream events of the immune response. Alterations in the expression of costimulatory molecules and receptors may influence

differences observed between immunological reactivity of T lymphocytes derived from umbilical cord blood (UCB) and adult peripheral blood (APB).

B7 costimulatory molecules are expressed on antigen presenting cells (APCs) and are important regulators of T cell activation (**Table 1**). Upon the engagement of the T cell receptor (TCR), the costimulatory signal from B7-1 (CD80) or B7-2 (CD86) via CD28 induces the production of IL-2 in T cells, thus protecting them from apoptosis and anergy. Both the TCR and CD28 are constitutively expressed by naive T cells, enabling them to respond to the antigen being presented [9]. Without costimulation, the signal from the TCR induces the tolerance of T cells to their cognate antigen instead of being activated [10].

APC	**T cell**	**Effect on T cell**
B7-1 (CD80)	CD28	stimulation
	CTLA-4 (CD152)	inhibition
B7-2 (CD86)	CD28	stimulation
	CTLA-4 (CD152)	inhibition
B7-H1 (CD274)	PD-1 (CD279)	inhibition
B7-H2 (CD275)	ICOS (CD278)	stimulation

Table 1. The investigated B7 family proteins on antigen presenting cells (APCs) and their receptors on T cells.

Nevertheless, B7 family members mediate not only stimulatory, but also inhibitory effects on T cells, and therefore may contribute to the altered reactivity of UCB T lymphocytes compared to APB [9]. Upon the stimulation of TCR, cytotoxic T lymphocyte antigen 4 (CTLA-4, CD152) becomes phosphorylated, resulting in its stabilisation on the cell surface. This way CTLA-4

can compete with CD28 for B7 binding, thus blocking the costimulatory signal and preventing IL-2 production. The affinity of the inhibitory receptor, CTLA-4 is higher than that of CD28 for B7-1 and B7-2. Besides its competitive role, CTLA-4 further emits inhibitory signals, thus contributing to the prevention of T cell activation [11].

Another B7 family member, B7-H1 (CD274) possesses mostly, but not exclusively inhibitory properties on T cells. Its inhibitory function occurs by signalling through the programmed death 1 receptor (PD-1, CD279), inducing apoptosis or anergy of self-reactive T cells [12]. Genetic deletion of PD-1 results in severe autoimmunity due to the loss of peripheral tolerance of self-reactive T cells [13].

B7-H2 (CD275) serves as the ligand for inducible costimulator of T cells (ICOS, CD278), and promotes T cell activation, differentiation, and effector responses [14]. In contrast to the costimulatory effect of CD28, ICOS most effectively induces IL-10, but does not influence IL-2 production [15]. ICOS also stabilizes IL-10R expression on T cells, increasing their sensitivity to IL-10 [16]. Thus, the B7-H2/ICOS pathway preferentially regulates the effector function of T cells [17].

2.3. The kynurenine pathway

Besides initiating signal transduction in T lymphocytes, B7-1 and B7-2 may back-signal into the APC and influence the local immune environment through induced expression of immunosuppressive factors independently of their effects on T cells [9]. For instance, reverse signalling through B7-1 and B7-2 after ligation by a soluble form of CTLA-4 was shown to upregulate the tryptophan (TRP) catabolic enzyme, indoleamine 2,3-dioxygenase (IDO) [18]. The potent immunosuppressive activity of IDO was first identified in pregnancy, when it was demonstrated that inhibition of IDO activity abolished allogenic gestation in mice [19].

In the first steps of the kynurenine (KYN) pathway, the rate-limiting step in KYN formation from TRP is mediated by IDO. KYN is then further metabolized by different enzymes. One of them is kynurenine aminotransferase, leading to the production of kynurenic acid (KYNA), a broad-spectrum endogenous antagonist of excitatory amino acid receptors [20,21] with emerging recent implications in immunomodulation [22,23]. The rate of TRP degradation, represented by the K/T (KYN to TRP) ratio, allows a good estimate of IDO activity.

The induction of IDO and the kynurenine system results in the inhibition of T cell functions, the activation of regulatory T cells and the inhibition of NK cells. Furthermore, the local depletion of TRP and the production of pro-apoptotic TRP metabolites of the kynurenine pathway such as 3-hydroxyanthranilic acid and quinolinic acid are among the mechanisms potentially responsible for the immunosuppressive effects related to IDO, as reviewed by Mándi and Vécsei [22]. Since the TRP metabolic pathway is activated by pro-inflammatory stimuli, the anti-inflammatory effect of KYN metabolites provides a feedback mechanism in modulating the immune response.

The interplay between the kynurenine system and cytokines is a regulator of both innate and adaptive immune responses, and it plays an important role in the interactions between the central nervous and the immune systems [24,25]. While some TRP metabolites, such as 3-hydroxykynurenine and quinolinic acid, may have neurotoxic potential, KYNA appears to be a potent neuroprotective agent as it ameliorates N-methyl-D-aspartate (NMDA) receptor-mediated excitotoxicity [26] and acts as a potent free radical scavenger and endogenous antioxidant [27]. The alterations of the kynurenine system appear to play a role in the pathophysiology of a broad spectrum of neurological disorders, including ischemic brain injury [23].

2.4. Regulatory T cell subtypes in preeclampsia

Preeclampsia (PE) is an immune-mediated syndrome usually developing in the third trimester of pregnancy characterized by an excessive maternal systemic inflammatory response with activation of both the innate and adaptive arms of the immune system [28,29]. The maternal immune tolerance towards the developing semi-allogeneic fetus present in healthy pregnancy (HP) is compromised in PE. Activated neutrophils, monocytes, and natural killer cells initiate inflammation, which induces endothelial dysfunction, and activated T cells may support inadequate maternal tolerance mechanisms. An important feature of systemic inflammation in PE is the absence of Th2 skewness characteristic for HP, and thus the predominance of a Th1-type immunity [30].

Regulatory T cells (Tregs) are mediators of the maternal immune tolerance towards the developing fetus. The FoxP3 transcription factor has been widely used as an intracellular marker to identify this subset. Tregs modulate the functions of other T cells (both CD4+ and CD8+), primarily through secretion of cytokines, including IL-10 and TGF-β [31,32]. Evidence for the role of Treg cells in establishing fetal tolerance during pregnancy comes from animal studies, demonstrating a significantly increased rate of fetal resorption in allogeneic gestations of Treg-deficient mice [33,34]. Lower than normal Treg frequency may contribute to the exaggerated systemic inflammation also in humans in PE. Indeed, a number of groups including ours demonstrated that the prevalence of peripheral Tregs is lower in PE compared to healthy pregnancy [35-38]. While these studies mainly investigated peripheral blood, the distribution of Tregs in the decidua might differ. Earlier investigations provided evidence for the selective migration of fetus-specific Tregs from peripheral blood to the decidua, further emphasizing the importance of studying Tregs at the fetomaternal interface [39,40]. Another study, evaluating both peripheral blood and decidual Treg cells in mostly severe PE patients

confirmed that the proportion of Tregs was decreased in both locations compared to normal term controls [41].

Based on different intra- and extracellular markers, recent investigations identified that Tregs are not a homogenous cell subset, but can divided into further subgroups. Tregs have been grouped according whether they originate from the thymus (naturally occurring or nTregs) or induced in the periphery (iTregs). The Helios transcription factor, belonging to the Ikaros family, has been identified as a marker of thymic-derived Treg cells [42]. Its function is not yet fully understood. Binding to the promoter region of FoxP3, it may have a role in regulating the expression of FoxP3 [43]. It does not seem to have a direct effect on Treg prevalence or function [44]. Both nTregs and iTregs have a high expression of CD25 and CTLA-4, and low expression of CD127. These two subsets are different in the cytokines they produce and their potential to suppress other cells: iTregs produce IL-10 and IL-17 and have a higher regulatory potential.

Miyara et al. categorized Tregs based on their expression of CD45RA and FoxP3. CD4+ FoxP3+ CD45RA+ cells were described as naive or resting Tregs, while CD4+ FoxP3hi CD45RA- cells were regarded as fully functional effector Tregs. CD4+ FoxP3+ CD45RA- cells are cytokine-secreting, non-suppressive T cells [45]. CD45RA was also used by other groups as a marker of distinction [46,47]. While naive Tregs have the potential to proliferate, effector Tregs are not capable of proliferation or further differentiation [48].

An “exhausted” and dysfunctional phenotype of Tregs has been reported in conditions of chronic disease and infection [49]. Exhausted Tregs express CD279 or programmed death receptor 1 (PD-1), a negative regulatory molecule. Lines of evidence indicate that CD279 expression on T cells is associated with limited proliferative capacity and reduced immune suppression in vivo [50-54]. Interestingly, one of the ligands for CD279, CD274 (PD-L1), has been shown to negatively regulate Tregs by inhibiting STAT-5 phosphorylation at sites of

chronic inflammation. Thus PD-1 and its ligand appears to be a major inhibitory receptor pathway involved in T cell exhaustion [51].

2.5. Infant nutrition and regulatory T cells

An important consideration in relation to neonatal immune function is the threshold of immune response versus tolerance in the early postnatal period. A range of factors act to limit alloreactive immune responses during pregnancy and avoid immunological rejection of the fetus. This includes an increase in both maternal and fetal-derived regulatory T cells (Tregs) [5,55] together with preferential differentiation of fetal CD4+ cells towards Treg phenotype [56] mediated through increased 'tolerogenic' dendritic cell activity [57]. It is likely that this balance towards relative immune suppression continues into neonatal life but the profile of this, and its relative dependence on the postnatal environment, as well as the presence of non-inherited maternal antigens (NIMA) remain unclear.

The perinatal establishment of the gut microbiome is likely to be a dominant regulator of neonatal immune development. Indeed, colonization with specific commensal bacteria can enhance the development of Treg responses [58], whilst dysbiosis disturbs stereotypic immune development and promotes T cell activation [7]. Vertical transmission of maternal microbiota is the initial, and potentially most important, determinant of the neonatal microbiome. In this regard it is notable that the mode of delivery is a critical factor and its influence on childhood microbiome extends for at least 7 years [59]. The influence of microbiome composition on long term health outcomes is an area of considerable interest and atypical colonization has been associated with a range of conditions including impaired immune function and increased risk of allergy [60].

The importance of nutrition as a determinant of the profile of neonatal immunity has been poorly investigated [61,62]. The natural nutrition for neonates is from breastmilk which

contains a range of complex nutrients as well as antimicrobial proteins. Breastmilk also contains bacteria and maternal cells, and as such it is not surprising that exposure to either breastmilk or formula milk significantly influences the composition of the gut microbiome [63]. Differential microbiome composition is likely to act as an indirect influence on how nutrition can modify the neonatal immune profile but there may also be a direct effect from exposure to maternal cells and antigenic proteins within milk.

2.6. The effects of phosphodiesterase inhibitors on T cells

Phosphodiesterase (PDE) inhibitors, such as caffeine, milrinone and sildenafil are widely used in the clinical management of preterm and term neonates. However, little is known about how these compounds interact with the neonatal adaptive immune system.

Caffeine is a non-selective PDE inhibitor and a non-specific adenosine receptor (AR) antagonist. Its main indication in neonatology is the treatment of apneas in preterm infants below 34 weeks of gestation [64]. The therapeutic plasma level of caffeine in the neonate is 25-125 uM (5-25 mg/L). In this concentration range, caffeine blocks A1 and A2A ARs, stimulating the central respiratory effort in the brainstem [65]. Furthermore, caffeine has also been linked to a decrease in the incidence of bronchopulmonary dysplasia and improved neurodevelopmental outcome in extremely premature infants [66], although the mechanisms explaining these findings are still to be clarified. The inhibition of ARs reduces cAMP levels and is therefore of a contrary effect to PDE inhibition (**Figure 1**).

Caffeine is also known to influence intracellular calcium homeostasis in two different ways [67]. On the one hand, it inhibits inositol trisphosphate (IP3), thus decreasing calcium release from the endoplasmic reticulum (ER). However, on the other hand, it activates ryanodine receptors (RyR), and contributes to calcium release from the ER and in turn to store-operated

calcium entry (SOCE) from the extracellular space (**Figure 1**). This is a key event in T cell activation and cytokine production.

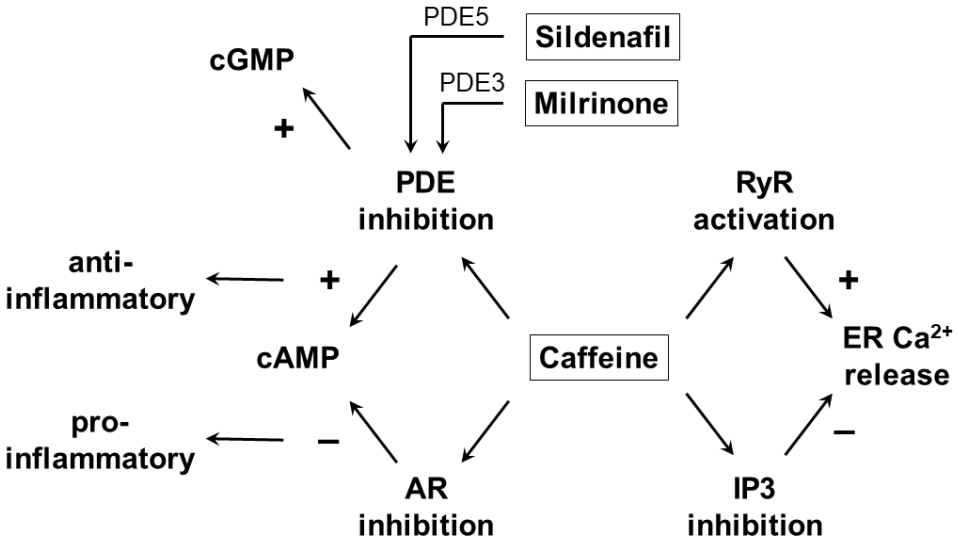

Figure 1. The effects of caffeine, milrinone and sildenafil on intracellular calcium, cAMP and cGMP homeostasis. Caffeine both increases and decreases cytosolic calcium levels by ryanodine receptor activation and the inhibition of inositol trisphosphate, respectively. It also has a dual effect on cAMP levels. Selective PDE inhibitors increase cAMP and cGMP levels. AR – adenosine receptor, ER – endoplasmic reticulum, IP3 – inositol trisphosphate, PDE – phosphodiesterase, RyR – ryanodine receptor.

In trials performed on adult populations, caffeine has been demonstrated to cause alterations in the immune system when applied in doses equivalent to regular coffee consumption. It is important to note that these concentrations are variable depending on the cohort studied but are generally lower than the target therapeutic plasma levels of caffeine in neonates. De Leon et

al. reported that the median plasma concentration of caffeine was 13 uM in individuals who consumed 1-2 cups of coffee throughout the day, and rose to 17 uM in individuals who drank 5-6 cups of coffee in a day [68]. Lelo et al. estimated a peak plasma caffeine concentration of 50 uM in habitual coffee consumers, with a mean 24 hr plasma level of 25 uM. These volunteers consumed 179-849 mg of caffeine over 24 h in the form of 1-5 cups of coffee or tea [69].

Caffeine reduces T cell proliferation and the production of tumor necrosis factor alpha (TNF-α), IFN-γ, IL-2, IL-4, IL-5 and IL-10 cytokines in human blood, as well as antibody production. A part of these immunomodulatory actions of caffeine are mediated via the inhibition of the hydrolysis of cAMP, and thus an increase in intracellular cAMP concentrations, promoting a largely anti-inflammatory and immunosuppressive effect [70].

On the other hand, caffeine also exerts immunomodulatory effects via the antagonism of ARs. Adenosine is known to have mainly suppressive effects on immune cells. For instance, adenosine increases the production of IL-10 [71]. The increase in TNF-α release by adult peripheral blood monocytes in response to lipopolysaccharide exposure can be abolished by pre-treatment with A2A receptor agonists [72].

Milrinone is a specific PDE3 inhibitor and is often used in cardiac failure as it improves the contractility of the myocardium. At the same time, it often causes peripheral vasodilation and hypotension. Sildenafil is a specific inhibitor of PDE5 is and used for the treatment of pulmonary hypertension as it reduces the increased pulmonary vascular resistance. Through increasing cAMP and cGMP levels, milrinone and sildenafil were also noted to exert immunosuppressive effects [73].

In spite of some evidence for immunomodulatory effects on adult T cells, little is known about how these compounds interact with the neonatal adaptive immune system. Taking into consideration their wide clinical application, this lack of knowledge needed to be addressed.

2.7. Perinatal asphyxia

Perinatal asphyxia evokes the injury of the central nervous system (CNS) due to the severe lack of oxygen and perfusion during labour and delivery, resulting in moderate to severe neurological dysfunction. Asphyxia primarily affects term and post-term neonates. It occurs in 2-4 of every 1000 live-born term neonates and is responsible for approximately 23% of neonatal deaths worldwide [74]. While some surviving children show favourable neurological outcome, others sustain severe neurodevelopmental problems such as learning difficulties, sensory impairment, cerebral palsy and seizures [75]. Identifying the factors responsible for such extent of individual variability regarding outcome would be critical, however, to date no definitive predictive factors have been validated.

The majority of hypoxic-ischaemic injuries happens during or in close proximity to delivery [76]. Term neonates generally present with symptoms of perinatal asphyxia directly after birth. The state-of-the-art treatment for asphyxia and its specific manifestation in the CNS, hypoxic-ischaemic encephalopathy (HIE) is therapeutic hypothermia. Eligibility for cooling therapy is established based on the presence of criteria A and B. Criteria A include: Apgar score of ≤ 5 at 10 minutes after birth, or continued need for resuscitation, including endotracheal or mask ventilation, at 10 minutes after birth, or acidosis within 60 minutes of birth (defined as any occurrence of umbilical cord or arterial or capillary pH < 7.00) or base deficit ≥ 16 mmol/L in umbilical cord or any blood sample (arterial, venous or capillary) within 60 minutes of birth. Criteria B include: seizures, or moderate to severe encephalopathy, consisting of altered state of consciousness (lethargy, stupor or coma), and abnormal tone (focal or general hypotonia or flaccidity), and abnormal primitive reflexes (weak or absent suck or Moro response) [77].

Symptoms usually evolve during the first days of life and their severity and persistence is in correlation with the severity and duration of the hypoxic-ischaemic insult. Based on the clinical presentation, HIE can be classified as mild, moderate or severe [78]. Mild hypoxic-ischaemic

insult might manifest in subtle neurological abnormalities (such as transient drowsiness) without multi-organ damage, whereas a severe insult usually leads to moderate-severe HIE and variable degree of multi-organ failure [78,79].

During the first 12-24 hours, neonates with mild HIE generally show some neurological alterations, such as restlessness or moderate hypertonia, often associated with periodic breathing and feeding difficulty. The most common systemic symptom is decreased urinary output. After 24 hours, neonates with mild-moderate HIE can improve in their overall clinical and neurological status. They often reach normal level of consciousness and begin to tolerate feeds during the first week of life. Laboratory parameters usually show a similar tendency [78]. Neonates with moderate-severe HIE on the other hand often show more profound neurological alterations during the first days, such as depressed state of consciousness, abnormal pupillary size, hypotonia, periodic breathing with apnea, bradycardia, and signs of seizure activity [80]. In the most severe cases, neonates are often lethargic, and stupor and early onset, overt seizure activity is also common. In term infants, seizures are usually multifocal and clonic, and can manifest in apneic spells. Systemic symptoms almost always include kidney damage and respiratory insufficiency with prolonged apnea, which often makes mechanic ventilation necessary. Hypoxic-ischaemic injury can cause cardiomyopathy, with the need for inotropic support, the severity of which is in close relations with the severity of the insult [81]. As HIE progresses, after 24 hours either a gradual stabilisation or deterioration can be observed. In the latter case, seizures often become refractory [80]. The patient’s level of consciousness progressively deteriorates, as brain stem functions begin to be affected. In the most severe cases, neonates die within the first week of life. Autopsy-based studies revealed cytotoxic brain oedema and extensive neuronal damage after lethal perinatal asphyxia [82].

2.8. The neuroinflammatory response in hypoxic-ischaemic encephalopathy

Inflammation of the CNS, or neuroinflammation is now recognised to be a feature of all neurological disorders, including that related to neonatal asphyxia. Microglia and astrocytes become activated and release pro-inflammatory cytokines and chemokines. Disruption of the blood-brain barrier allows infiltration of peripheral monocytes into the brain that further enhances the inflammatory response, leading to neuronal injury and apoptosis. However, the inflammatory reaction following asphyxia is not limited to the CNS, but can also be detected in the periphery. Systemic immune activation is characterized by increased synthesis of pro-inflammatory cytokines [83]. A key player in the mediation of the inflammatory response both in the brain and peripheral blood during asphyxia is the subset of T lymphocytes. T lymphocytes have a pivotal role in the evolution of hypoxic injury. The mechanisms by which T cells are neurotoxic include the production of perforin and granzyme B, the release of free radicals, the triggering of apoptotic pathways within neurons, and most importantly, the production of pro- and anti-inflammatory cytokines [84,85].

2.9. The neuroregenerative response following hypoxic-ischaemic encephalopathy

An extensive dataset describes neuroinflammation to have detrimental consequences, but results have indicated over the past decade that some aspects of the inflammatory response are beneficial for CNS outcomes [86,87]. Benefits of neuroinflammation include neuroprotection, the mobilisation of neural precursors for repair, remyelination, and axonal regeneration. In vitro studies demonstrated that pro-inflammatory cytokines, such as TNF-α and IFN-γ are toxic for oligodendrocytes [88-90]. Although inflammatory cytokines contribute to injury progression, they also play a vital role in the fast elimination of cellular debris, and in the processes of growth and repair, contributing to functional recovery [91,92]. The results of Saliba et al. support the positive role of certain cytokines in neuronal regeneration [93]. In addition to its

toxic effect, TNF-α also plays a role in neuronal progenitor cell proliferation, lineage commitment and cellular differentiation. IL-1 also has neurotrophic properties which might be mediated by the stimulation of nerve growth factor production. Direct intracerebral injection of IL-1 or TNF-α have been shown to stimulate astrogliosis and angiogenesis in the developing rodent brain [94]. The transforming growth factor beta (TGF-β) family consists of pleiotropic proteins with potent immune regulatory properties, which might also play key roles in the development, repair and survival of neurons [93].

2.10. The effects of therapeutic hypothermia on inflammation

Previous investigations in asphyxia demonstrated that pro-inflammatory IL-1β, TNF-α and IFN-γ play an outstanding role in the pathophysiology. IL-6, IL-8, and IL-17 also have an important contribution [93,95-97]. On the other hand, anti-inflammatory TGF-β and IL-10 have a protective role, and are important for regenerative processes [98]. Prolonged moderate hypothermia improves neurological outcome, and has become standard care for term infants with HIE over the recent years [77]. One mechanism by which hypothermia exerts a neuroprotective effect may be by reducing systemic inflammation [99]. In an earlier study, we measured cytokine levels at the 6th, 12th and 24th postnatal hours in neonates with perinatal asphyxia treated with hypothermia or standard intensive care on normothermia [100]. Our results indicated that IL-6 levels (at 6 hours of age) and IL-4 levels (at all time points) were significantly lower in neonates treated with hypothermia compared to normothermic neonates. The duration of hypothermia initiated before 6 hours of age correlated with lower levels of IL-6, TNF-α and IFN-γ measured at 6 hours of age. These data suggest that therapeutic hypothermia may rapidly suppress and modify the immediate cytokine response in perinatal asphyxia.

2.11. The regulation of the neuroinflammatory response

The permeability of the blood brain barrier (BBB) is higher in neonates compared to adults and is further disrupted by the hypoxic injury itself. The release of IL-1β, TNF-α and IFN-γ also increase the permeability of the BBB [101,102]. CD49d is part of the very late antigen-4 (VLA-4) which mediates the migration of activated leukocytes to the site of tissue inflammation via binding to vascular cell adhesion molecule-1 (VCAM-1), expressed by endothelial cells [103]. VLA-4 is thus crucial for the migration of activated T lymphocytes through the BBB to the site of inflammation in the brain [104,105], making it a primary therapeutic target in multiple sclerosis [106] and in primary neuroinflammatory brain disease in murine ischemic stroke models [107]. Although VCAM-1 is not exclusively expressed in the CNS, the level of CD49d expression can be correlated with the capacity of T lymphocytes to enter the site of inflammation, more specifically the brain tissue in case of neuroinflammation [108].

The challenge in neonatal asphyxia is to harness the beneficial aspects of neuroinflammation following the insult to allow neuroprotection and regeneration within the CNS, while at the same time minimising its harmful effects. Significant barriers remain in understanding the benefits of inflammation in contrast to its detriments following perinatal asphyxia. Identification of factors that differentiate between infants with an extensive and potentially damaging neuroinflammatory response and infants with moderate inflammation would present new options for a more individualised therapeutic approach in perinatal asphyxia.

2.12. Neonatal arterial ischaemic stroke

The perinatal period carries the highest risk for stroke in the entire childhood, with almost similar incidence to that in the elderly population. “Perinatal stroke” is a broad term defining a group of heterogeneous conditions characterised by the focal disruption of cerebral blood flow, of which neonatal arterial ischaemic stroke (NAIS) is one of the most common subtypes, with

an incidence of 1 per 8000 live births. NAIS by definition is an arterial ischaemic stroke, with clinical symptoms occurring in the neonatal period (within the first 28 days of life) which are supported by radiological evidence [109,110]. NAIS generally occurs in term neonates and presents a major risk for life-long motor, cognitive, and/or behavioural disabilities ranging from fine motor impairment to unilateral cerebral palsy, which develops in around 20-30% of affected neonates. Thus, NAIS is a leading cause of cerebral palsy [111].

Interestingly, in almost all cases of NAIS the intra-cranial arteries developing from the carotid arterial tree are affected, i.e. the proximal parts of the anterior cerebral artery, the middle cerebral artery (MCA) and the posterior cerebral artery – while the basilar artery and the extra-cranial arteries are unaffected [112-114]. The area of the left MCA is the most common localisation of the ischaemic lesion, resulting in a higher incidence of right sided congenital hemiplegia [109]. The clinical presentation of NAIS is often subtle and non-specific, the most frequent symptoms being seizures, general hypotonia, lethargy and poor feeding, making the timely diagnosis of NAIS difficult [115]. The diagnosis of NAIS is often delayed, due to the prenatal onset or absence of specific signs, therefore the primary therapeutic focus is on prevention and post-insult anti-inflammatory mechanisms [111]. Another challenge regarding the diagnosis of NAIS is the fact that the risk factors and clinical signs of global HIE due to perinatal asphyxia show a significant overlap with NAIS and the two often co-occur [115-117]. Differentiating between the two pathologies is a complex question, some studies list perinatal asphyxia as an independent risk factor for NAIS [118], while neuroinflammation following ischaemia appears to be a common feature of the both.

2.13. Pathophysiology of neonatal arterial ischaemic stroke

According to the classic pathophysiological hypothesis, most ischaemic lesions are a result of thromboembolic events, where the presumable source of the thrombi are the placenta or the

umbilical vessels [119]. While in some instances this could be the case, this hypothesis does not give a plausible explanation to why NAIS is almost exclusively affecting the intracranial arterial territories developing from the carotid arterial tree, while the incidence of basilary arterial or extracerebral infarcts is negligible [119]. In addition, there is angiographic evidence indicating a possibility of local arterial wall defects and in situ thrombus generation [117, 120]. Based on these findings, Giraud et al. proposed a different pathomechanism, where feto-maternal inflammation induces focal arteritis specific to the intracranial arteries developing from the carotid arterial tree, which are susceptible to NAIS [111]. Using a preclinical rat model of chorioamnionitis, they were able to demonstrate that classic prothrombotic stress applied alone to the MCA was not enough to induce NAIS. However, when combined with in-utero exposure to lipopolysaccharide (LPS), the same stress lead to the classical symptoms of NAIS and motor impairment. They also examined the walls of arteries susceptible to NAIS and found that the constitutive expression of certain pro-inflammatory cytokines, such as TNF-α and IL-1β was higher in the susceptible intra-cerebral arteries compared to extra-cerebral arteries. Furthermore, pups born from LPS-exposed dams developed a specific cerebral arteritis with increased presence of macrophages and elevated levels of pro-inflammatory cytokines IL-1β, TNF-α, and monocyte chemoattractant protein-1 (MCP-1) with increased IL-1/IL-1 receptor antagonist (IL-1ra) ratio in NAIS susceptible arteries, but not elsewhere [113].

2.14. The neuroinflammatory response in neonatal arterial ischaemic stroke

The primary aim of current research efforts in the field of perinatal stroke is to gain a better understanding of the pathomechanism of the disease with specific regard to the activation of the inflammatory pathway, that could present a possibility for more specific diagnosis, intervention and even prevention [111]. Human experimental data on inflammatory markers is scarce. Only one case-control study is available, where the authors aimed to describe the levels

of different cytokines in the plasma of paediatric stroke patients. Elevated levels of TNF-α, IL-2, IL-6, and IL-8 were observed 6 months following stroke compared to healthy controls. However, no differences were observed in soluble endothelial protein C receptor, IL-11, and FVIII median levels [121]. The limitation of this study is that they included both neonatal and paediatric stroke cases (from birth until 18 years of age), which are now viewed as clinically distinct syndromes. These results indicate that an ongoing inflammation could be observed up to 6 months following stroke, however, they do not provide information regarding the acute phase of NAIS.

The pivotal role of inflammatory pathways in ischaemic brain injury is supported by recent investigations. T lymphocytes appear to play a central role in ischaemic infarct development, they appear in the brain tissue within hours of the hypoxic insult and can be detected for up to a month after the injury. T cell deficiency has been shown to result in smaller infarct size and improved neurological outcome in murine models [122,123]. Several cytokines have been connected to acute ischemic stroke in adults. Pro-inflammatory cytokines IL-1β, IL-8, MCP-1, TNF-α and IFN-γ appear to exacerbate cerebral injury in adults, whereas anti-inflammatory cytokines such as TGF-β and IL-10 appear to be neuroprotective [124-126]. Although the immune system of neonates shows many differences compared to adults, the inflammatory network appears to play a similarly critical role in ischaemic brain injury. Therefore, it is reasonable to hypothesise that the same cytokines might also influence the course of neuroinflammation in the neonatal brain.

3. AIMS

3.1. B7 costimulation in the neonate

1. To determine the frequency of activated monocytes expressing B7-1, B7-2, B7-H1 and B-7H2 costimulatory molecules, as well as that of T cells and T helper cells expressing CD28, CTLA-4, PD-1 and ICOS in UCB compared to APB.
2. To examine the intracellular expression of IDO in activated monocytes and T cells, along with plasma levels of TRP, KYN and KYNA in UCB compared to APB.

3.2. B7 costimulation in healthy pregnancy and preeclampsia

3. To determine the frequency of activated monocytes expressing B7-1, B7-2, B7-H1 and B-7H2 costimulatory molecules, as well as that of T cells and T helper cells expressing CD28, CTLA-4, PD-1 and ICOS in non-pregnant, HP and PE women.
4. To examine the intracellular expression of IDO in activated monocytes and T cells in non-pregnant, HP and PE women.

3.3. Regulatory T cell subtypes in preeclampsia

5. To compare the peripheral prevalence of Treg subtypes, such as naive and effector, thymic and extrathymic, as well as exhausted Tregs in HP and PE.

3.4. Breastfeeding and immune development

6. To analyse how immune phenotype of T cells evolve between birth and three weeks of age in breastfed and formula fed healthy neonates with a specific focus on regulatory T cells.

7. To study the interaction of the maternal and neonatal immune systems in the first three weeks of life following delivery using mixed lymphocyte reactions in breastfed and formula fed healthy neonates.
8. To study prospective changes in the neonatal gut microbiome in the first three weeks of life in relation to the source of nutrition and the immune phenotype of T cells.

3.5. The impact of phosphodiesterase inhibitors on T cells

9. To describe the effects of caffeine, milrinone and sildenafil on the activation of T cells from UCB compared to APB.
10. To describe the effects of caffeine, milrinone and sildenafil on cytokine production of T cells from UCB compared to APB.
11. To examine the expression of CD203c, an ectoenzyme responsible for the extracellular hydrolysis of cAMP in UCB compared to APB.
12. To examine the expression nuclear factor of activated T cells (NFAT), a key transcription factor in T cell cytokine production in UCB compared to APB.

3.6. Perinatal asphyxia and neonatal arterial ischaemic stroke

13. To assess the prevalence and cytokine production of T lymphocyte subsets in moderate and severe perinatal asphyxia up to one month of age following the hypoxic event in order to identify components of the inflammatory response that may influence patient outcome.
14. To describe the alterations of plasma cytokine levels in moderate and severe perinatal asphyxia up to one month of age following the hypoxic event.

15. To describe the alterations of plasma TRP, KYN and KYNA levels as well as IDO activity in moderate and severe perinatal asphyxia up to one month of age following the hypoxic event.
16. To assess the prevalence and cytokine production of T lymphocyte subsets in NAIS in comparison to perinatal asphyxia up to one month of age after birth.
17. To assess the alterations of plasma cytokine levels in NAIS in comparison to perinatal asphyxia up to one month of age after birth.

4. METHODS

4.1. B7 costimulation in the neonate, in healthy pregnancy and preeclampsia

4.1.1. Neonatal sample collection

Peripheral blood samples were taken from 20 healthy adults (8 women and 12 men; age: 26.5 (24-28) years, median (interquartile range)) and cord blood samples from the umbilical vein of 17 healthy, term neonates (7 girls and 10 boys; gestational age: 39 (38-40) weeks, median (interquartile range); birth weight: 3300 (3150-3650) grams, median (interquartile range)). Informed consent was obtained from all subjects or, in the case of neonates, parents of subjects, and our study was reviewed and approved by an independent ethical committee of Semmelweis University (TUKEB). The study was adhered to the tenets of the most recent revision of the Declaration of Helsinki.

4.1.2. Sample collection in healthy pregnancy and preeclampsia

For comparisons between non-pregnant (NP) and HP women, peripheral blood samples were taken from 20 HP women in the third trimester (34-37 weeks) and 14 age-matched, healthy NP women. The latter group was synchronized in terms of menstrual cycle for the luteal phase. Informed consent was obtained from all subjects, and our study was reviewed and approved by an independent ethical committee of Semmelweis University (TUKEB). The study was adhered to the tenets of the most recent revision of the Declaration of Helsinki.

For comparisons between PE and HP, we took peripheral blood samples from an additional 20 PE women in the third trimester of pregnancy (30-38 weeks). PE was defined by increased blood pressure (≥ 140 mmHg systolic and/or ≥ 90 mmHg diastolic on ≥ 2 occasions at least 6 hours apart) that occurred after 20 weeks of gestation in a woman with previously normal blood

pressure, accompanied by proteinuria (≥ 0.3 g/24h or ≥ 1 + on dipstick in the absence of urinary tract infection). Exclusion criteria were multifetal gestation, chronic hypertension, diabetes mellitus, autoimmune disease, angiopathy, renal disorder, maternal or fetal infection and fetal congenital anomaly. Informed consent was obtained from all subjects, and our study was reviewed and approved by an independent ethical committee of Semmelweis University (TUKEB). The study was adhered to the tenets of the most recent revision of the Declaration of Helsinki.

4.1.3. Peripheral blood mononuclear cell isolation

Peripheral blood mononuclear cells (PBMCs) were separated by a standard density gradient centrifugation (Ficoll Paque, Amersham Biosciences AB, Uppsala, Sweden, 25 minutes, 400 *g*, 22 °C) from freshly drawn blood collected in lithium heparin-treated tubes (BD Vacutainer, BD Biosciences, San Jose, CA, USA). Cells were kept at -80 ºC in Fetal Bovine Serum (FBS) containing 10% dimethyl sulfoxide (DMSO) until analysis. After thawing, cells were washed twice in phosphate-buffered saline and their viability was assessed by trypan blue exclusion (consistently > 90%).

4.1.4. Flow cytometry

PBMCs were stained for 30 min at room temperature in the dark with PerCP-conjugated CD3, PE Cy7-conjugated CD4, PE-conjugated CD28, APC-conjugated CD152 (CTLA-4), FITC-conjugated CD278 (ICOS) and APC-Cy7-conjugated CD279 (PD-1) monoclonal antibodies (mAbs), or PerCP-conjugated CD3, PE Cy7-conjugated CD11b, APC-conjugated CD80 (B7-1) and PE-conjugated CD275 (B7-H2) mAbs, or PerCP-conjugated CD3, PE Cy7-conjugated CD11b, APC-conjugated CD86 (B7-2) and PE-conjugated CD274 (B7-H1) mAbs in separate tubes, respectively (BioLegend, San Diego, CA, USA). After washing, cells were fixed with

Fixation/Permeabilization solution and treated with Permeabilization Buffer according to the manufacturer's instructions (eBioscience, San Diego, CA, USA). They were then stained with a mouse anti-human IDO monoclonal antibody (Millipore, USA) for 30 min at 4 ºC in the dark. After washing, cells were stained with FITC-labelled goat anti-mouse antibody (Millipore, USA) for 15 min at 4 ºC in the dark. After washing, cells were analysed on a BD FACSAria flow cytometer (BD Biosciences) equipped with 488 nm and 633 nm excitation lasers. Data were processed using the FACSDiVa software. 100,000 cells were recorded. The populations of lymphocytes and monocytes were gated from PBMCs according to Forward Scatter Characteristics and Side Scatter Characteristics. As control of FITC-labelled goat anti-mouse specificity staining, PBMCs were incubated with surface antibodies and FITC-labelled goat anti-mouse antibody in the absence of mouse anti-human IDO monoclonal antibody. Gating strategy is represented in **Figure 2**.

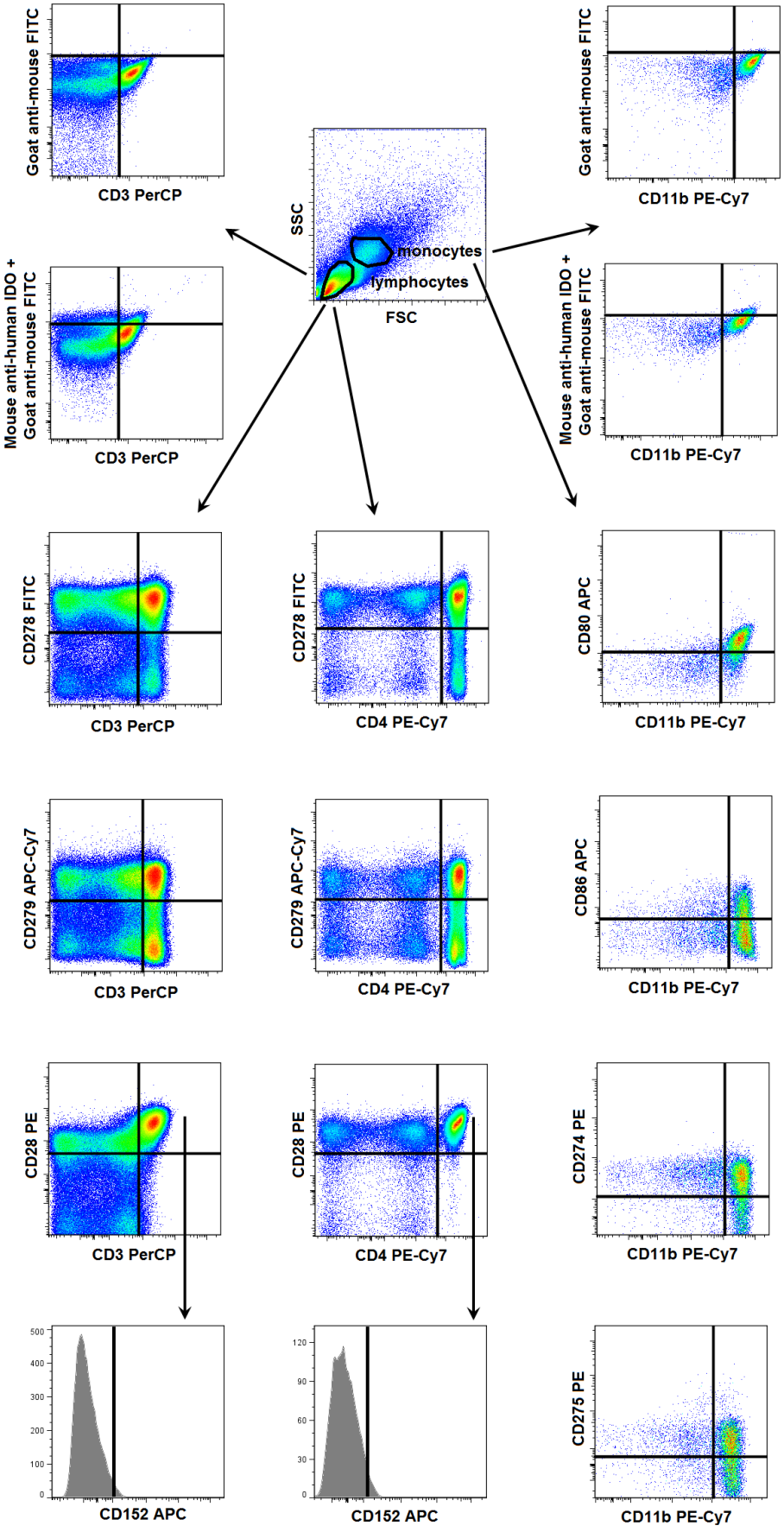
Goat anti-mouse FITC
CD3 PerCP
SSC
monocytes
lymphocytes
FSC
Goat anti-mouse FITC
CD11b PE-Cy7
Mouse anti-human IDO + Goat anti-mouse FITC
CD3 PerCP
Mouse anti-human IDO + Goat anti-mouse FITC
CD11b PE-Cy7
CD278 FITC
CD3 PerCP
CD278 FITC
CD4 PE-Cy7
CD80 APC
CD11b PE-Cy7
CD279 APC-Cy7
CD3 PerCP
CD279 APC-Cy7
CD4 PE-Cy7
CD86 APC
CD11b PE-Cy7
CD28 PE
CD3 PerCP
CD28 PE
CD4 PE-Cy7
CD274 PE
CD11b PE-Cy7
CD152 APC
CD152 APC
CD275 PE
CD11b PE-Cy7

Figure 2. Gating strategy applied for discrimination of the investigated cell subsets in flow cytometry measurements in the B7 costimulation experiments. FSC – forward scatter characteristics, SSC – side scatter characteristics.

4.1.5. High-performance liquid chromatography

The investigated reference compounds (L-TRP, L-KYN sulphate salt, KYNA) and zinc acetate dihydrate were purchased from Sigma-Aldrich (Saint Louis, MO, USA), acetonitrile and perchloric acid were purchased from Scharlau (Barcelona, Spain) and acetic acid was purchased from VWR International (Radnar, PA, USA).

Plasma samples were stored at -80 °C until analysis. Before analysis, the samples were thawed and after brief vortexing 300 µl of plasma sample was "shot" onto 700 µl precipitation solvent (containing 3.57 w/w% perchloric acid and 2.857 µM 3-nitro-L-tyrosine as internal standard). Following that the samples were centrifuged at 13000 *g* for 10 min at 4 °C, and the supernatant was collected.

The KYN, KYNA and TRP concentrations of the samples were quantified based on the slightly modified method of Herve et al. [127], with an Agilent 1100 high-performance liquid chromatography (HPLC) system (Agilent Technologies, Santa Clara, CA, USA). The system was equipped with a fluorescent and a UV detector, the former was applied for the determination of KYNA and TRP, and the latter for the determination of KYN and the internal standard. Chromatographic separations were performed on an Onyx Monolithic C18 column, 100 mm x 4.6 mm I.D. (Phenomenex Inc., Torrance, CA, USA) after passage through a Hypersil ODS pre-column, 20 x 2.1 mm I.D., 5 um particle size (Agilent Technologies, Santa Clara, CA, USA) with a mobile phase composition of 0.2 M zinc acetate/ACN = 95/5 (v/v%) with a pH adjusted to 6.2 with glacial acetic acid, applying isocratic elution. The flow rate and the injection volume were 1.5 ml/min and 20 µl, respectively. The fluorescent detector was set

at excitation and emission wavelengths of 344 nm and 398 nm, and after 3.5 min of each run the wavelengths were changed to 254 nm and 398 nm. The UV detector was set at a wavelength of 365 nm.

4.1.6. Statistical analysis

Data are expressed as median and interquartile range. Comparisons between sample populations were made with Mann-Whitney test. Correlation analyses were performed using Spearman tests. p-values less than 0.05 were considered significant. Statistics were calculated using the STATISTICA software (version 8.0; StatSoft, Inc., Tulsa, Oklahoma, USA).

4.2. Regulatory T cell subtypes in preeclampsia

4.2.1. Sample collection

Peripheral blood samples were collected from 19 women with PE at on average the 34th gestational week of pregnancy. PE was diagnosed according to standard internationally accepted criteria. These include hypertension (defined as systolic blood pressure and/or diastolic blood pressure ≥ 140 mmHg and ≥ 90 mmHg, respectively) occurring after 20 weeks of gestation, and proteinuria (defined as presence of ≥ 0.3 g protein in a 24 hour urine specimen). As controls, 21 healthy, age-matched pregnant women at on average the 36th gestational week were enrolled. Exclusion criteria were multifetal gestation, chronic hypertension, diabetes mellitus, autoimmune disease, angiopathy, renal disorder, maternal or fetal infection and fetal congenital anomaly. Informed consent was obtained from all subjects, and our study was reviewed and approved by an independent ethical committee of Semmelweis University (TUKEB). The study was adhered to the tenets of the most recent revision of the Declaration of Helsinki.

4.2.2. Flow cytometry

PBMCs were separated by a standard density gradient centrifugation (Ficoll Paque, Amersham Biosciences AB, Uppsala, Sweden, 25 minutes, 400 g, 22 °C) from freshly drawn blood collected in lithium heparin-treated tubes (BD Vacutainer, BD Biosciences, San Jose, CA, USA). Cells were kept at -80 °C in Fetal Bovine Serum containing 10% DMSO until analysis. After thawing, cells were washed twice in phosphate buffered saline.

PBMCs were stained for 30 min at room temperature in the dark with PE Cy7-conjugated CD4, APC-conjugated CD25, APC-Cy7-conjugated CD279 and FITC-conjugated CD45RA (BioLegend, San Diego, CA, USA). After washing, cells were fixed with Fixation/Permeabilization solution and treated with Permeabilization Buffer according to the manufacturer's instructions (eBioscience, San Diego, CA, USA). They were then stained with PE-conjugated FoxP3 PE, and PerCP-conjugated Helios for 30 min at 4 °C in the dark. Mouse IgG1 antibodies were used as isotype control.

After washing, cells were analyzed on a BD FACSAria flow cytometer (BD Biosciences). Data were processed using the FACSDiVa software. 200,000 cells per sample were recorded.

4.2.3. Statistical analysis

Data are expressed as median and interquartile range (IQR). Comparisons between two sample populations were made with the Mann-Whitney U test, as a test of normality (according to Kolmogorov-Smirnoff) indicated non-normal distribution of data; p-values less than 0.05 were considered significant. Statistics were calculated using the GraphPad software (Prism version 5.00 for Windows, GraphPad Software, San Diego, CA, USA).

4.3. Breastfeeding and immune development

4.3.1. Sample collection

A total of 38 healthy pregnant women who were planned to deliver electively at gestational term by caesarean section were sampled in our study at Birmingham Women's Hospital, UK. Peripheral blood samples were collected prior to the caesarean section and all women were not in labour and had intact membranes. Sixteen out of 38 babies (42%) were exclusively breastfed for the duration of the study, while 9 babies received mixed feeding and 13 babies were exclusively formula-fed. Further characteristics of the neonatal population are: male/female: 17/21, gestational age: 39 (39-39) weeks, birth weight: 3530 (3298-3733) g (median (interquartile range)).

Cord blood samples were taken immediately after delivery. A peripheral blood sample (up to 2 ml) was taken from the neonate at 3 weeks of age. In addition to the blood samples, a neonatal stool sample was collected at birth and at 3 weeks of age from 29 of the recruited neonates. Exclusion criteria included multiple pregnancy, sepsis risk factors (especially maternal fever or chorioamnionitis), Group B Streptococcus positivity in the current pregnancy, genetic conditions of the fetus or the mother, maternal HIV, maternal tuberculosis, maternal new-onset viral infection, maternal hypertensive disorder, maternal endocrine condition or diabetes, maternal asthma and maternal autoimmune conditions, as well as maternal medication other than pregnancy supplements. Peripheral blood samples were also collected from 13 healthy, non-pregnant adults (male/female: 6/7) who were age-matched to the pregnant women.

Informed written consent was obtained from all pregnant women and healthy volunteers. The study was reviewed and approved by the East Midlands – Nottingham 2 NHS Research Ethics Committee.

4.3.2. Peripheral blood mononuclear cell isolation

Blood samples were collected into EDTA anticoagulated tubes. PBMCs were isolated by density centrifugation using Lymphoprep (Stemcell Technologies, Seattle, WA, USA). PBMCs were washed with RPMI-1640 medium (Sigma-Aldrich, St. Louis, MO, USA) and used either directly or cryopreserved in FBS containing 10% DMSO (Sigma-Aldrich). After thawing, cells were washed with RPMI and re-suspended in enriched media (RPMI-1640 + FBS 10% + 2mM glutamine). Viability of thawed cells was consistently >90% as assessed by methylene blue exclusion. For immunophenotyping, a small portion of cells was frozen from all blood samples and samples were processed in batches after thawing. For mixed lymphocyte reactions, cord blood and neonatal blood samples at 3 weeks of age were used directly. Pregnant and non-pregnant adult samples were split at the time of sampling and one part of the samples was used directly with cord blood, while the other part was frozen and retained to be used 3 weeks later with the neonatal blood.

4.3.3. Immunophenotyping

Mononuclear cells were prepared as described above for two immunophenotyping panels. Panel 1 was designed to study intracellular cytokine production following stimulation, using unstimulated cells as controls. Cells were stained with FITC-conjugated CD107a (Biolegend, San Diego, CA, USA) at the time of stimulation, as this marker is only detectable on the cell surface upon degranulation in conjunction with stimulation [128]. Stimulation was performed with phorbol myristate acetate (PMA, 50 ng/mL, Sigma-Aldrich) and ionomycin (1 ug/mL, Sigma-Aldrich) for a total of 3.5 hours at 37 °C. After 30 minutes, 1.25 ug/mL of monensin (Sigma-Aldrich) was added to stimulated cells for the remaining 3 hours. Cells were then washed with phosphate-buffered saline (PBS, Sigma-Aldrich) and re-suspended in MACS buffer. Cell surface staining was performed for 30 minutes on ice in the dark as follows:

BV510-conjugated CD4, PerCP-Cy5.5-conjugated CD8, ECD-conjugated CD14/CD19/CD56, APC-Cy7-conjugated CD3 (all from Biolegend) and Live/Dead (red, 488nm, Invitrogen, Carlsbad, CA, USA). After washing, cells were fixed with fixation/permeabilization solution (eBioscience, San Diego, CA, USA) for 30 minutes at room temperature in the dark. Cells were washed with permeabilization buffer (eBioscience). Following centrifugation and re-suspension in MACS buffer, the following intracellular dyes were added for 30 minutes at room temperature in the dark: PE-Cy7-conjugated IL-6, AF700-conjugated IFN-γ, AF647-conjugated IL-4, BV421-conjugated IL-17A and PE-conjugated IL-8 (all from Biolegend). Cells were then washed and run on an LSRII flow cytometer equipped with blue, red and violet lasers (BD Biosciences, San Jose, CA, USA). The staining procedure was identical for unstimulated cells. At least 50,000 cells were recorded per sample. Unstained and single-stained samples were used as compensation controls in flow cytometry experiments. All antibodies and dyes were used in concentrations recommended by the relevant manufacturer.

Panel 2 assessed the immunophenotype of cells without mitogenic stimulation. Cells were surface stained in MACS buffer with PE-Cy7-conjugated HLA-DR, BV510-conjugated CD4, PerCP-conjugated CD69, ECD-conjugated CD14/CD19/CD56, AF700-conjugated CD45RA, APC-Cy7-conjugated CD3, BV421-conjugated CD25, BV605-conjugated CD31 (all from Biolegend) and Live/Dead (red, 488nm, Invitrogen). After washing, cells were fixed with fixation/permeabilization solution (eBioscience) for 30 minutes at room temperature in the dark. Cells were washed with permeabilization buffer (eBioscience). Following centrifugation and re-suspension in MACS buffer, AF647-conjugated FoxP3 (Biolegend) antibodies were added for 30 minutes in the dark. Cells were then washed and run on an LSRII flow cytometer equipped with blue, red and violet lasers (BD Biosciences). At least 50,000 cells were recorded per sample. Unstained and single-stained samples were used as compensation controls in flow

cytometry experiments. All antibodies and dyes were used in concentrations recommended by the relevant manufacturer.

In both panels during the gating process, doublets were first excluded based on FSC-A and FSC-H characteristics. Lymphocytes were then identified based on FSC-A and SSC-A characteristics. Dead, as well as CD14+, CD19+ and CD56+ cells were excluded based on positivity in the ECD channel. Further gating was performed within CD3+ cells (**Figure 3**). Flow cytometry data was analysed using the FlowJo software package.

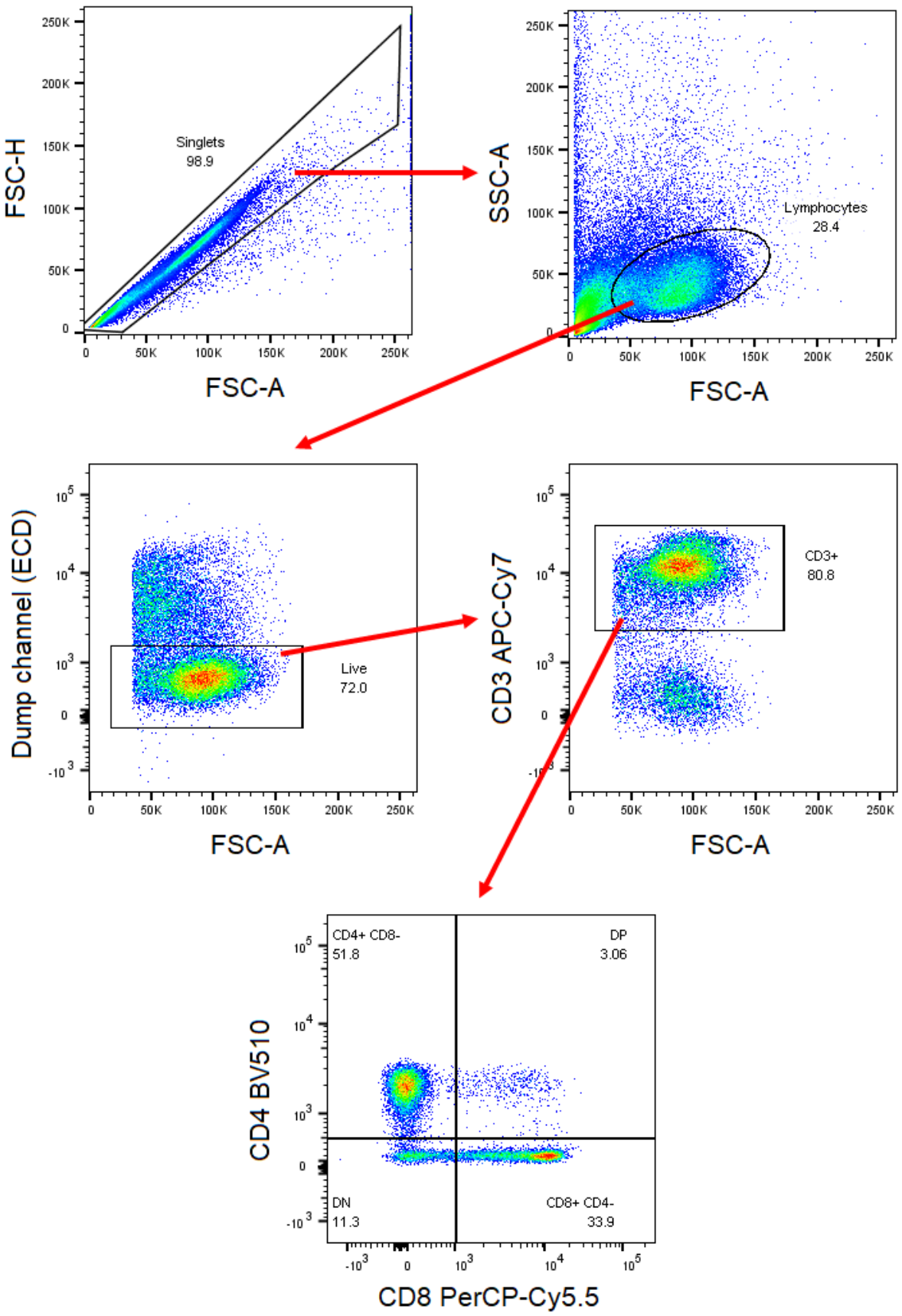
FSC-H
FSC-A
Singlets
98.9
SSC-A
FSC-A
Lymphocytes
28.4
Dump channel (ECD)
FSC-A
Live
72.0
CD3 APC-Cy7
FSC-A
CD3+
80.8
CD4 BV510
CD8 PerCP-Cy5.5
CD4+ CD8-
51.8
DP
3.06
DN
11.3
CD8+ CD4-
33.9

Figure 3. Gating strategy applied for discrimination of the investigated cell subsets in flow cytometry measurements in the breastfeeding experiments. Doublets were first excluded based on FSC-A and FSC-H characteristics. Lymphocytes were then identified based on FSC-A and SSC-A characteristics. Dead, as well as CD14+, CD19+ and CD56+ cells were excluded based on positivity in the ECD channel. Further gating was performed within CD3+ cells.

4.3.4. Mixed lymphocyte reaction assay

Mononuclear cells were prepared as described above. Stimulator cells were extracted and re-suspended in enriched media for irradiation. Cells were irradiated at 3000 rad. For responder cells, T cell enrichment was performed using the Easy Sep T cell enrichment antibody mix (1 uL per 10^6 cells), magnetic beads and Easy Sep Purple Magnet separation (Stemcell Technologies) as described earlier [129]. Mixed lymphocyte reactions (MLRs) were applied in the following combinations: maternal T cell responders vs irradiated cord blood cells, cord blood T cell responders vs irradiated maternal cells, maternal T cell responders vs irradiated neonatal cells and neonatal T cell responders vs irradiated maternal cells. For the setup of neonatal MLRs, all corresponding maternal cells had undergone prior cryopreservation and were thawed as described above. In selected maternal, cord blood and neonatal samples (n = 6 each), the T cell enriched suspensions were split between non-CD25-depleted and CD25-depleted samples. Suspensions that were retained for CD25-depletion were depleted using CD25 MicroBeads with magnetic MACS microcolumn separation (Miltenyi Biotec, Bergisch Gladbach, Germany).

To trace proliferation of responder T cells in the assay, 1 uL of CellTrace Violet dye (Invitrogen) was added per 10^6 cells and incubated at 37 °C for 20 minutes. 2 x 10^5 irradiated stimulator mononuclear cells were added at a 2:1 ratio to each responder sample of 1 x 10^5 in a 96-well round-bottom plate in enriched media. Each sample was run in duplicate. Positive

control samples were established with the addition of 5 uL of CD3/CD28 activator Dynabeads (Thermo Fisher Scientific, Waltham, MA, USA) instead of stimulator cells. Negative controls were established in enriched media only. To each sample and positive control, 10 U of IL-2 cytokine was added. Samples were incubated for 5 days. At day 3, 150 uL of media per well was replaced with fresh media. Each sample was harvested and washed with PBS (Sigma Aldrich). Surface staining was performed in MACS buffer using APC-Cy7-conjugated CD3, BV510-conjugated CD4 and PerCP-Cy5.5-conjugated CD8 (all from Biolegend). Samples were washed and then re-suspended. 1 uL of propidium iodide (Biolegend) was added for live/dead discrimination to each sample immediately before flow cytometry was performed on an LSRII flow cytometer equipped with blue, red and violet lasers (BD Biosciences). At least 20,000 cells were recorded per sample. Unstained and single-stained samples were used as compensation controls in flow cytometry experiments. All antibodies and dyes were used in concentrations recommended by the relevant manufacturer.

During the gating process, doublets were first excluded based on FSC-A and FSC-H characteristics. Lymphocytes were then identified based on FSC-A and SSC-A characteristics. Dead cells were excluded based on positivity in the ECD channel. Further gating was performed within CD3+ cells (**Figure 3**). Flow cytometry data was analysed using the FlowJo software package.

4.3.5. Cytokine production

MLRs were applied in the combinations as described above. On day 5, supernatants from each well (100 uL) of selected samples (n = 13) were collected and frozen. The concentration of cytokines in each supernatant sample was analysed in batches after thawing using a custom designed Luminex plate as per the manufacturer's instructions (Bio-Techne, Minneapolis, MI, USA). The concentration of IFN-γ, IL-4, IL-6, IL-8, IL-10, IL-17 and TNF-α were analysed

using a Bio-Plex 200 plate reader and the Bio-Plex Manager 6.1 software (Bio-Rad, Hercules, CA, USA).

4.3.6. Stool DNA extraction, amplification and sequencing

4.3.6.1. Neonatal stool collection

Whole nappies were removed by the parents and placed into a transport bag. Samples were then taken from the nappies by a gloved study personnel using a sterile scoop and then placed into sterile glass containers. Stool samples were frozen immediately and stored at -20 °C until DNA extraction.

4.3.6.2. DNA extraction

DNA was extracted from thawed stool samples using the QIAamp Fast DNA Stool Mini Kit (Qiagen, Hilden, Germany). For all extractions 290-310 mg of stool was transferred into Lysing Matrix E 2mL tubes (MP Biomedicals, Illkirch-Graffenstaden, France). Tubes without stool were used as negative controls for each batch of samples. Samples underwent 4 cycles of bead beating for 30 seconds using the FastPrep-24 5G Instrument (MP Biomedicals). The suspensions were heated to 95 °C for 5 minutes and then centrifuged (2 minutes, 12000 rpm). The remaining extraction steps were performed according to the manufacturer's instructions. DNA was eluted using 100 uL of elution buffer and samples were centrifuged for 2 minutes to elute the DNA. DNA yield was assessed using the Qubit dsDNA HS Assay kit with a Qubit 2.0 fluorometer (Invitrogen). Extracted DNA was stored at -80 °C until amplified.

4.3.6.3. Amplification of bacterial DNA

16S rRNA genes were amplified with primers targeting the V4 region using the standardized Earth Microbiome 16S Illumina Amplicon protocol [130]. Samples were processed in batches with appropriate negative controls to ensure there were no contaminants arising from the DNA extraction kits as described earlier [131]. Following clean up, the amplicon fragment lengths were assessed for quality using Tapestation (Agilent, Santa Clara, CA, USA). DNA was quantified for each amplicon using the Qubit dsDNA HS Assay kit with a Qubit 4.0 fluorometer (Invitrogen). Each DNA library was normalized to a DNA concentration of 4 nM and then pooled to contain 5 uL DNA from each sample. The quality of the pooled DNA sample was assessed on Tapestation and demonstrated an average base pair length of 401 bp. Using the Qubit method described above, the pooled DNA was quantified to an average 1.61 ng/uL.

4.3.6.4. Sequencing and identification of bacterial DNA

The pool of stool DNA was sequenced in one sequencing run. Sequences were obtained using an Illumina MiSeq paired-end 250-bp protocol for 500 cycles. The PCR was performed in one batch with appropriate negative controls following which paired-end sequencing (2×250bp) was performed on the Illumina MiSeq platform (Illumina, San Diego, CA, US) and processed using the Quantitative Insights Into Microbial Ecology 2 (QIIME2) pipeline [132]. Samples were rarefied prior to alpha and beta diversity analysis. Taxonomy assignment was done against the Silva-132-99% OTUs database and differences in relative abundance of taxa between cohorts were analysed using linear discriminant analysis (LDA) effect size (LEfSe). Taxa with LDA > 2 at a p value < 0.05 were considered significant.

4.3.7. Univariate statistical modelling

4.3.7.1. Statistical analysis

Comparisons were made using the Kruskal-Wallis test or the Mann-Whitney U test as the distribution of data appeared to be non-normal according to the Shapiro-Wilk test. p values < 0.05 were considered significant. Data are presented as median (interquartile range). Statistics were calculated using the GraphPad Prism 5 and 8 software.

4.3.7.2. Random Forest machine learning method

We used Random Forest (RF) for data integration and individual data set analysis. RF is a machine learning ensemble method in conjunction with multiple learning algorithms to obtain better predictive performance [133]. RF can be used for both classification and regression. In our analysis we used RF for classification using the feeding method (exclusively breastfed vs exclusively formula-fed) as outcome variable and treating each of the data sets separately. We used ntree = 500 and mtry = square root of variables in our models. We used two packages for RF analysis (randomForest and varSelRF) in R (v3.6.1).

4.3.7.3. The Backward elimination method

To select features automatically we iteratively fitted random forests, at each iteration building a new forest after discarding 20% of the features with the smallest variable importance. The selected set of features was used as a predictor to fit the model to check the "out of bag" (OOB) error rate. We examined the OOB error rates from all fitted random forests. We chose the solution with the smallest number of variables whose error rate was within one standard error. This procedure was performed iteratively using the varSelRF package in R (v3.6.1).

4.3.7.4. Network analysis

We used the qgraph package in R (v3.6.1) to perform network analysis. A network is a set of nodes and a set of edges, where each node represents either an immune parameter or an operational taxonomic unit (OTU) from microbiome analysis whereas the edges represent associations amongst them. Pearson correlation coefficients were used to quantify the strength of associations between combinations of immune parameters or OTUs.

4.4. The impact of phosphodiesterase inhibitors on T cells

4.4.1. Sample collection

Peripheral blood samples were taken from 10 healthy adults (5 women and 5 men; age: 26.5 (25.25-29.5) years, median (interquartile range)) and cord blood samples from 6 healthy, term neonates (3 girls and 3 boys; gestational age: 39.5 (38.25-40) weeks, median (interquartile range); birth weight: 3675 (3310-3890) grams, median (interquartile range)). Healthy adults and women in labour abstained from the consumption of PDE inhibitors for a minimum of 72 h before sampling. Informed consent was obtained from all subjects or, in the case of neonates, parents of subjects, and our study was reviewed and approved by an independent ethical committee of Semmelweis University (TUKEB). The study was adhered to the tenets of the most recent revision of the Declaration of Helsinki.

4.4.2. Peripheral blood mononuclear cell isolation

PBMCs and cord blood mononuclear cells (CBMCs) were separated by a standard density gradient centrifugation (Ficoll Paque, Amersham Biosciences AB, Uppsala, Sweden, 25 min, 400 g, 22 °C) from freshly drawn blood collected in lithium heparin-treated tubes (BD

Vacutainer, BD Biosciences, San Jose, CA, USA). Cells were distributed for the following experiments.

4.4.3. Kinetic measurements

Cells were incubated for 24 h at 37 °C in 5% CO_2 in a modified RPMI-1640 medium, ie. the calcium concentration of this medium was set to 2 mM by the addition of crystalline $CaCl_2$. Clinically relevant concentrations of caffeine (50 uM) milrinone (30 uM) or sildenafil (30 uM) were applied for 24 h prior to fluorescent staining, respectively, or 100 uM of a synthetic cAMP analogue, dbcAMP was applied for 60 min or 10 uM of ZM241385, a specific inhibitor of the A2A AR was applied for 75 min prior to fluorescent staining, respectively. Untreated cells were used as controls. Mononuclear cells were then incubated with anti-CD4 PE-Cy7 mAbs (BioLegend, San Diego, CA, USA) according to the manufacturer's instructions. Cytoplasmic free calcium and reactive oxygen species (ROS) levels were detected by loading the cells with Fluo-4 AM and dihydroethidium (DHE) dyes, respectively for 20 min at 30 °C (both Invitrogen, Carlsbad, CA, USA). Cells were washed once before measurement.

At the beginning of the kinetic measurements, a one min baseline of calcium and ROS levels was recorded. T cell activation was initiated by the addition of phytohemagglutinin (PHA, 15 ug/mL final concentration) to the samples. Fluorescence emission of sequentially measured cells was monitored for 10 min. Average cell acquisition rate was 1000 cells/s. At the end of the kinetic measurements, 5 ug of ionomycin was used as positive control (Sigma-Aldrich, St. Louis, MO, USA). Cells were analysed on a BD FACSAria flow cytometer (BD Biosciences) equipped with 488 nm and 633 nm excitation lasers.

4.4.4. Kinetic data analysis

The population of lymphocytes was gated according to forward and side scatter characteristics. CD4 cells were gated based on mAb positivity. Data acquired from the measurements were evaluated with specific software developed at our laboratory as described earlier (FacsKin, available at: www.facskin.bitbucket.org) [134,135]. The core of this software is an algorithm [136] based on the calculation of logistic functions for each recording. The software also calculates parameter values describing each function, including the End value, representing the maximal cytoplasmic calcium or ROS concentration and the area under the curve (AUC) value, corresponding to the sum cytoplasmic calcium or ROS increase over the measurement period. These two parameters were used for further statistical analysis to describe calcium influx and ROS production of lymphocytes. Gating strategy is demonstrated in **Figure 4**.

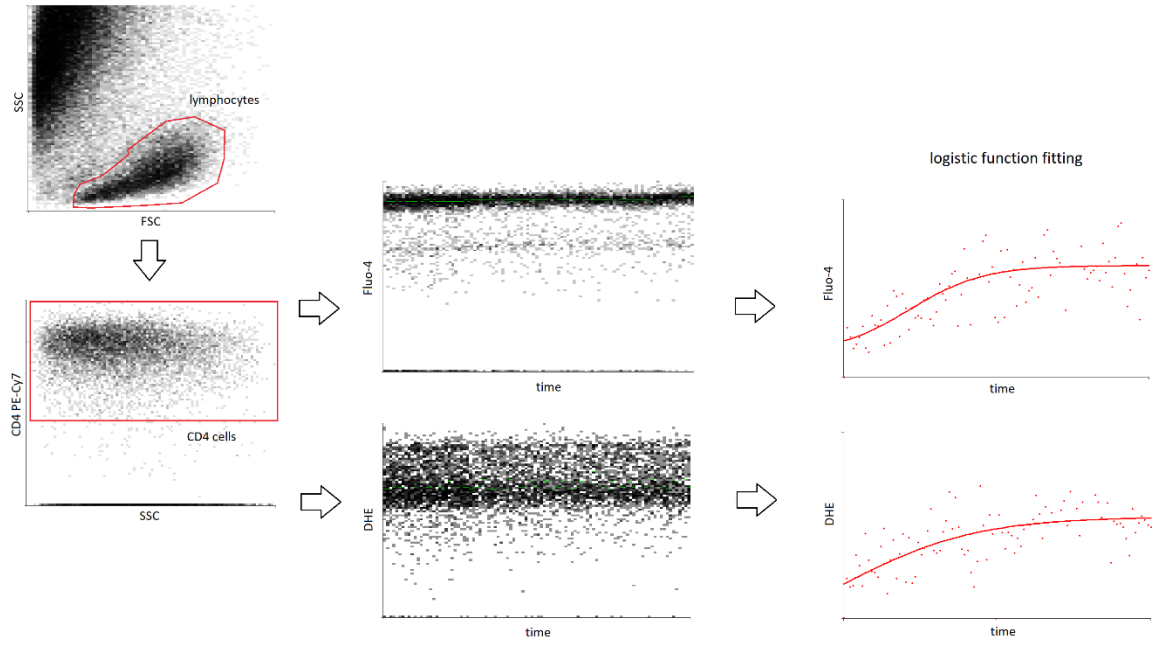

Figure 4. Gating strategy of kinetic flow cytometry measurements demonstrated on a representative sample using the FacsKin software. Following the gating of lymphocytes, the

population of CD4 cells were identified. Logistic functions were fitted to study the kinetics of cytosolic calcium influx (Fluo-4) and reactive oxygen species production (DHE) over a period of 10 minutes. DHE – dihidroethydium, FSC – forward scatter characteristics, SSC – side scatter characteristics

4.4.5. Intracellular cytokines

Cells were incubated for 24 h at 37 °C in 5% CO_2 in a modified RPMI-1640 medium. The calcium concentration of this medium was set to 2 mM by the addition of crystalline CaCl2. 50 uM of caffeine, 30 uM of milrinone or 30 uM of sildenafil was applied for 24 h prior to fluorescent staining, respectively. Untreated cells were used as controls. PMA (50 ng/mL), ionomycin (1 ug/mL) and Brefeldin A (BFA, 10 ug/mL) were added for stimulation 6 h prior to measurement to allow intracellular accumulation of cytokines (all Sigma-Aldrich). For surface marker staining, samples were then incubated with anti-CD4 APC-Cy7 mAb (clone SK3, BioLegend) according to the manufacturer's instructions. Cells were permeabilized using FACS Permeabilizing (2) solution (BD Biosciences). Cells were washed and resuspended in phosphate buffer saline (PBS) and stained according to the manufacturer's instructions for intracellular cytokines using the following conjugated anti-human monoclonal antibodies: IFN-γ PE-Cy7, IL-2 APC, IL-4 PE, IL-6 FITC, IL-17 PerCP, respectively (all from BioLegend). Following labelling, cells were washed and resuspended in PBS for flow cytometry analysis. Samples were analysed immediately on a FACSAria flow cytometer (BD Biosciences) equipped with 488 and 633 nm excitation lasers. 100,000 cells were recorded. The population of lymphocytes was gated from mononuclear cells according to forward and side scatter characteristics. CD4 cells were gated based on mAb positivity. Data acquired from the measurements were evaluated with FlowJo software (version X, Tree Star, Ashland, OR, USA).

4.4.6. CD203c and Nuclear Factor of Activated T cells expression

Cells were incubated for 24 h at 37 °C in 5% CO_2 in a modified RPMI-1640 medium. The calcium concentration of this medium was set to 2 mM by the addition of crystalline CaCl2. For surface marker staining, samples were incubated with the following conjugated anti-human monoclonal antibodies: anti-CD4 PE-Cy7 (clone SK3), anti-CD8 APC-Cy7 (clone SK1), anti-CXCR3 APC, anti-CCR4 PE and anti-CD203c PerCP (all from BioLegend) according to the manufacturer's instructions. Cells were permeabilized using FACS Permeabilizing (2) solution (BD Biosciences). Cells were then washed and resuspended in PBS and stained according to the manufacturer's instructions with anti-NFATc1 Alexa Fluor 488 mAb (BioLegend). Following labelling, cells were washed and resuspended in PBS for flow cytometry analysis. Samples were analysed immediately on a FACSAria flow cytometer (BD Biosciences) equipped with 488 and 633 nm excitation lasers. 100,000 cells were recorded. The population of lymphocytes was gated from mononuclear cells according to forward and side scatter characteristics. Th1 cells were regarded as CD4+ CXCR3+ CCR4-, while Th2 cells were regarded as CD4+ CXCR3- CCR4+. Data acquired from the measurements were evaluated with FlowJo software (version X, Tree Star).

4.4.7. Statistical analysis

Data are expressed as median (interquartile range). Comparisons of the calculated parameters were made with Mann-Whitney, Wilcoxon and Friedman tests as Kolmogorov-Smirnoff analysis indicated non-normal distribution of data. Statistics were calculated at 5% significance level ($p = 0.05$) using the GraphPad Prism 5 software (La Jolla, CA, USA).

4.5. Perinatal asphyxia and neonatal arterial ischaemic stroke

4.5.1. Sample collection

We enrolled 33 term neonates admitted to the regional neonatal intensive care unit at the First Department of Pediatrics at Semmelweis University, Budapest, Hungary with the initial diagnosis of perinatal asphyxia requiring therapeutic hypothermia. The diagnosis of moderate-to-severe hypoxic-ischemic encephalopathy and the eligibility for cooling were assessed according to the TOBY criteria [77,137]. Infants fulfilled both criteria A (Apgar score ≤ 5 at 10 minutes after birth OR continued need for resuscitation, including endotracheal or mask ventilation, at 10 minutes after birth OR umbilical cord, arterial or capillary pH < 7.00 within 60 minutes of birth OR base deficit ≥ 16 mmol/L in umbilical cord or any blood sample (arterial, venous or capillary) within 60 minutes of birth) AND criteria B (clinical seizures OR altered state of consciousness (reduced response to stimulation or absent response to stimulation) AND abnormal tone (focal or general hypotonia, or flaccid) AND abnormal primitive reflexes (weak or absent suck or Moro response)). All enrolled neonates were outborn and hypothermia was initiated between 1-5 h of life (mostly within 2 h of life as hypothermia was started before and maintained during transport). Rectal temperature was maintained between 33-34 °C and was recorded every hour during the 72 h intervention period. 2 ml venous blood samples were collected between 3-6 h of life (at admission), as well as at 24 h, 72 h and 1 week of life during intensive care treatment, adjusted to blood sampling related to clinical care. A further venous blood sample was obtained at 1 mo of age during a routine outpatient follow-up appointment.

Neonates with congenital abnormalities or CNS malformations, maternal chorioamnionitis or perinatal infections were excluded from the study. Blood cultures and ear swabs were obtained at admission from all infants and bacterial infection was excluded. Clinical or culture-proven

sepsis was not detected in any of the participating infants. All infants received regular preventive intravenous antibiotics, i.e. ampicillin and gentamicin during the hypothermic treatment. One infant was excluded due to suspected metabolic disease (peroxisomal fatty acid C26/C22 ratio above the normal range) as well as the presence of multiple minor anomalies and mutation of the ROBO1 gene.

The data of four infants were analysed and published separately as their MRI scan results showed signs of neonatal stroke rather than hypoxic-ischemic insult. Therefore, in our publication on neonatal asphyxia, data from a total of 28 neonates were analysed. These neonates were divided into two groups based on the severity of hypoxic-ischemic insult, determined by initial and recovery time of amplitude-integrated EEG (aEEG) monitoring [138] as well as MRI results performed up to 12 days of life. MRI data were interpreted by radiologists who were blinded to the clinical status of the neonates, based on criteria defined by Rutherford et al. [139]. The reporting template was developed in the ISORT (intelligent structured online reporting tool) software framework created by Bioscreen Ltd., Debrecen, Hungary. In cases where MRI was not performed due to the critical condition of the patient or MRI data were missing, grouping was done solely based on the aEEG results. The severe group (n = 11) consisted of newborns with moderate-to-severe HIE signs on MRI scans AND burst-suppression or continuous extremely low voltage or flat tracing background activity on aEEG OR normalization of aEEG after 48th hour of life or never, OR early death (< 28 days). Neonates that met none of the above listed criteria constituted the moderate group (n = 17) (normal MRI scans or mild HIE signs on MRI scans AND continuous or discontinuous normal voltage background activity on aEEG OR normalization of aEEG activity before 48th hour of life).

In the severe group, 3 infants deceased before one month of age due to severity of the insult. Available data from these neonates were included at the relevant time points within the severe

group. Therefore, 72 h, 1 week and 1 month data were missing in case of 2 infants and 1 month data were missing from 1 infant.

Our study was reviewed and approved by the Hungarian Medical Research Council and written informed consent was obtained from parents of all participants. The study was adhered to the tenets of the most recent revision of the Declaration of Helsinki. Clinical characteristics and laboratory parameters of participants are summarized in **Table 2**.

	Moderate HIE (n = 17)	**Severe HIE** (n = 11)	**NAIS** (n = 4)
Male gender (%)	10 (59%)	7 (64%)	2 (50%)
Birthweight (g)	3330 (2860-3605)	3000 (2490-3300)	3115 (2540-3885)
Gestational age (week)	39 (37-40)	38 (37-40)	39.5 (38.25-40)
No. of C-sections (%)	10 (59%)	8 (73%)	3 (75%)
Apgar at 1 min	3 (0.5-4.5)	1 (0-3)	4[b] (3-5)
Apgar at 5 min	6 (5-7)	2[a] (0-4)	5.5[b] (5-6)
Apgar at 10 min	7 (5-8)	4[a] (1.75-5.25)	7[b] (6-7)
Worst pH	7.03 (6.87-7.12)	6.86 (6.62-7.06)	6.94 (6.88-7.00)
Worst BD (mmol/L)	18.05 (16.65-21.28)	20.4 (19.38-23.5)	14[b] (14-17)
S100 (ug/L)	7.5 (2.33-28.85)	21.8 (3.8-30.0)	3.6[b] (1.88-18.35)
LDH (U/L)	2072 (1371-5274)	3335 (1879-5792)	1874 (1676-3187)

Table 2. Clinical characteristics of neonates in the moderate and severe HIE and NAIS groups upon admission (within 12 h of age). Data are presented as median and interquartile range; a = moderate vs severe HIE, $p < 0.05$; b = severe HIE vs NAIS, $p < 0.05$.

4.5.2. Flow cytometry

Plasma was separated from peripheral blood samples by centrifugation. Plasma samples were aliquotted and immediately frozen and stored at -80 °C for later determination of cytokine concentrations and HPLC measurements.

Flow cytometry experiments and analysis were performed in line with European Federation of Immunological Societies guidelines [140]. Remaining cells were resuspended in RPMI-1640 medium (Sigma-Aldrich, St. Louis, MO, USA). Cells were incubated with PMA (50 ng/ml), ionomycin (1 ug/ml) and BFA (10 ug/ml) for 6 h at 37 °C to allow intracellular accumulation of cytokines. For surface marker staining, samples were then incubated with the following fluorochrome-conjugated anti-human mAbs: CD4 PE-Cy7 and CD8 APC-Cy7 (panel 1), or CD4 APC-Cy7 and CD49d PerCP (panel 2), respectively, according to the manufacturer's instructions (all from BioLegend, San Diego, CA, USA). Red blood cells were lysed and PBMCs were permeabilized using FACS Lysing and FACS Permeabilizing solutions (BD Biosciences, San Jose, CA, USA). Cells were washed and resuspended in PBS and divided into two equal aliquots and stained according to the manufacturers' instructions for intracellular cytokines using the following conjugated anti-human monoclonal antibodies or the appropriate isotype controls: IL-6 PE, IL-17A PerCP, IL-10 APC, IFN-γ FITC (for panel 1), or TNF-α PE-Cy7, FoxP3 PE, TGF-β APC, IL-1β FITC (for panel 2), respectively (all from BioLegend). Following labelling, cells were washed and resuspended in PBS for flow cytometry analysis. Samples were analysed immediately on a FACSAria flow cytometer (BD Biosciences) equipped with 488 and 633 nm excitation lasers. Data were processed using the FACSDiVa software (BD Biosciences). 100,000 cells were recorded. Evaluators of flow cytometry data were blinded to the clinical status of the neonates.

4.5.3. Immunoassays

Plasma samples were stored at -80 °C until analysis. The plasma levels of the following cytokines, chemokines and growth factors were determined using Bio-Plex Pro Assays (Bio-Rad Laboratories, Hercules, CA, USA): IL-1b, IL-2, IL-4, IL-5, IL-6, IL-7, IL-8, IL-10, IL-12, IL-13, IL-17, IFN-γ, TNF-α, TGF-β, granulocyte colony stimulating factor (G-CSF), granulocyte-macrophage colony-stimulating factor (GM-CSF), MCP-1, macrophage inflammatory protein 1b (MIP-1b) and VCAM-1. Bio-Plex Pro Assays are immunoassays formatted on magnetic beads that utilize principles similar to those of a sandwich ELISA. Capture antibodies against the biomarker of interest are covalently coupled to the beads. A biotinylated detection antibody creates the sandwich complex and the final detection complex is formed by the addition of a streptavidin-phycoerythrin conjugate, where PE serves as the fluorescent reporter. Reactions are read using a Luminex-based reader.

4.5.4. High-performance liquid chromatography

Plasma samples were stored at -80 °C until analysis. Samples were processed and measured as described in **Section 4.1.5.** of this thesis.

4.5.5. Statistical analysis

Data are expressed as median and interquartile range. Comparisons between sample populations were performed with Mann-Whitney tests, as a test of normality (performed according to Kolmogorov-Smirnoff) indicated non-normal distribution of data. Comparisons between the paired values (samples collected at different time points) in the same population were made with Friedman tests. p values less than 0.05 were considered significant. Outliers were identified using Grubbs' tests and were excluded from analyses. Statistics were calculated using the GraphPad Prism 5 software (La Jolla, CA, USA).

5. RESULTS

5.1. B7 costimulation in the neonate

5.1.1. The expression of B7 costimulatory molecules and their receptors

A statistically significant, but biologically modest decrease in the frequency of CD4+ CD28+ lymphocytes was observed in UCB in comparison with APB. At the same time, a more considerable increase was noticed in the expression of the regulatory receptor CD152 (CTLA-4) on these cells. The frequency of CD11b+ CD86+ monocytes was higher in UCB than in APB.

The prevalence of CD3+ CD278+ lymphocytes was also higher in UCB than in APB, however, this difference was not significant in the CD4+ subset. The frequency of the corresponding costimulatory molecule, CD275 on CD11b+ monocytes was comparable in the two groups. In contrast, that of CD11b+ CD274+ monocytes, providing inhibitory signal via CD279, was lower in UCB compared to APB.

5.1.2. Intracellular indoleamine dioxygenase expression and plasma indoleamine dioxygenase activity

A tendency was observed for an increased prevalence of IDO-expressing cells among CD3+ lymphocytes in UCB compared to ABP ($p = 0.069$), while their frequency in the CD11b+ subset was comparable. The mean fluorescence intensity (MFI) values for IDO were lower in UCB than in APB both in case of CD3+ lymphocytes and CD11b+ monocytes.

Plasma KYN and TRP levels were higher in UCB than in APB, with a more pronounced increase in KYN, resulting in a more than two-fold higher K/T ratio in UCB compared to APB. KYNA levels were also considerably, almost ten-fold higher in UCB (**Table 3**).

In order to explore the presence of reverse signalling via CD80 and CD86, correlation analyses were performed. A negative correlation between the frequency of CD11b+ CD86+ monocytes and IDO-expressing CD11b+ monocytes was found in UCB (Spearman's Rho = -0.59), while no correlation was present in APB. Furthermore, a positive correlation was detected between MFI of IDO in CD3+ cells and the prevalence of CD11b+ CD80+ monocytes in APB (Spearman's Rho = 0.48).

	APB (n=20)	**UCB** (n=17)
CD3+ CD28+ cells/ CD3+ lymphocytes	77.2 (65.8-82.5) %	80.7 (71.2-88.4) %
CD3+ CD28+ CD152+ cells/ CD3+ CD28+ lymphocytes	8.74 (6.46-11.7) %	12.0 (6.09-15.8) %
CD3+ CD278+ cells/ CD3+ lymphocytes	56.4 (50.4-74.9) %	73.6* (67.9-77.7) %
CD3+ CD279+ cells/ CD3+ lymphocytes	51.2 (45.3-61.2) %	52.7 (28.0-61.6) %
CD4+ CD28+ cells/ CD4+ lymphocytes	97.9 (96.8-99.1) %	95.4* (93.1-98.3) %
CD4+ CD28+ CD152+ cells/ CD4+ CD28+ lymphocytes	6.15 (4.55-8.57) %	9.21* (6.53-13.1) %
CD4+ CD278+ cells/ CD4+ lymphocytes	59.2 (54.8-74.0) %	69.4 (59.3-79.2) %
CD4+ CD279+ cells/ CD4+ lymphocytes	54.2 (49.1-63.3) %	54.5 (42.5-57.3) %
CD11b+ cells/ monocytes	80.4 (75.0-87.3) %	81.0 (73.2-86.1) %
CD11b+ CD80+ cells/ CD11b+ monocytes	54.2 (19.6-68.8) %	34.0 (19.7-56.7) %
CD11b+ CD86+ cells/ CD11b+ monocytes	27.6 (19.6-29.8) %	43.1* (30.0-51.9) %
Continued on next page		

	APB (n=20)	**UCB** (n=17)
CD11b+ CD274+ cells/ CD11b+ monocytes	74.1 (68.2-84.9) %	57.2* (51.5-72.7) %
CD11b+ CD275+ cells/ CD11b+ monocytes	61.2 (34.5-70.0) %	46.6 (39.1-57.9) %
CD3+ IDO+ cells/ CD3+ lymphocytes	3.33 (2.12-5.95) %	4.57 (3.00-10.8) %
IDO MFI in CD3+ IDO+ cells (arbitrary unit)	9888 (7461-11175)	7627* (6551-9768)
CD11b+ IDO+ cells/ CD11b+ monocytes	2.45 (1.92-2.99) %	2.90 (1.65-4.52) %
IDO MFI in CD11b+ IDO+ cells (arbitrary unit)	21400 (19075-24175)	15200* (13300-18700)
KYN (uM)	1.80 (1.63-2.26)	4.77* (3.73-5.45)
KYNA (nM)	29.8 (22.9-42.8)	294.7* (253.8-360.6)
TRP (uM)	53.4 (46.3-59.6)	62.4* (56.6-70.4)
K/T ratio	0.036 (0.032-0.041)	0.075* (0.063-0.086)

Table 3. Frequency of the investigated cell surface and intracellular markers and plasma levels of kynurenine (KYN), kynurenic acid (KYNA) and tryptophan (TRP) in adult peripheral blood (APB) versus umbilical cord blood (UCB). * $p < 0.05$ versus APB. Data are presented as median (interquartile range). IDO – indoleamine 2,3-dioxygenase, MFI – mean fluorescence intensity.

5.2. B7 costimulation in healthy pregnancy and preeclampsia

5.2.1. The expression of B7 costimulatory molecules and their receptors

A significant increase in the prevalence of CD28+ T cells was observed in HP compared to NP women. At the same time a decrease was shown in the expression of CD152 on these cells.

	Non-pregnant women (n=14)	Healthy pregnant women (n=20)
CD3+ CD28+ cells/CD3+ lymphocytes	76.0 (64.7-82.9) %	88.4* (81.8-90.6) %
CD3+ CD28+ CD152+ cells/CD3+ CD28+ lymphocytes	8.90 (7.57-11.4) %	6.64* (5.07-9.89) %
CD3+ CD278+ cells/CD3+ lymphocytes	55.7 (49.5-56.7) %	89.9* (75.7-91.6) %
CD3+ CD279+ cells/CD3+ lymphocytes	46.3 (39.3-51.2) %	51.9* (47.9-67.7) %
CD4+ CD28+ cells/CD4+ lymphocytes	97.8 (96.7-98.8) %	97.3 (93.0-99.2) %
CD4+ CD28+ CD152+ cells/CD4+ CD28+ lymphocytes	6.92 (4.93-8.63) %	5.61 (3.65-9.09) %
CD4+ CD278+ cells/CD4+ lymphocytes	56.7 (52.8-59.5) %	87.7* (76.3-92.2) %
CD4+ CD279+ cells/CD4+ lymphocytes	49.4 (42.1-54.5) %	44.2 (37.5-65.2) %
CD11b+ CD80+ cells/CD11b+ monocytes	55.5 (17.3-69.8) %	17.6* (13.6-25.4) %
CD11b+ CD86+ cells/CD11b+ monocytes	23.8 (17.3-29.5) %	20.7 (14.9-31.9) %
CD11b+ CD274+ cells/CD11b+ monocytes	78.4 (70.3-85.9) %	80.7 (77.2-87.8) %
CD11b+ CD275+ cells/CD11b+ monocytes	63.8 (59.0-72.1) %	17.3* (14.1-27.0) %
CD3+ IDO+ cells/CD3+ lymphocytes	5.90 (2.65-16.9) %	24.1* (13.3-56.4) %
IDO mean fluorescence intensity in CD3+ IDO+ cells (arbitrary unit)	9888 (7482-11475)	62500* (19800-84475)
CD11b+ IDO+ cells/CD11b+ monocytes	2.59 (1.99-11.7) %	22.5* (13.6-50.5) %
IDO mean fluorescence intensity in CD11b+ IDO+ cells (arbitrary unit)	21400 (19075-23875)	70450* (38775-114000)

Table 4. Frequency of the investigated cell surface and intracellular markers in non-pregnant versus healthy pregnant women. * $p < 0.05$ versus non-pregnant women. Data are presented as median (interquartile range). IDO – indoleamine-2,3-dioxygenase, MFI – mean fluorescence intensity

The prevalence of both CD278+ and CD279+ T cells was higher in HP than in NP women. Within the CD4 subset, the ratio of CD28+, CD28+ CD152+ and CD279+ cells was comparable in HP and NP women, while that of CD278+ cells was higher in HP than in NP individuals. The frequency of both CD80+ and CD275+ monocytes was lower in HP women, however, no difference was observed regarding CD86+ and CD274+ monocytes (**Table 4**).

The frequency of CD11b expressing (activated) monocytes was higher in PE samples than in HP. The frequency of CD80 and CD86 expressing activated monocytes was lower in PE than in HP. No difference was observed in the expression of the other investigated cell surface markers between the two groups (**Table 5**).

5.2.2. Intracellular indoleamine dioxygenase expression

The prevalence of IDO-expressing T cells and monocytes was higher in HP compared to NP women. At the same time, the mean fluorescence intensity (MFI) values for IDO were also significantly higher in both cell subsets in HP (**Table 4**).

In order to explore whether reverse signalling via CD80 and CD86 is present in monocytes, correlation analyses were performed. However, we could not detect a correlation between the frequency of CD80+ or CD86+ monocytes and the frequency of IDO-expressing T cells or monocytes or the MFI of IDO in the investigated study groups.

The frequency of IDO expressing T lymphocytes was lower in PE than in HP. The mean fluorescence intensity (MFI) of IDO was also lower in T cells of PE patients compared to HP (**Table 5**).

	Healthy pregnant women (n=20)	Preeclamptic patients (n=20)
CD3+ CD28+ cells/CD3+ lymphocytes	88.4 (81.8-90.6) %	90.3 (84.8-91.1) %
CD3+ CD28+ CD152+ cells/CD3+ CD28+ lymphocytes	6.64 (5.07-9.89) %	5.15 (4.07-9.25) %
CD3+ CD278+ cells/CD3+ lymphocytes	89.9 (75.7-91.6) %	91.3 (86.5-92.9) %
CD3+ CD279+ cells/CD3+ lymphocytes	51.9 (47.9-67.7) %	55.1 (48.6-77.2) %
CD4+ CD28+ cells/CD4+ lymphocytes	97.3 (93.0-99.2) %	97.9 (93.0-99.0) %
CD4+ CD28+ CD152+ cells/CD4+ CD28+ lymphocytes	5.61 (3.65-9.09) %	5.45 (3.17-13.6) %
CD4+ CD278+ cells/CD4+ lymphocytes	87.7 (76.3-92.2) %	90.9 (77.3-92.4) %
CD4+ CD279+ cells/CD4+ lymphocytes	44.2 (37.5-65.2) %	49.7 (45.3-75.6) %
CD11b+ cells/monocytes	77.4 (73.3-81.6) %	84.1* (77.6-88.9) %
CD11b+ CD80+ cells/CD11b+ monocytes	17.6 (13.6-25.4) %	12.1* (8.82-16.3) %
CD11b+ CD86+ cells/CD11b+ monocytes	20.7 (14.9-31.9) %	15.7* (12.1-20.5) %
CD11b+ CD274+ cells/CD11b+ monocytes	80.7 (77.2-87.8) %	82.3 (78.0-87.3) %
CD11b+ CD275+ cells/CD11b+ monocytes	17.3 (14.1-27.0) %	13.4 (10.2-30.3) %
CD3+ IDO+ cells/CD3+ lymphocytes	24.1 (13.3-56.4) %	12.9* (6.63-28.1) %
IDO mean fluorescence intensity in CD3+ IDO+ cells (arbitrary unit)	62500 (19800-84475)	33150* (21000-44500)
CD11b+ IDO+ cells/CD11b+ monocytes	22.5 (13.6-50.5) %	23.7 (12.3-45.7) %
IDO mean fluorescence intensity in CD11b+ IDO+ cells (arbitrary unit)	70450 (38775-114000)	54850 (36050-86875)

Table 5. Frequency of the investigated cell surface and intracellular markers. * $p < 0.05$ versus normal pregnant women. Data are presented as median (interquartile range). IDO – indoleamine-2,3-dioxygenase

Correlation analysis revealed a positive correlation between the expression of CD86 on the cell surface and that of IDO intracellularly within activated monocytes in the investigated groups ($p = 0.021$, $r = 0.36$) (**Figure 5**). Intracellular IDO expression was not in correlation with any other investigated cell surface markers in activated monocytes or T cells.

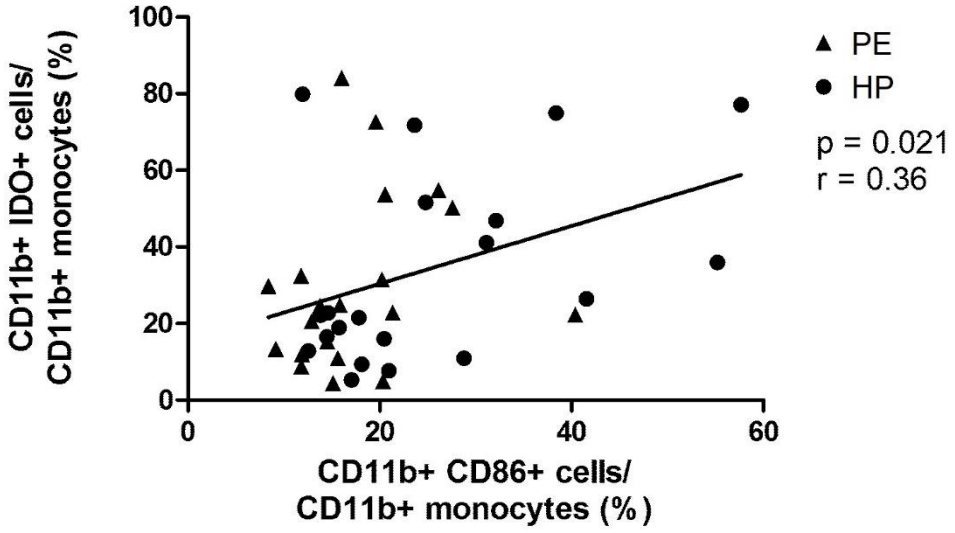

Figure 5. Correlation between the expression of cell surface CD86 and intracellular indoleamine dioxygenase (IDO) in CD11b+ monocytes in peripheral blood of healthy pregnant (HP) and preeclamptic (PE) women

5.3. Regulatory T cell subsets in preeclampsia

Within CD4+ T cells, the prevalence of CD4+ CD25hi FoxP3+ regulatory T cells was lower in women with PE than in HP women (4.63 (4.22-5.56) % vs. 3.69 (3.32-4.09) %, $p = 0.0003$). In PE, the prevalence of CD45RA- effector regulatory T cells among CD4+ cells was also decreased (2.44 (1.02-6.78) % vs. 0.87 (0.45-1.22) %, $p = 0.0098$), while that of CD45RA+ naive regulatory T cells did not differ between the two groups. However, when investigating

the prevalence of naive Tregs within the Treg subset, an increase in PE was detected (57.3 (30.9-77.8) % vs. 75.2 (46.0-87.9) %, p = 0.0014).

The percentage of activated CD4+ T cells was higher in women with PE than in the control group (2.56 (0.55-7.02) % vs. 4.30 (1.78-7.85) %, p = 0.0456).

Within the regulatory T cells, the prevalence of CD279+ exhausted Tregs was higher in women with PE than in HP women (8.08 (4.16-13.5) % vs. 18.2 (9.27-36.3) %, p = 0.0223).

The prevalence of other regulatory T cell subtypes (Helios+ effector Tregs, Helios+ naive Tregs, thymic Tregs, extrathymic Tregs) did not differ between the two groups (**Figure 6**).

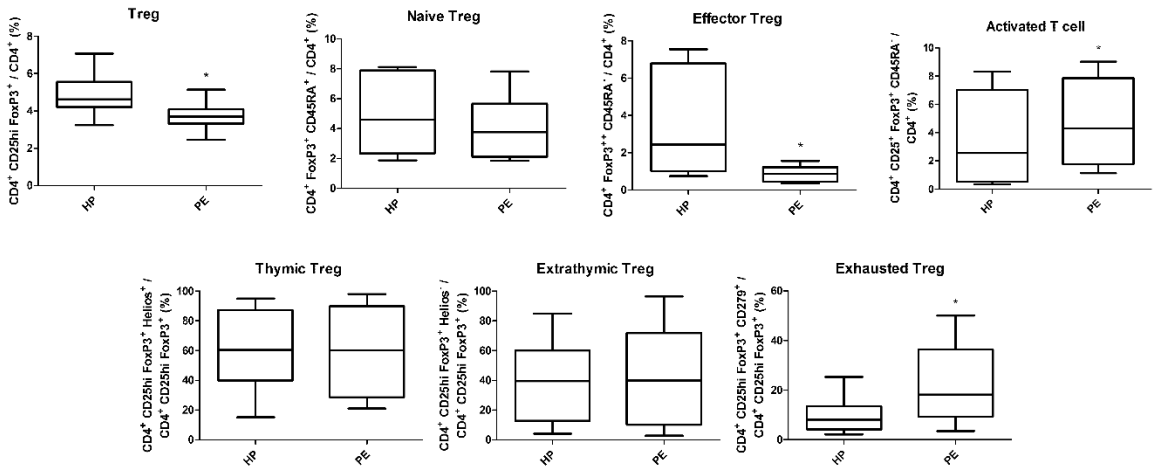

Figure 6. Box-plots representing the frequency of the investigated regulatory T cell subsets in healthy pregnancy (HP) and preeclampsia (PE). Horizontal line: median; Box: interquartile range (25-75 percentile); Whisker: range. * p < 0.05 versus HP

5.4. Breastfeeding and immune development

5.4.1. Neonates develop both protective and tolerogenic adaptive immune responses in the first three weeks of life

The proportion of CD3+ cells was lower in cord blood compared to maternal blood, while that of CD4+ cells was nearly two-fold higher. CD8+ cell percentages both at birth and at 3 weeks of age were nearly half of those seen in maternal and non-pregnant adult samples (**Figure 7A**). The proportion of CD4+ FoxP3+ CD25hi Tregs increased from 6.4% in cord blood to 8.0% within the first 3 weeks of life, comparable to the level in non-pregnant adults but remained lower than third trimester maternal samples (**Figure 7B**).

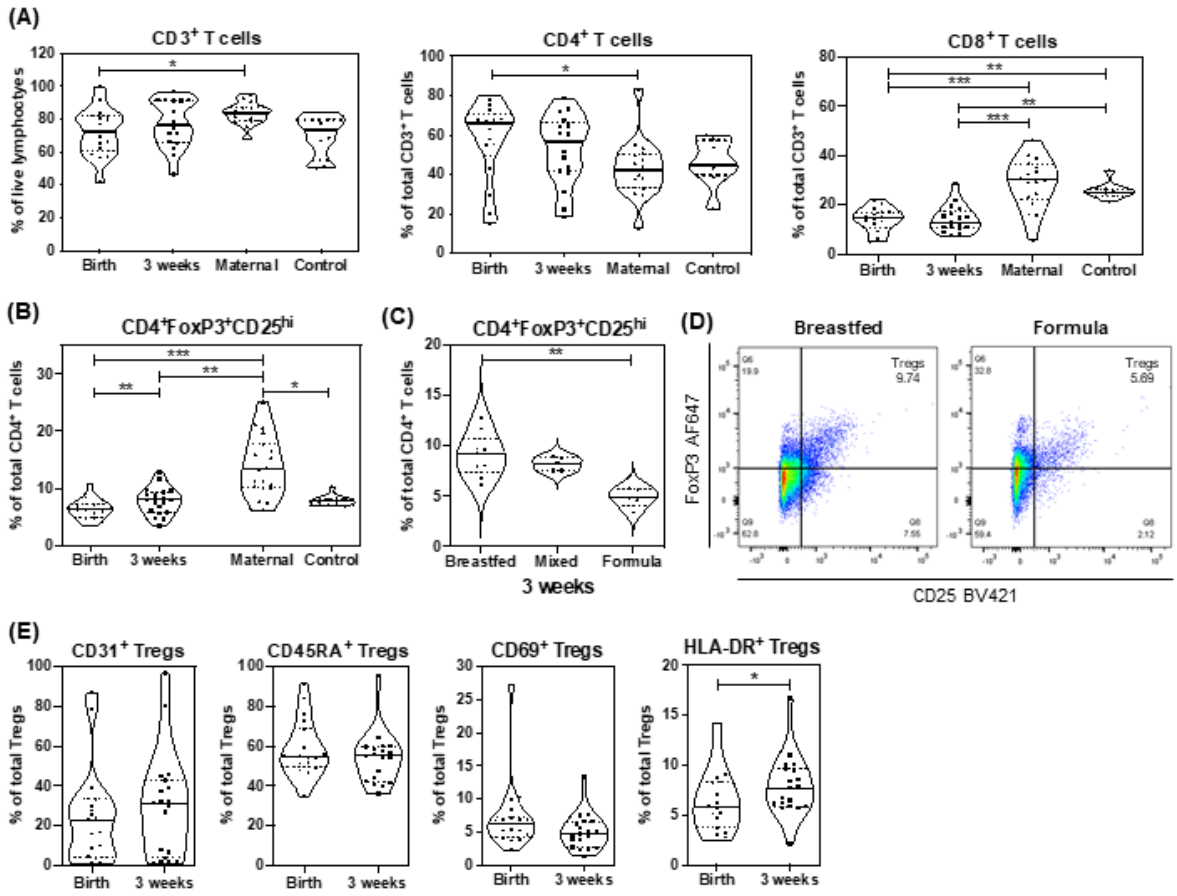

Figure 7. Alterations of T cell subsets and the regulatory T cell (Treg) phenotype in neonates between birth and 3 weeks of age. **A,** The frequency of CD3+, CD4+ and CD8+ cells in neonatal blood samples (n = 17) at birth and at 3 weeks of age, as well as in maternal blood (n = 17) and healthy controls (n = 8). **B,** The frequency of CD4+ FoxP3+ CD25hi cells in neonatal blood samples (n = 19) at birth and at 3 weeks of age, as well as in maternal blood (n = 19) and healthy controls (n = 13). **C,** The frequency of CD4+ FoxP3+ CD25hi cells in neonatal blood samples at 3 weeks of age grouped according to the feeding method: exclusively breastfed (n = 9), mixed feeding (n = 5) and formula-fed (n = 5) neonates. **D,** Representative dot-plots of CD4+ FoxP3+ CD25hi cells in a breastfed and a formula fed neonate at 3 weeks of age, gated within CD4+ cells. **E,** The expression of selected cell surface markers on Tregs in neonatal blood samples at birth and at 3 weeks of age (n = 19). Horizontal lines represent medians and interquartile ranges. * $p < 0.05$, ** $p < 0.01$, *** $p < 0.001$

Interestingly, within the different feeding groups at 3 weeks of age, the frequency of Tregs was nearly two-fold higher (9.3% vs 4.9%) in exclusively breastfed compared to exclusively formula-fed neonates (**Figure 7C&D**). We also examined the expression of selected cell surface markers on Treg cells at birth and at 3 weeks of age. HLA-DR expression increased during the first 3 weeks of life, potentially reflecting recent activation, however, no difference was detected in the expression of CD45RA, CD31 or CD69 between the two time points (**Figure 7E**). Of note, no difference was observed in the expression of these markers between the different feeding groups.

We then went on to determine the functional activity of T cells through analysis of intracellular cytokine and surface CD107a expression, a marker of degranulation in response to mitogenic stimulation. The proportion of IL-8+ CD4+ cells was lower, whereas that of IFN-γ+ CD4+ cells was higher in maternal compared to neonatal samples (**Figure 8**). No differences were

observed in the profile of IFN-γ, IL-4, IL-6 or IL-8 expression by CD4+ and CD8+ cells between birth and 3 weeks of age.

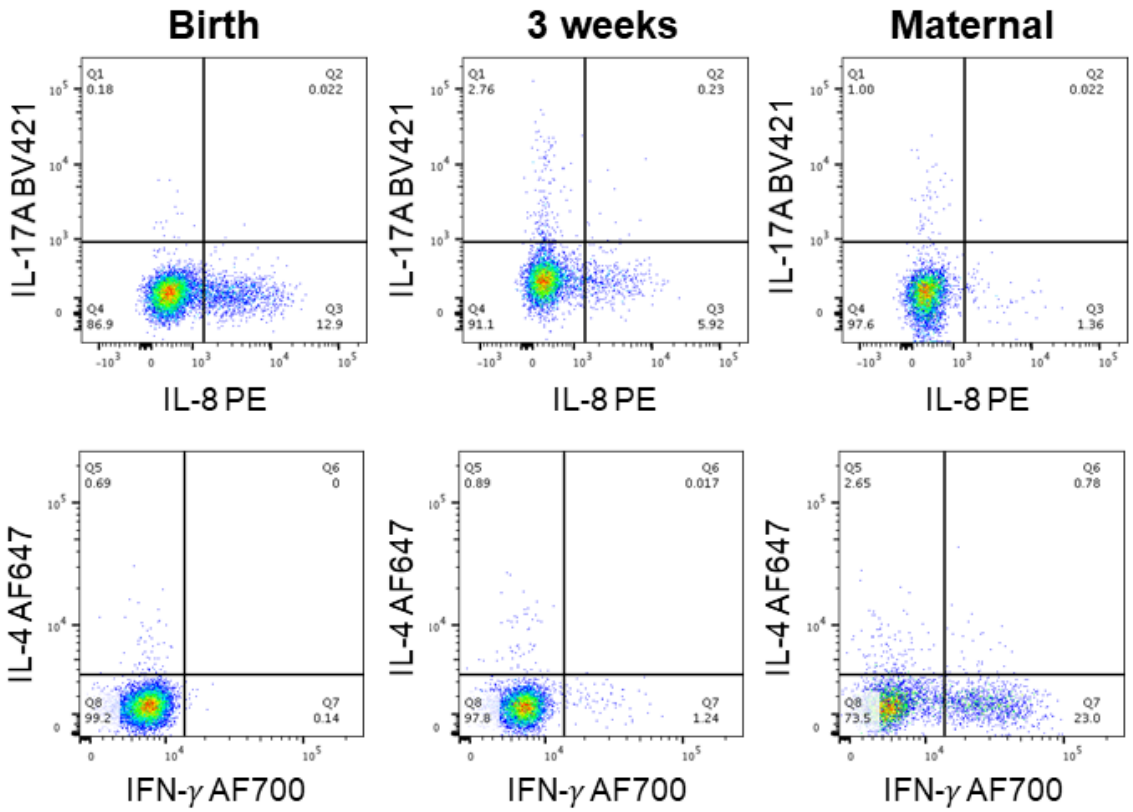

Figure 8. Representative dot-plots of intracellular cytokine markers following mitogenic stimulation in a neonatal blood sample at birth and at 3 weeks of age as well as in a maternal blood sample. Intracellular cytokines were gated within CD4+ cells.

However, the number of IL-17+ CD8+ cells, as well as the mean fluorescence intensity of IL-17 in CD4+ and CD8+ cells, increased during the first three weeks **(Figure 9**). Interestingly, at 3 weeks of age the mean fluorescence intensity of IFN-γ in CD4+ and CD8+ cells was nearly three times higher in exclusively formula-fed neonates compared to those receiving breastmilk (**Figure 10A**). No further differences were observed between feeding groups.

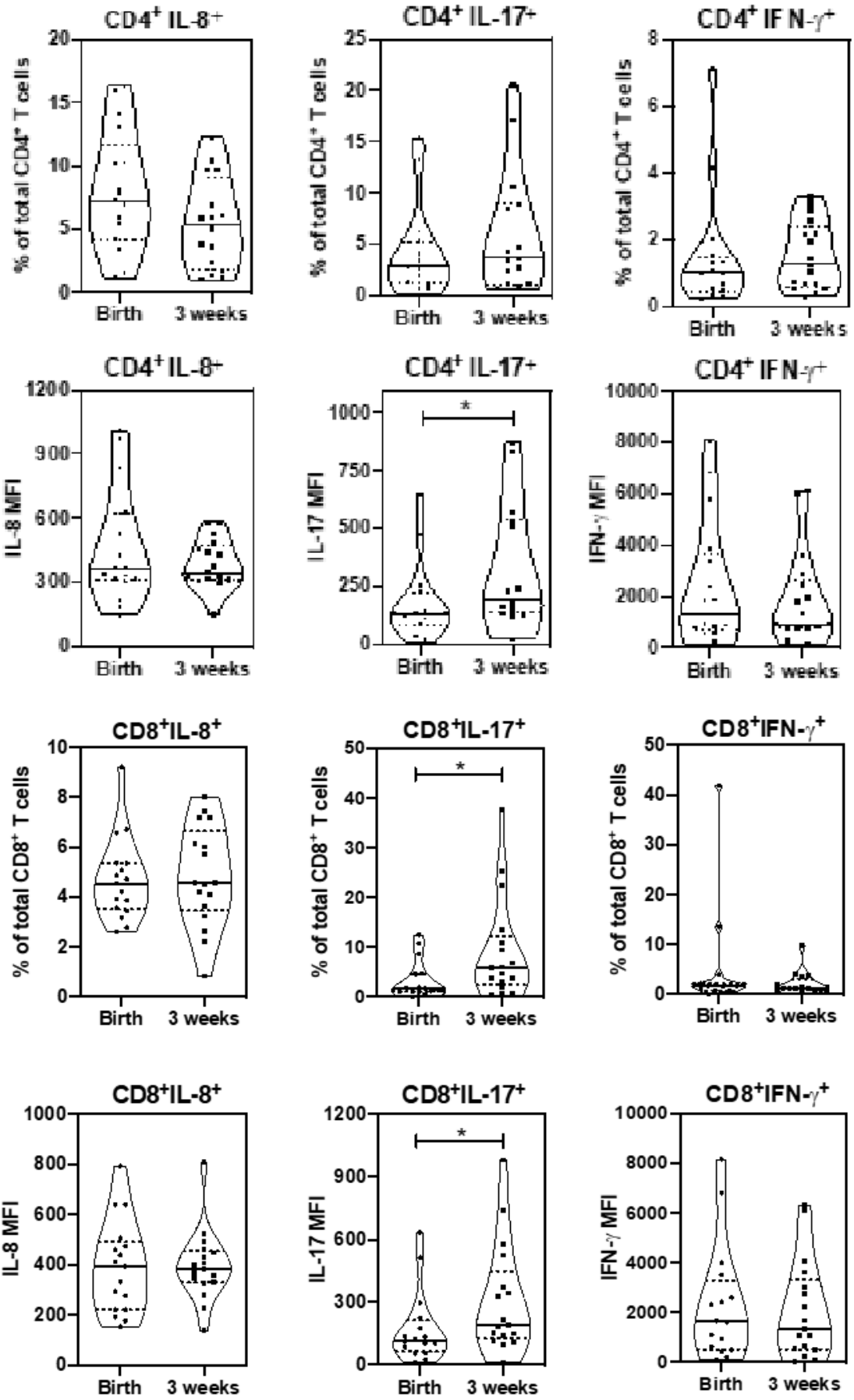
CD4+ IL-8+
% of total CD4+ T cells
CD4+ IL-17+
% of total CD4+ T cells
CD4+ IFN-γ+
% of total CD4+ T cells
CD4+ IL-8+
IL-8 MFI
CD4+ IL-17+
IL-17 MFI
*
CD4+ IFN-γ+
IFN-γ MFI
CD8+IL-8+
% of total CD8+ T cells
CD8+IL-17+
% of total CD8+ T cells
*
CD8+IFN-γ+
% of total CD8+ T cells
CD8+IL-8+
IL-8 MFI
CD8+IL-17+
IL-17 MFI
*
CD8+IFN-γ+
IFN-γ MFI
Birth
3 weeks

Figure 9. The intracellular frequency and mean fluorescence intensity (MFI) of selected pro-inflammatory cytokines in CD4+ and CD8+ cells in neonatal blood samples at birth and at 3 weeks of age (n = 17). Horizontal lines represent medians and interquartile ranges. * $p < 0.05$

A higher proportion of CD8+ cells expressed CD107a, a marker of cytotoxic degranulation, in non-pregnant adult samples compared to neonatal samples at birth and 3 weeks of age. The mean fluorescence intensity of CD107a expression on CD8+ cells was higher in adult compared to neonatal samples (**Figure 10B&C**). No differences were observed between feeding groups.

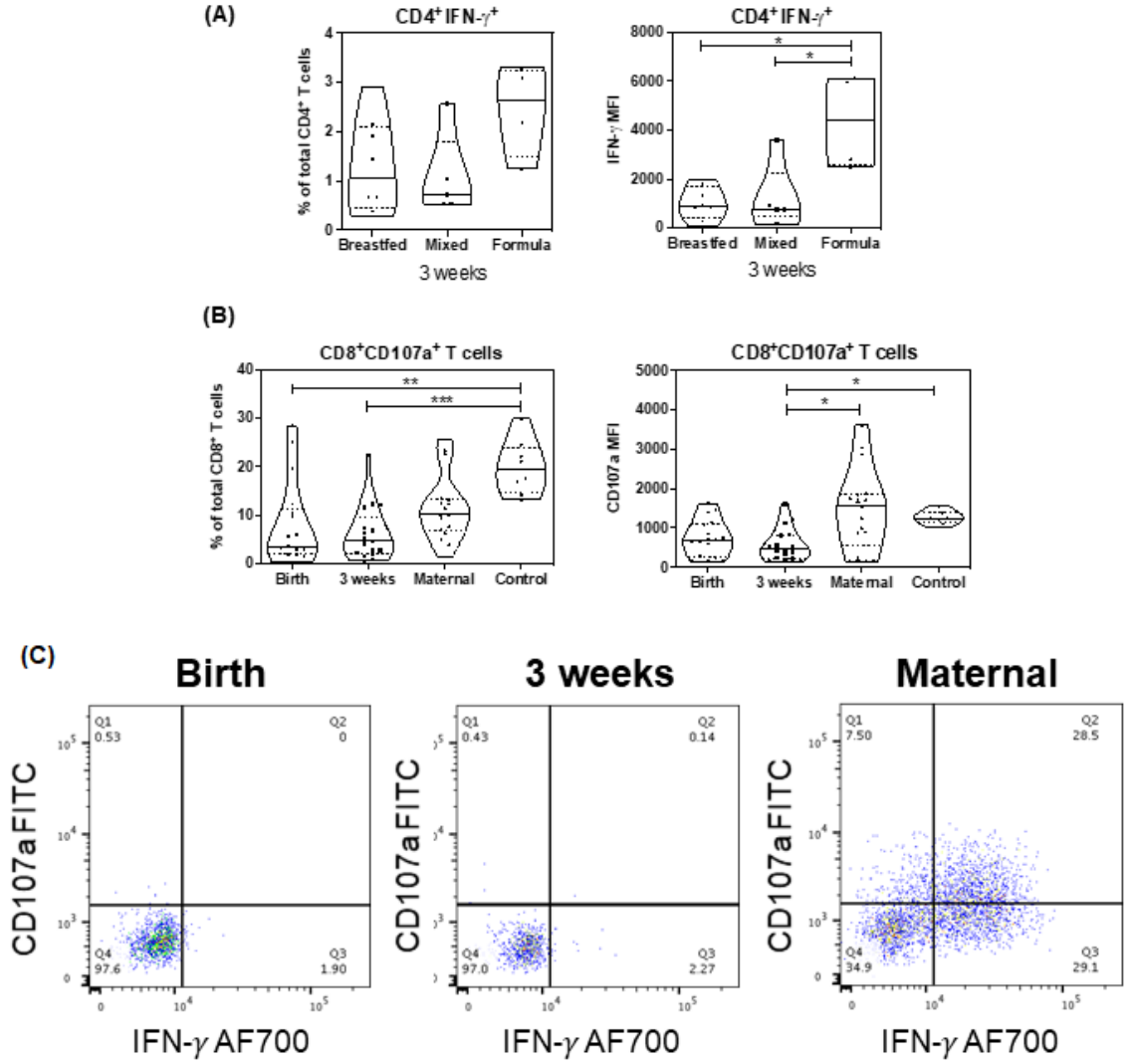

Figure 10. Alterations of the pro-inflammatory and cytotoxic immunophenotype in neonates between birth and 3 weeks of age. **A,** The intracellular frequency and MFI of interferon gamma (IFN-γ) in CD4+ cells in neonatal blood samples at 3 weeks of age grouped according to the feeding method: exclusively breastfed (n = 8), mixed feeding (n = 5) and formula-fed (n = 4) neonates. **B,** The frequency of CD8+ and CD8+ CD107a+ cells and MFI of CD107a in CD8+ cells in neonatal blood samples (n = 17) at birth and at 3 weeks of age, as well as in maternal blood samples (n = 17) and healthy controls (n = 8). Horizontal lines represent medians and interquartile ranges. * $p < 0.05$, ** $p < 0.01$, *** $p < 0.001$. **C,** Representative dot-plots of intracellular cytokine and cell surface cytotoxic markers following mitogenic stimulation in a neonatal blood sample at birth and at 3 weeks of age as well as in a maternal blood sample. Cell surface expression of CD107a, a marker of cytotoxic degranulation and the intracellular expression of IFN-γ are shown within CD8+ cells.

5.4.2. T cells of exclusively breastfed neonates show reduced proliferation in response to stimulation by maternal cells

We performed MLRs on blood samples of 37 mother-and-baby dyads. Initially, maternal cells were stimulated with irradiated cord or neonatal cells and here we observed increased proliferation of CD3+ and CD4+ cells in response to neonatal PBMCs at 3 weeks of age compared to birth (**Figure 11A**). A similar increase (CD3+: 5.4 vs 15.5% median proliferating cells, CD4+: 5.3 vs 18% median proliferating cells) was observed when responder T cells of a non-pregnant healthy adult were used in combination with neonatal stimulator cells (**Figure 11B**).

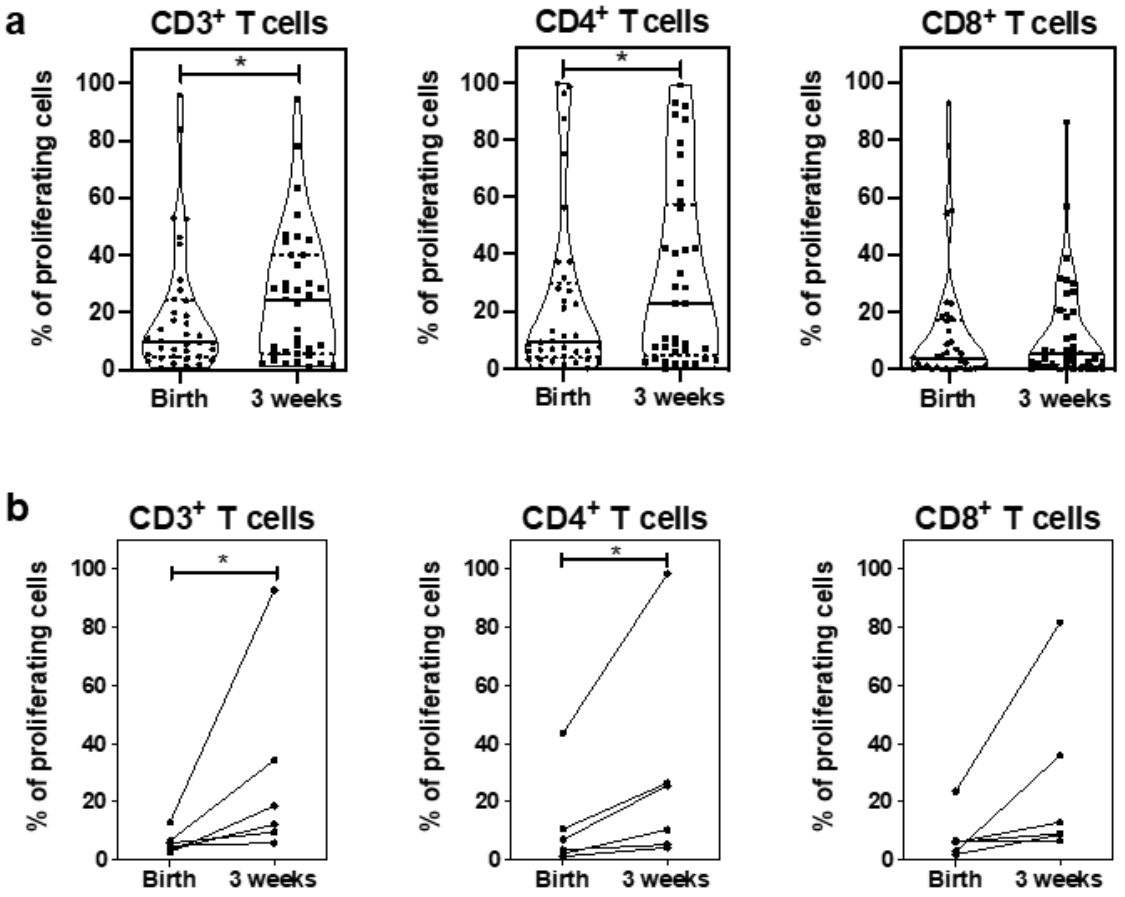

Figure 11. Maternal T cell response upon neonatal antigen stimulation from birth and 3 weeks of age. **A,** Percentage of maternal proliferating T cells (n = 37) in the CD3+, CD4+ and CD8+ cell subsets in response to neonatal irradiated cells. **B,** Percentage of proliferating T cells of a third-party, non-pregnant control individual (n = 6) in the CD3+, CD4+ and CD8+ cell subsets in response to neonatal irradiated cells. Horizontal lines represent medians and interquartile ranges. * $p < 0.05$

We next utilized cord and neonatal T cells in MLRs against irradiated maternal PBMCs (**Figure 12A**). The rate of proliferation on Figure 3a is represented by the proportion of cells with a lower concentration of the CellTrace Violet dye, signifying the dilution of the dye in proliferating cells. Interestingly, here we observed decreased proliferation in neonatal CD3+

and CD8+, but not CD4+ cells in response to maternal stimulator cells at 3 weeks of age compared to birth (**Figure 12B**).

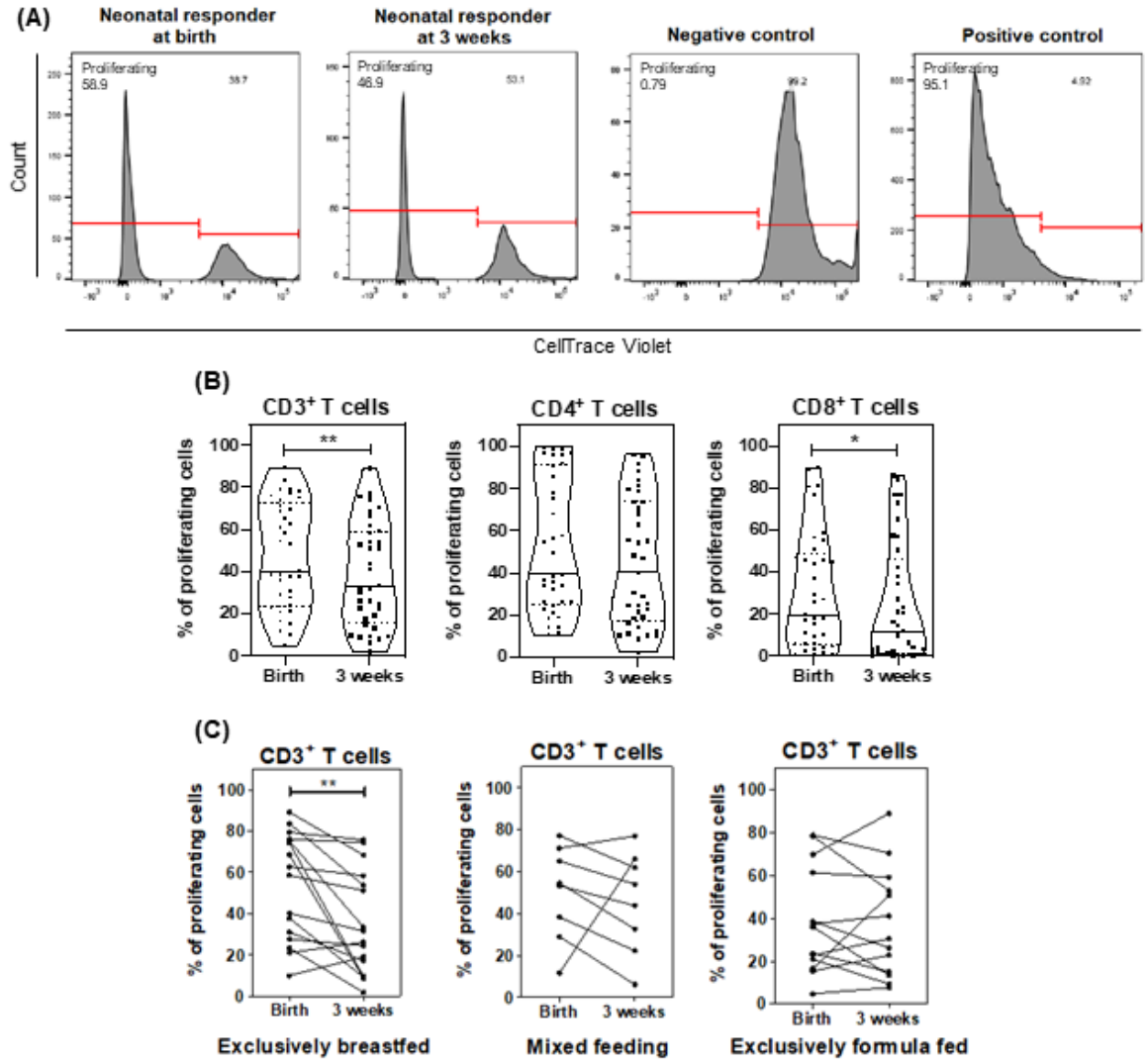

Figure 12. Neonatal T cell response upon maternal antigen stimulation. **A,** Representative sample of a mixed lymphocyte reaction (MLR) at birth and at 3 weeks of age with negative and positive controls. Positive controls were established with the addition of CD3/CD28 activator beads instead of stimulator cells. Negative controls were established in enriched media only. Samples were incubated for 5 days. **B,** Percentage of neonatal proliferating T cells (n = 37) at birth and at 3 weeks of age in response to maternal irradiated cells in the CD3+,

CD4+ and CD8+ cell subsets. **C,** Percentage of neonatal proliferating CD3+ cells at birth and at 3 weeks of age in response to maternal irradiated cells grouped according to the feeding method: exclusively breastfed (n = 16), mixed feeding (n = 8) and formula-fed (n = 13) neonates. Horizontal lines represent medians and interquartile ranges. * $p < 0.05$, ** $p < 0.01$

We further examined the influence of neonatal nutrition on these proliferative responses at 3 weeks of age. Sixteen neonates had been exclusively breastfed whereas 13 had received only formula and 8 had undergone a mixed milk intake. The decrease in the proliferation rate of CD3+ cells was still evident in exclusively breastfed neonates (60.7 vs 28.9% median proliferating cells) but was not present in the mixed feeding and exclusively formula-fed groups (**Figure 12C**). The same pattern was observed in CD4+ and CD8+ cells. Interestingly, the proliferation rate of CD3+, CD4+ and CD8+ cells of exclusively breastfed neonates was comparable at birth and at 3 weeks of age when PBMCs of a non-pregnant healthy adult were used as stimulators (n = 6), reflecting that the neonatal tolerance is specific to maternal antigens.

5.4.3. Neonatal immune tolerance promoted by breastfeeding is mediated by regulatory T cells and is associated with a reduction in release of inflammatory cytokines

Having observed that breastfeeding promotes the expansion of Tregs and suppresses proliferative responses against maternal antigen, we next investigated if this immune tolerance was dependent on the presence of Tregs. To this end, we repeated the MLRs on a set of 6 mother-and-baby dyads where babies were exclusively breastfed following the depletion of CD25+ cells (**Figure 13A**). Pregnancy is associated with peripheral accumulation of Tregs and the proliferation of maternal CD3+ cells in response to neonatal antigens increased both at birth (20.4 vs 59.7% median proliferating cells) and at 3 weeks of age (34.1 vs 57.1% median

proliferating cells) following depletion of CD25+ cells (**Figure 13B**). The same pattern was observed for CD4+ but not in CD8+ cells. Of note, the proliferation of neonatal CD3+ cells in response to maternal antigens increased after depletion of CD25+ cells in samples taken at 3 weeks of age (71.4 vs 85.1% median proliferating cells) but this was not seen with the use of cord blood cells (**Figure 13C**). The same pattern was observed for CD4+ but not in CD8+ cells. We also measured the concentration of cytokines in MLR supernatants (n = 11) produced by neonatal T cells of exclusively breastfed neonates in response to maternal antigens. The concentration of IFN-γ and TNF-α was found to be lower at 3 weeks of age compared to birth, whereas no difference was observed in case of the other cytokines tested (IL-4, IL-6, IL-8, IL-10, IL-17). The maximal IFN-γ and TNF-α producing capacity of neonatal T cells, tested by culturing with CD3/CD28 activator beads, was higher both at birth and at 3 weeks of age compared to the level seen in response to maternal antigens at 3 weeks (**Figure 13D**). As such, breastfeeding is seen to suppress the inflammatory Th1 cytokine response of neonatal T cells in response to maternal antigen stimulation.

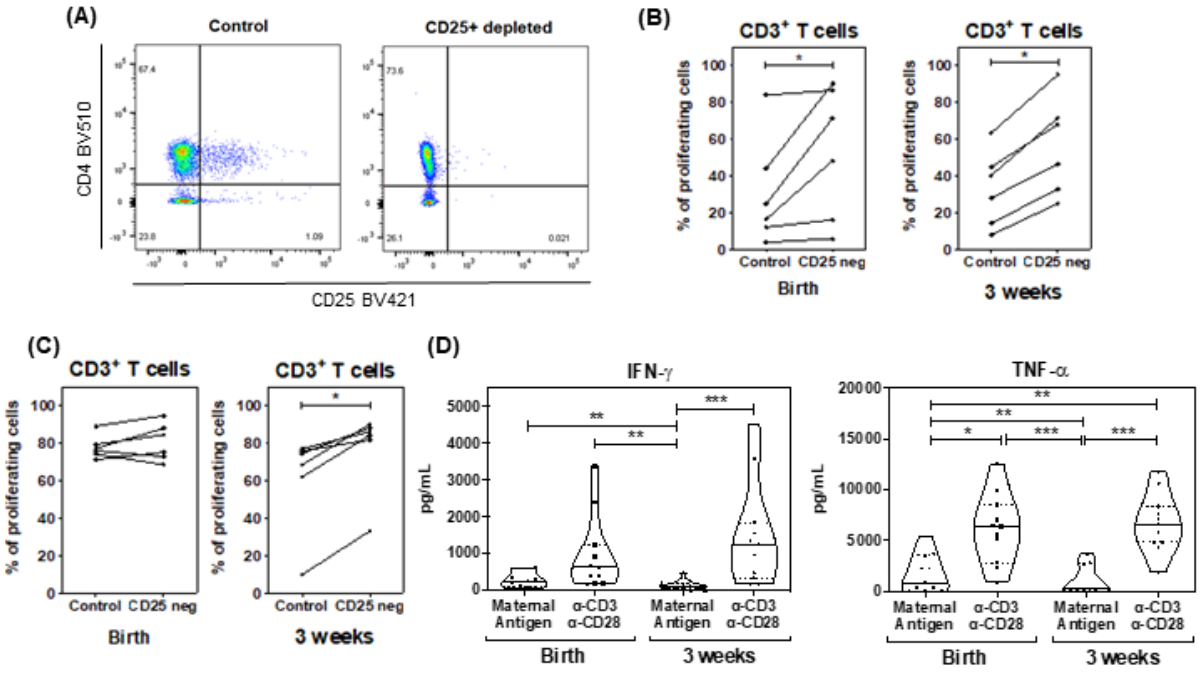

Figure 13. Maternal and neonatal T cell response in mixed lymphocyte reactions (MLR) following the depletion of CD25+ cells and pro-inflammatory cytokine production by neonatal T cells in exclusively breastfed neonates in MLR upon maternal antigen stimulation at birth and at 3 weeks of age. **A,** Representative dot-plots with and without the depletion of CD25+ cells in a neonatal sample at 3 weeks of age, gated within CD3+ cells. CD25+ cells were depleted using magnetic microbead separation. **B,** Percentage of maternal proliferating T cells (n = 6) in response to neonatal stimulator cells of exclusively breastfed neonates from birth and 3 weeks of age in the CD3+ subset. **C,** Percentage of neonatal proliferating T cells (n = 6) in response to maternal stimulator cells at birth and at 3 weeks of age in the CD3+ subset of exclusively breastfed neonates. **D,** The concentration of IFN-γ and TNF-α was found to be lower at 3 weeks of age compared to birth (n = 11). The maximal IFN-γ and TNF-α producing capacity of neonatal T cells was also assessed at birth and at 3 weeks of age by culturing them with CD3/CD28 activator beads. The production of IFN-γ and TNF-α was higher both at birth and at 3 weeks of age compared to the level seen in response to maternal antigens at 3 weeks. Horizontal lines represent medians and interquartile ranges. * $p < 0.05$, ** $p < 0.01$, *** $p < 0.001$

5.4.4. Breastfeeding has modest impact on the gut microbiome in neonates born by caesarean section within the first 3 weeks of life

To evaluate the impact of breastfeeding on the neonatal gut microbiome, we analysed stool samples from exclusively breastfed and exclusively formula-fed neonates collected at 3 weeks of age. Meconium samples had also been collected at birth but the amount of DNA extracted from these samples was consistently < 0.15 ng/uL. PCR amplification using 16S primers on these DNA samples yielded undetectable product for further analysis, reflecting minimal or no microbial colonization immediately after birth.

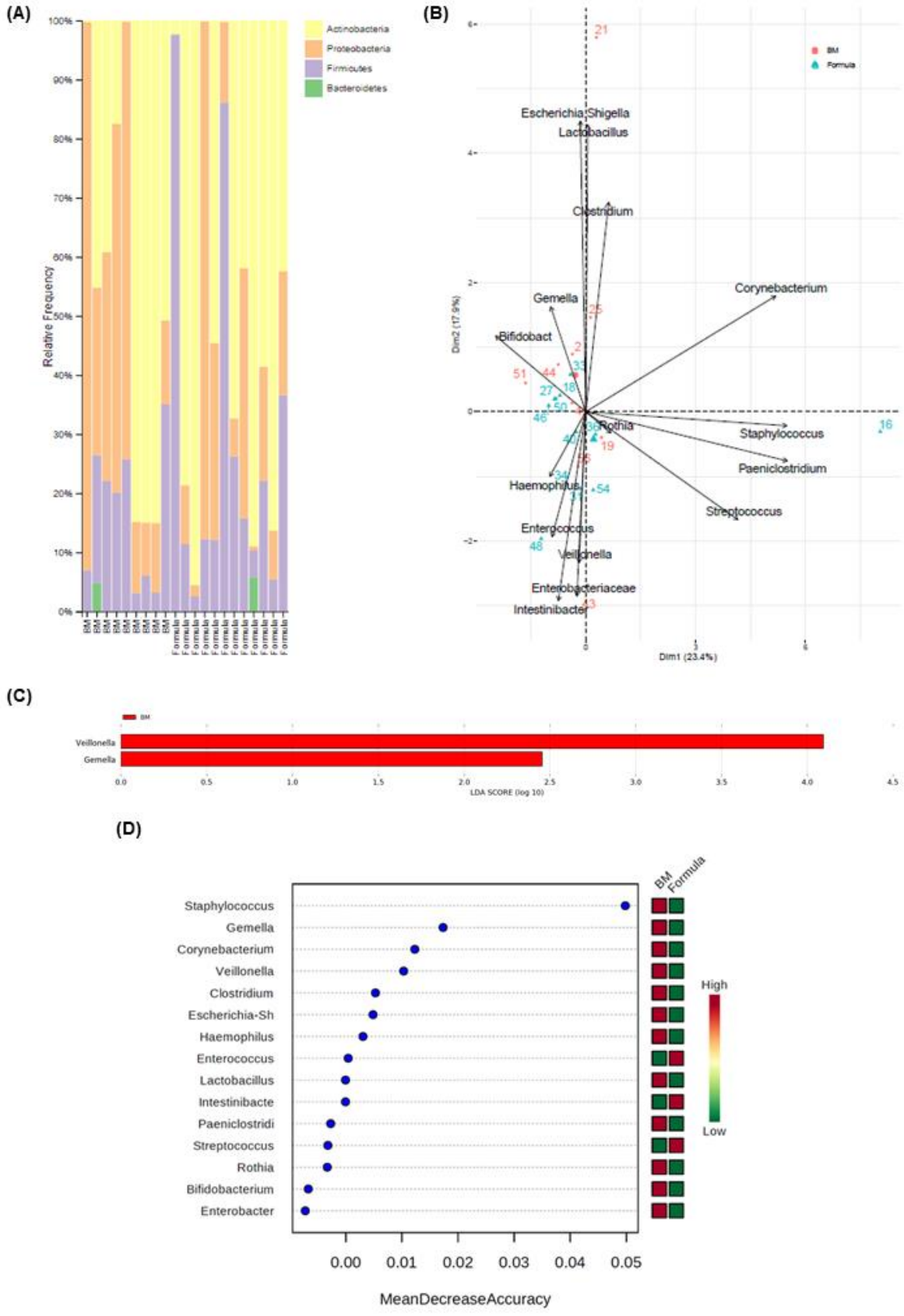
(A)
Actinobacteria
Proteobacteria
Firmicutes
Bacteroidetes
Relative Frequency
(B)
BM
Formula
Escherichia.Shigella
Lactobacillus
Clostridium
Gemella
Corynebacterium
Bifidobact
Rothia
Staphylococcus
Paeniclostridium
Haemophilus
Streptococcus
Enterococcus
Veillonella
Enterobacteriaceae
Intestinibacter
Dim1 (23.4%)
Dim2 (17.9%)
(C)
BM
Veillonella
Gemella
LDA SCORE (log 10)
(D)
Staphylococcus
Gemella
Corynebacterium
Veillonella
Clostridium
Escherichia-Sh
Haemophilus
Enterococcus
Lactobacillus
Intestinibacte
Paeniclostridi
Streptococcus
Rothia
Bifidobacterium
Enterobacter
BM
Formula
High
Low
MeanDecreaseAccuracy

Figure 14. Microbiome analysis of neonatal stool samples at 3 weeks of age in exclusively breastfed (n = 9) and exclusively formula-fed (n = 12) neonates. **A,** Relative frequency of bacterial phyla in the two cohorts. **B,** Principal component analysis (PCA) of gut microbiota composition of exclusively breastfed (red) and exclusively formula-fed (blue) neonates at 3 weeks of age determined by bacterial 16S rRNA amplification. Numbers represent the individual study number of each participant. Pooled variables of milk received are represented by the large red circle for breastmilk and the large blue triangle for formula, respectively. **C,** Association of specific microbial taxa with the feeding method by linear discriminant analysis (LDA) effect size (LEfSe). Red indicates taxa enriched in exclusively breastfed neonates. **D,** Ranking of gut microbial strains using the Random Forest (RF) method in exclusively breastfed (BM) and exclusively formula-fed neonates at 3 weeks of age.

In the stool samples at 3 weeks of age, following microbial 16S rRNA gene amplification, a median frequency of 18,354 amplicon sequence variants (ASV) per sample were retained after trimming and filtering. The composition of gut microbiota from exclusively breastfed and exclusively formula-fed neonates was broadly similar and no differences in any alpha or beta diversity metrics were seen (**Figure 14A**). Principal component analysis (PCA) of gut microbiota composition of exclusively breastfed and exclusively formula-fed neonates demonstrated that individuals in these groups cluster closely together, and breastfeeding is associated with the presence of *Gemella* (**Figure 14B**). Linear discriminant analysis (LDA) effect size (LEfSe) revealed enrichment of the *Veillonella* and *Gemella* taxa in exclusively breastfed neonates (**Figure 14C**). Random Forest (RF) analysis identified the presence of *Staphylococcus*, followed by that of *Gemella* to be the most significant parameters distinguishing the two groups of exclusively breastfed and exclusively formula-fed neonates (**Figure 14D**).

5.4.5. Network modelling links Veillonella to regulatory T cell expansion whilst skin-associated bacteria enhance T cell proliferation in breastfed neonates

Finally, we undertook an integrative analysis of the combined data from flow cytometry, MLR and microbiome sequencing of neonates at 3 weeks of age.

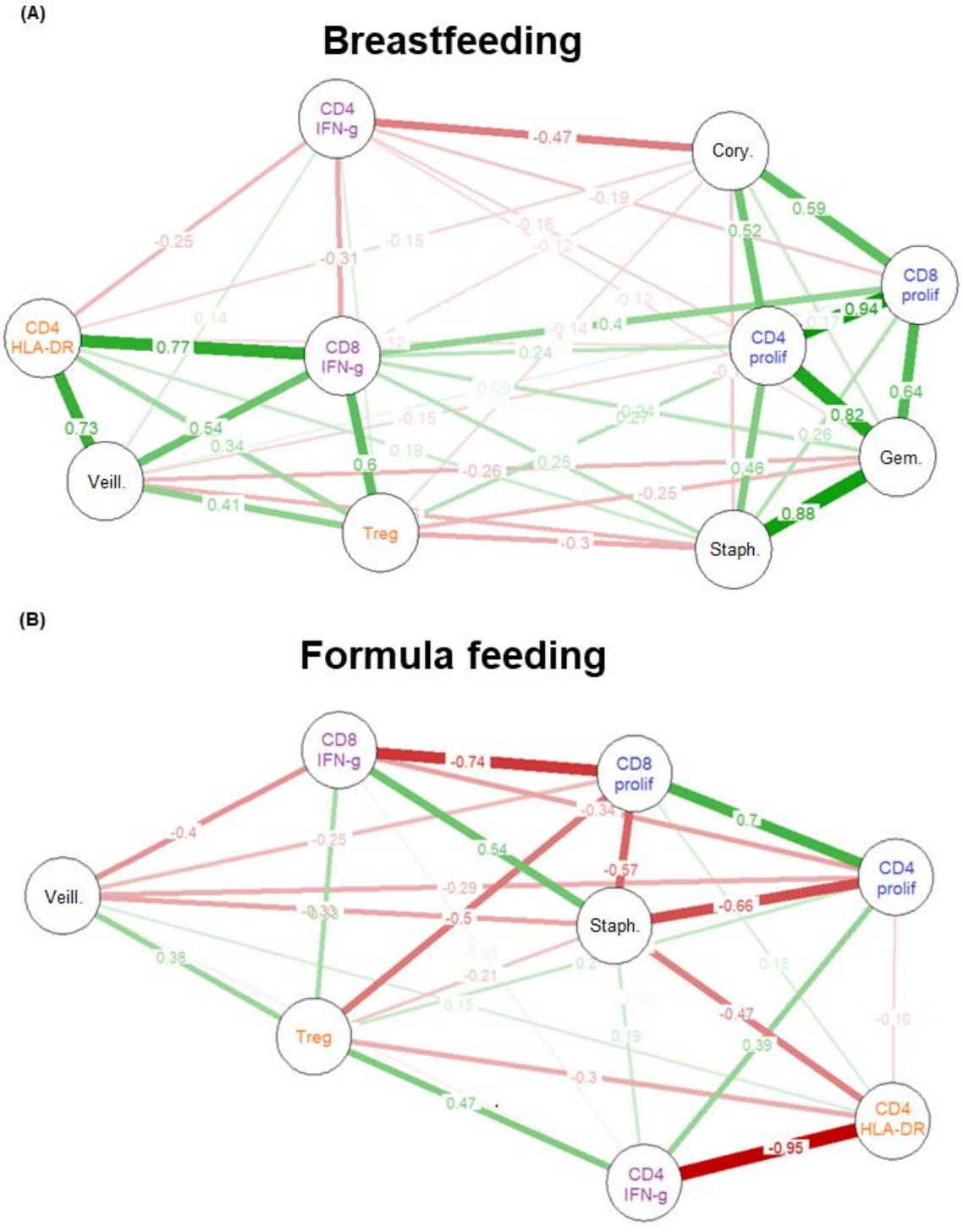

Figure 15. Integrated analysis of mixed lymphocyte reaction (MLR), flow cytometry and microbiome data of **A,** exclusively breastfed (n = 9) and **B,** exclusively formula-fed (n = 5) neonates at 3 weeks of age. Various positive and negative correlations between the studied parameters were revealed. Green represents a positive correlation, whereas red represents a negative correlation. Thicker lines represent stronger correlations. Nodes in blue represent MLR data, nodes in black represent microbiome data, and nodes in purple and orange represent flow cytometry data from the panels with and without mitogenic stimulation, respectively.

Network modelling revealed a range of positive and negative correlations between these parameters. In breastfed neonates CD4+ and CD8+ proliferative responses against maternal antigen were strongly correlated with *Gemella* and skin-associated taxa (**Figure 15A**). The presence of *Veillonella* within the microbiome correlated with the prevalence of Tregs at 3 weeks and this effect was independent of nutrition history (**Figure 15B**). In breastfed neonates *Veillonella* was also associated with HLA-DR expression on CD4+ cells and IFN-γ production in CD8+ cells. These findings suggest that *Veillonella* may act to enhance regulatory responses in the early period of life whereas skin-associated bacteria, potentially acquired through breastfeeding, may act to promote proliferative responses.

5.5. The impact of phosphodiesterase inhibitors on T cells

5.5.1. Kinetic measurements

In order to assess short-term activation of T lymphocytes following activation with PHA, we measured calcium influx using Fluo-4 AM dye and ROS production using DHE in APB and UCB CD4 cells. AUC and End values of Fluo-4 were higher in ZM241385 treated samples compared to untreated, caffeine treated and sildenafil treated samples in APB. AUC values of

Fluo-4 were elevated in caffeine (1.41-fold), dbcAMP (1.3-fold), milrinone (1.22-fold), sildenafil (1.23-fold) and ZM241385 (1.23-fold) treated samples compared to untreated samples in UCB (**Figure 16A**). End value of Fluo-4 was also raised in caffeine (1.61-fold) and dbcAMP (1.34-fold) treated samples, but comparable in milrinone, sildenafil and ZM241385 treated samples compared to untreated samples in UCB (**Figure 16B**). AUC value of Fluo-4 was higher in untreated APB compared to untreated UCB samples (630 (601-744) au vs. 534 (411-645) au, p = 0.045).

AUC and End values of DHE were influenced by treatment of samples with caffeine, dbcAMP, milrinone, sildenafil or ZM241385 neither in APB nor in UCB samples.

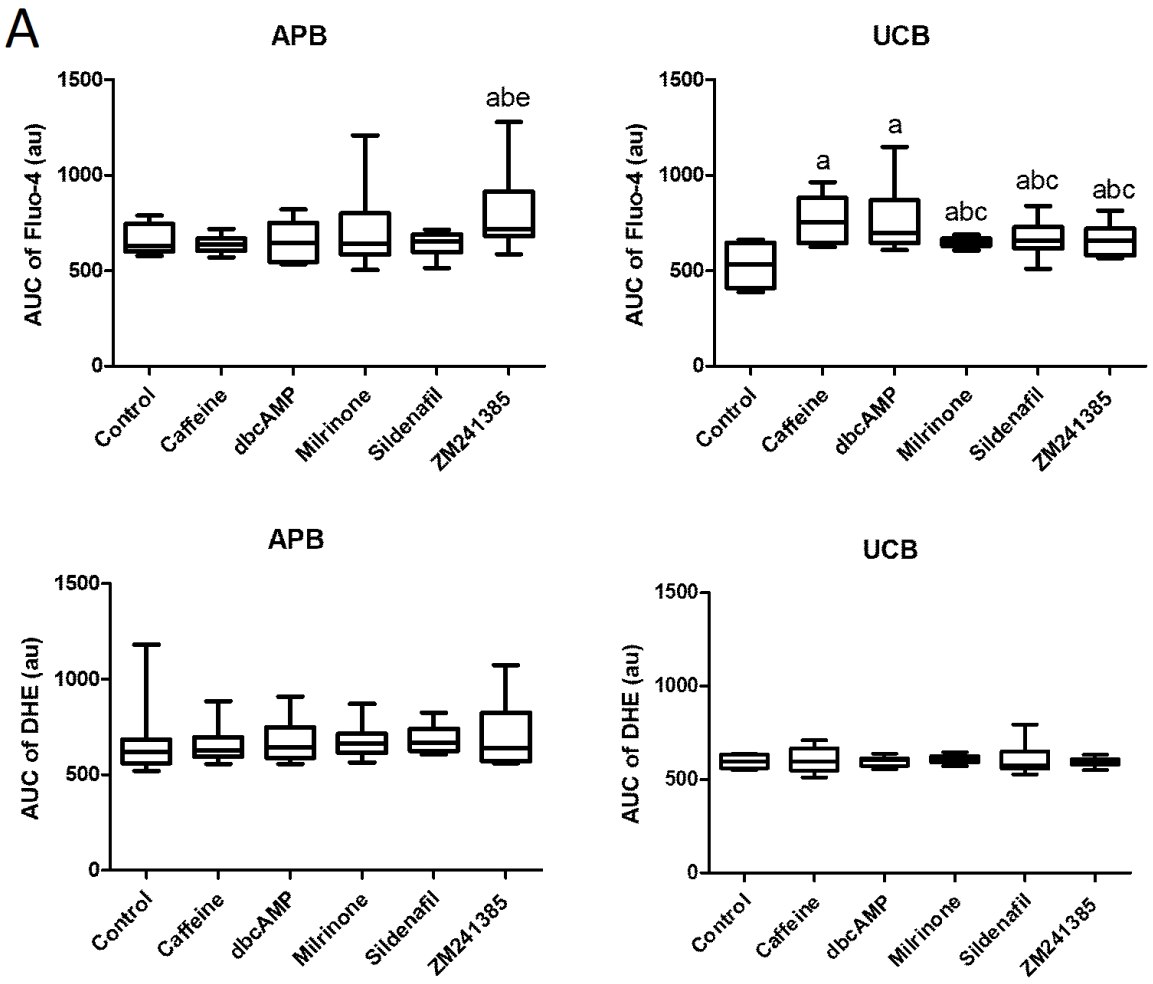

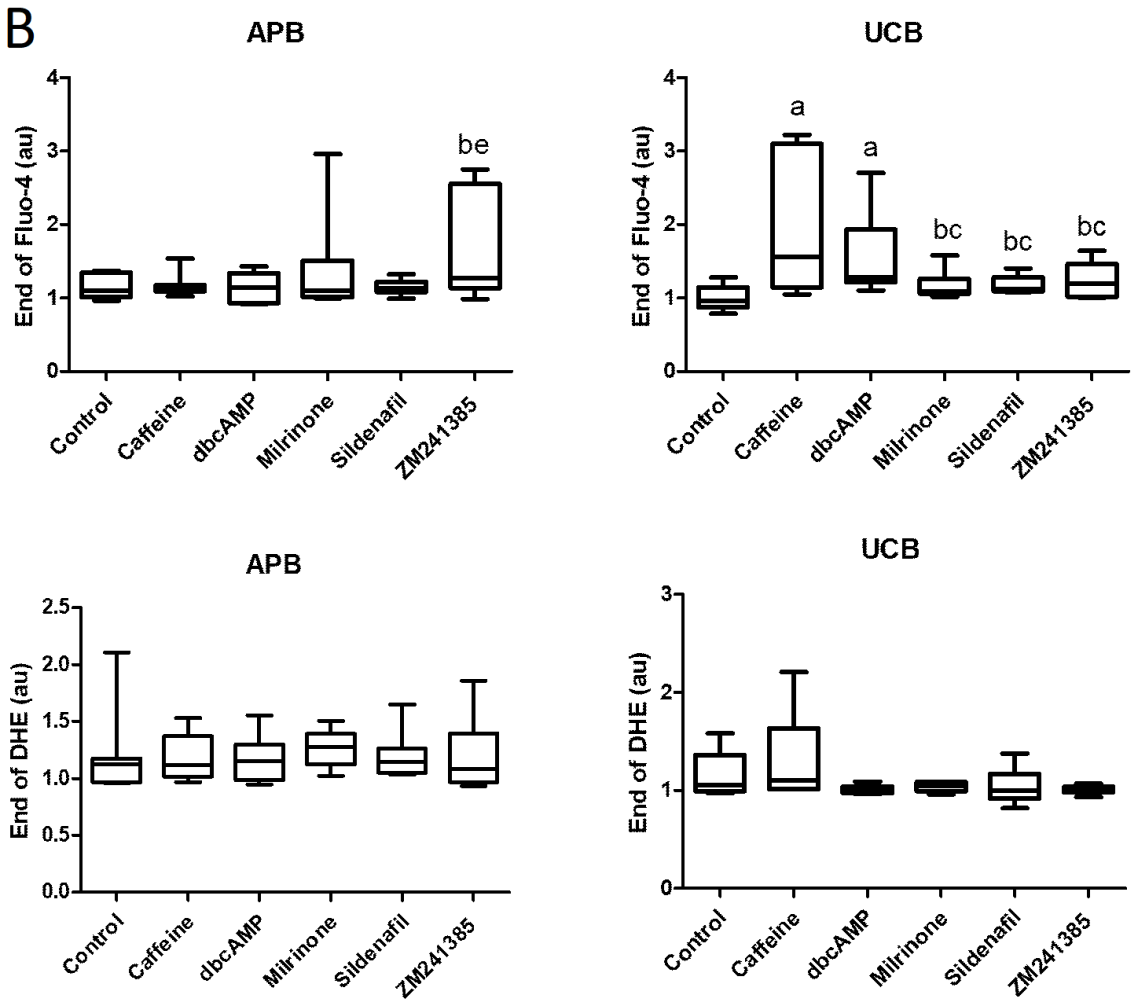

Figure 16. A, Area under the curve (AUC) and **B,** End values of kinetic measurements in adult peripheral blood (APB) and umbilical cord blood (UCB) samples. AUC values of Fluo-4 were elevated in caffeine (1.41-fold), dbcAMP (1.3-fold), milrinone (1.22-fold), sildenafil (1.23-fold) and ZM241385 (1.23-fold) treated samples compared to untreated samples in UCB. End value of Fluo-4 was also raised in caffeine (1.61-fold) and dbcAMP (1.34-fold) treated samples, but comparable in milrinone, sildenafil and ZM241385 treated samples compared to untreated samples in UCB. The studied compounds did not influence AUC or End values of DHE. Horizontal line – median, box – interquartile range, whiskers – range. $p < 0.05$ a vs. Control, b vs. Caffeine, c vs. dbcAMP, d vs. Milrinone, e vs. Sildenafil. au – arbitrary unit

5.5.2. Intracellular cytokine production

We performed intracellular cytokine staining of CD4 cells to demonstrate their cytokine producing capacity. Mean fluorescence intensity (MFI) of IFN-γ in CD4 cells was lower in UCB compared to APB (3940 (1945-8901) au vs. 1568 (145-2635) au, p = 0.036). The prevalence of CD4+ IFN-γ+ cells did not differ between the two groups. MFI and prevalence values of all other cytokines were comparable between APB and UCB samples.

PDE inhibitors did not alter CD4+ IL-2+ cell prevalence in APB. In contrast, the prevalence of CD4+ IL-2+ cells increased following treatment with sildenafil in UCB (**Figure 17**). MFI of IL-2 was unaffected. MFI and prevalence values of all other cytokines studied were not influenced by treatment with PDE inhibitors.

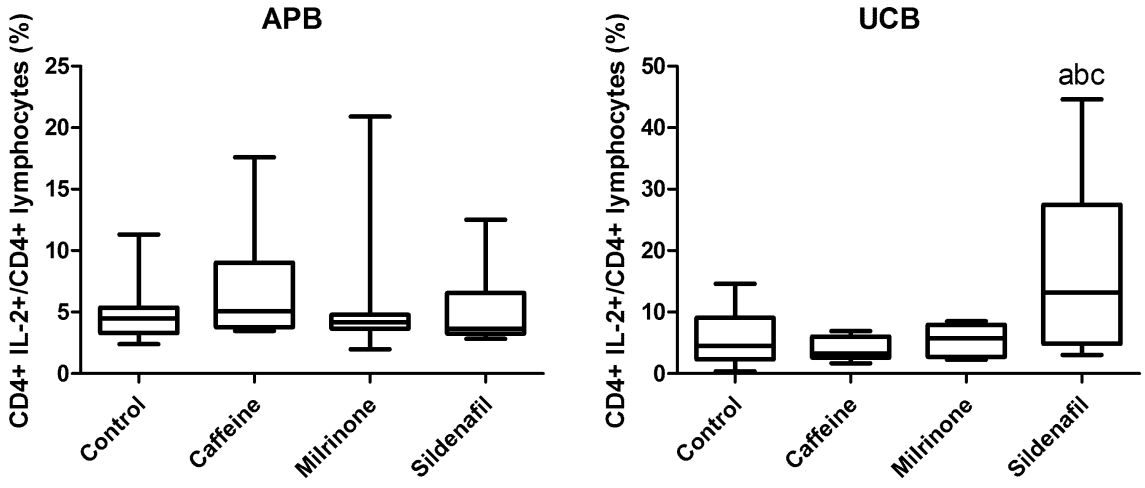

Figure 17. Prevalence of IL-2-producing CD4+ lymphocytes in adult peripheral blood (APB) and umbilical cord blood (UCB) samples. Sildenafil increased the prevalence of IL-2-producing CD4 cells in UCB. Horizontal line – median, box – interquartile range, whiskers – range. $p < 0.05$ a vs. Control, b vs. Caffeine, c vs. Milrinone

5.5.3. CD203c and Nuclear Factor of Activated T cells expression

We performed cell surface staining in order to demonstrate the expression of CD203c, an ectoenzyme responsible for the extracellular hydrolysis of cAMP. The density of CD203c (represented by MFI values) was lower in Th1 and CD8 cells in UCB than APB (**Table 6**). The density of CD203c on the cell surface was higher in Th2 compared to Th1 cells in both APB and UCB (**Figure 18**).

In order to study NFAT expression, intracellular staining was applied. The amount of intracellular nuclear factor of activated T cells (NFAT, represented by MFI values) was lower in Th1 and CD8 cells in UCB than in APB (**Table 6**). The amount of intracellular NFAT was higher in Th2 compared to Th1 and CD8 cells in both APB and UCB (**Figure 18**).

	APB (n = 10)	**UCB** (n = 6)
MFI of NFAT in CD4+ (au)	2019 (907-3780)	1088 (31-2836)
MFI of NFAT in CD4+ CXCR3+ CCR4- (au)	1166 (792-1835)	346* (27-1099)
MFI of NFAT in CD4+ CXCR3- CCR4+ (au)	2817 (1043-5902)	1765 (107-6665)
MFI of NFAT in CD8+ (au)	1622 (687-2519)	664* (22-1197)
MFI of CD203c in CD4+ (au)	672 (373-2014)	449 (34-1313)
MFI of CD203c in CD4+ CXCR3+ CCR4- (au)	565 (418-1032)	195* (10-386)
MFI of CD203c in CD4+ CXCR3- CCR4+ (au)	937 (240-3352)	1135 (399-9037)
MFI of CD203c in CD8+ (au)	1041 (475-1871)	547* (6-1029)

Table 6. Mean fluorescence intensity (MFI) values of nuclear factor of activated T cells (NFAT) and CD203c in adult peripheral blood (APB) and umbilical cord blood (UCB) samples. Data are presented as median (interquartile range). * $p < 0.05$ vs. APB. au – arbitrary unit

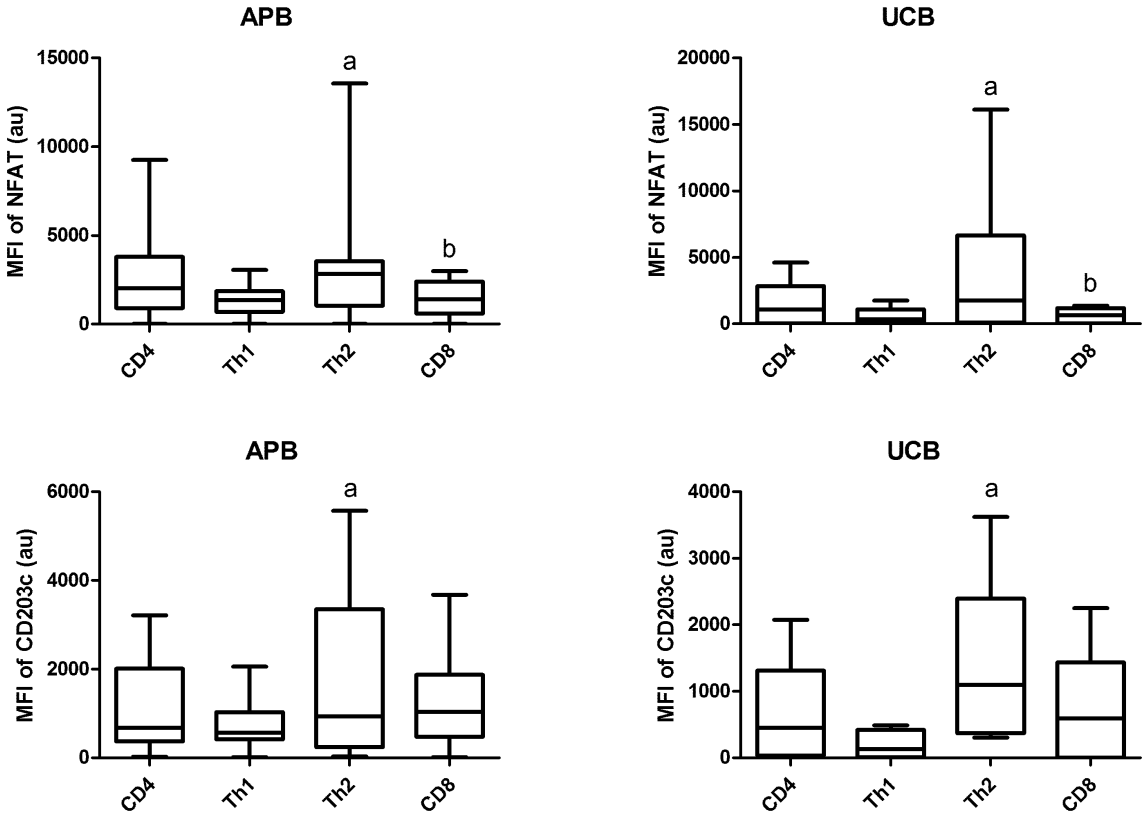

Figure 18. Mean fluorescence intensity (MFI) values of nuclear factor of activated T cells (NFAT) and CD203c in adult peripheral blood (APB) and umbilical cord blood (UCB) samples. NFAT and CD203c expression is elevated in Th2 compared to Th1 cells in both APB and UCB samples. Horizontal line – median, box – interquartile range, whiskers – range. $p < 0.05$ a vs. Th1, b vs. Th2. au – arbitrary unit

5.6. Perinatal asphyxia and neonatal arterial ischaemic stroke

5.6.1. Pro-inflammatory cytokines in perinatal asphyxia

Our results suggest that CD4+ IL-1β+ cells are early mediators of the inflammatory response, as their prevalence is higher at 6 h after birth in severe compared to moderate asphyxia. The extravasation of these cells is also increased at this time point in severe asphyxia as evidenced

by the lower prevalence of CD49d-expressing CD4+ IL-1β+ cells in peripheral blood. Therefore, although plasma levels of IL-1β are not different in moderate and severe asphyxia, IL-1β may play an important role in initiating tissue damage in the brain following the hypoxic insult. Intracellular (MFI) levels of IL-1β in both groups and plasma levels in the moderate group are highest at 6 h and comparably lower at the following time points, suggesting that its main role is the initiation of the inflammatory response (**Figures 19&20** and **Table 7**).

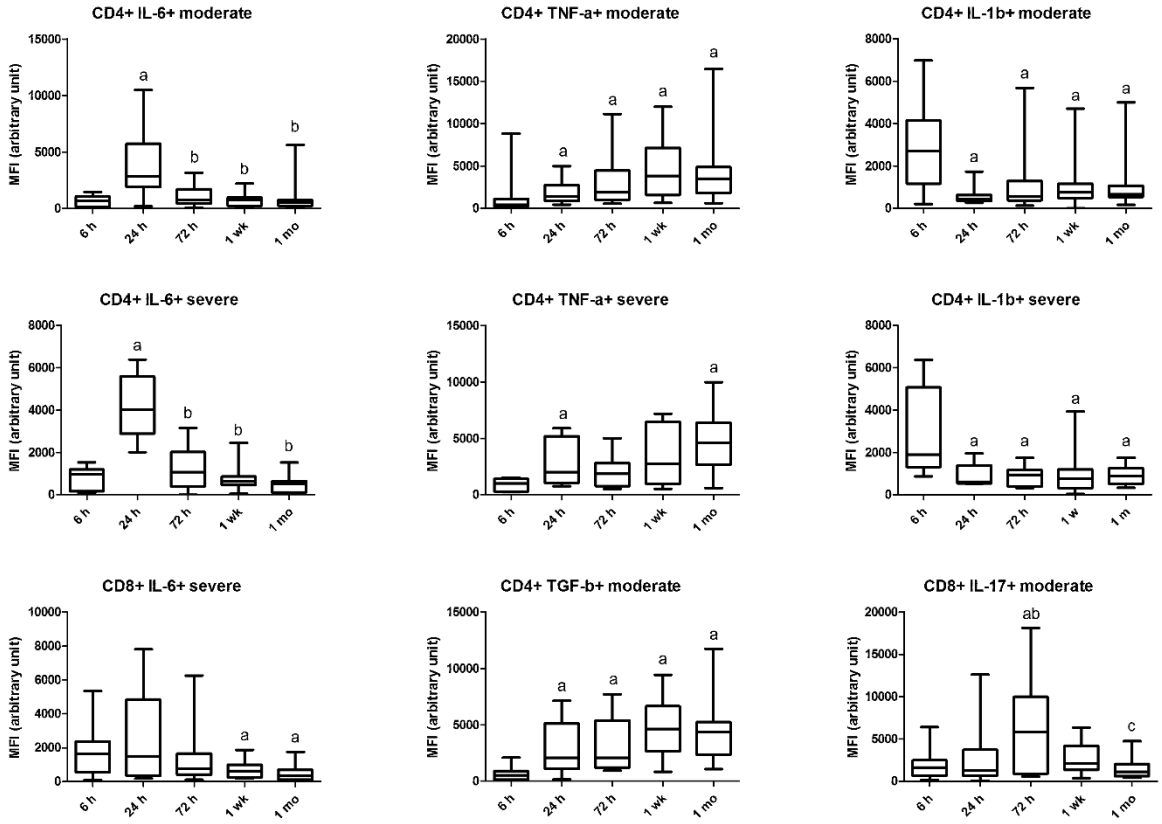

Figure 19. Intracellular cytokine level alterations in time represented by mean fluorescence intensity (MFI) values in moderate and severe asphyxia. Horizontal line: median, box: interquartile range, whisker: range. $p < 0.05$ a vs 6 h, b vs 24 h, c vs 72 h, d vs 1 wk.

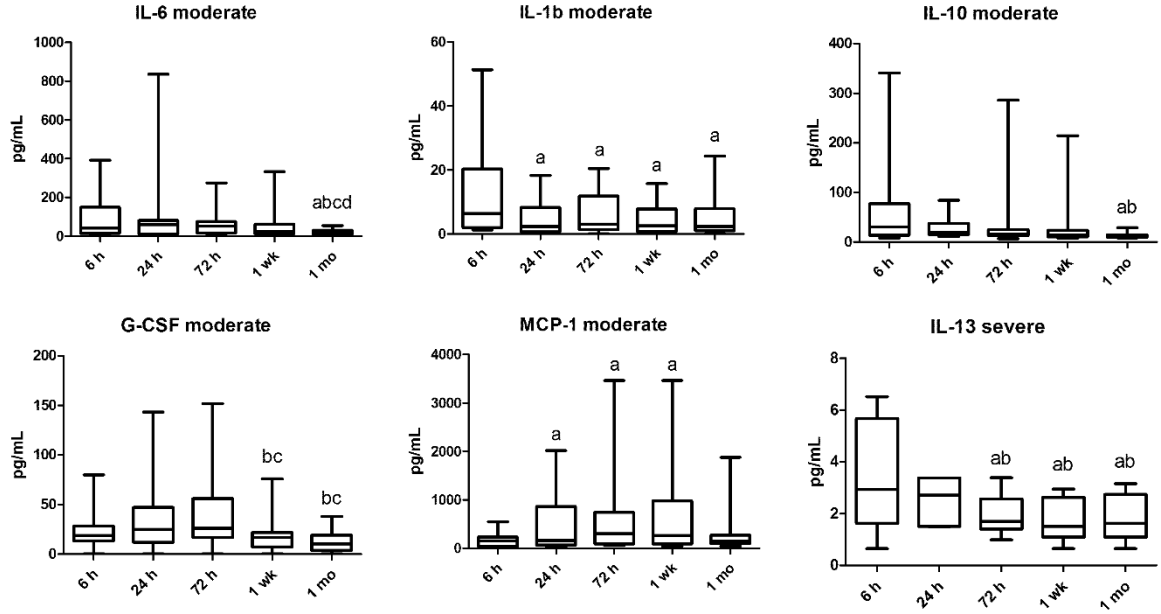

Figure 20. Plasma cytokine level alterations in time in moderate and severe asphyxia. Horizontal line: median, box: interquartile range, whisker: range. $p < 0.05$ a vs 6 h, b vs 24 h, c vs 72 h, d vs 1 wk.

Plasma IL-6 levels were higher at 1 wk in the severe compared with the moderate group. Plasma IL-6 levels decreased by 1 mo following the insult in the moderate group. MFI of CD4+ IL-6+ cells peaked at 24 h in both patient groups and declined later, indicating that it may play a role in the initial inflammatory response. MFI of CD8+ IL-6+ cells in the severe group also decreased by 1 wk (**Figures 19&20** and **Table 7**).

The prevalence of CD8+ IL-17+ cells was higher in the moderate group than in the severe group at 6 h. In contrast, the prevalence of CD4+ IL-17+ cells was lower in the moderate than in the severe group at 1 wk. The prevalence of CD4+ IL-17+ was lower at 6 h than at other time points in the severe group and remained high until 1 mo. MFI of CD8+ IL-17+ cells at 24 h and that of CD4+ IL-17+ cells at 72 h were also higher in the severe group. The MFI of CD8+

IL-17+ cells peaked at 72 h in the moderate group. No difference was observed in plasma levels of IL-17 (**Figures 19&20** and **Table 7**).

	Time	**Moderate**	**Severe**
Intracellular cytokines – cell prevalence data (% of parent population)			
CD4+ IL-1b+/CD4+	6 h	3.52 (2.13-5.16) %	6.77 (3.18-10.26) %
CD4+ IL-1b+ CD49d+/ CD4+ IL-1b+	6 h	6.98 (4.61-9.32) %	4.08 (2.86-5.46) %
CD4+ TNF-a+ CD49d+/ CD4+ TNF-a+	6 h	6.63 (4.47-13.45) %	3.52 (2.12-7.23) %
CD8+ IL-17+/CD8+	6 h	5.26 (3.89-14.40) %	2.63 (1.75-5.18) %
CD4+ FoxP3+/CD4+	24 h	2.35 (1.96-3.13) %	3.02 (2.60-4.13) %
CD4+ TNF-a+ CD49d+/ CD4+ TNF-a+	72 h	4.77 (3.43-7.70) %	9.75 (6.31-10.80) %
CD4+ IL-17+/CD4+	1 wk	3.08 (1.80-4.59) %	5.13 (3.40-13.76) %
Intracellular cytokines – mean fluorescence intensity (MFI) data (arbitrary unit)			
CD8+ IL-17+/CD8+	24 h	1069 (639-3265)	4187 (1274-6133)
CD4+ IFN-g+/CD4+	72 h	455 (150-770)	887 (496-1427)
CD4+ IL-17+/CD4+	72 h	939 (566-1674)	1760 (1614-3508)
CD4+ TNF-a+/CD4+	1 mo	3281 (1752-4326)	4729 (3959-6714)
Plasma cytokines (pg/mL)			
G-CSF	24 h	19.85 (10.87-30.70)	42.74 (22.27-131.3)
IL-5	72 h	1.37 (0.00-4.69)	0.20 (0.00-0.46)
IL-13	72 h	2.35 (2.01-3.67)	1.70 (1.40-2.56)
IL-6	1 wk	21.06 (11.89-43.24)	70.25 (33.73-134.1)
G-CSF	1 wk	13.33 (5.52-17.72)	32.90 (16.65-94.76)
HPLC results (uM)			
KYN	1 mo	3.62 (2.72-4.47)	2.28 (1.45-3.14)

Table 7. Significant differences in intracellular cytokine, plasma cytokine and high-performance liquid chromatography (HPLC) data between the moderate and severe group. $p < 0.05$ for all comparisons.

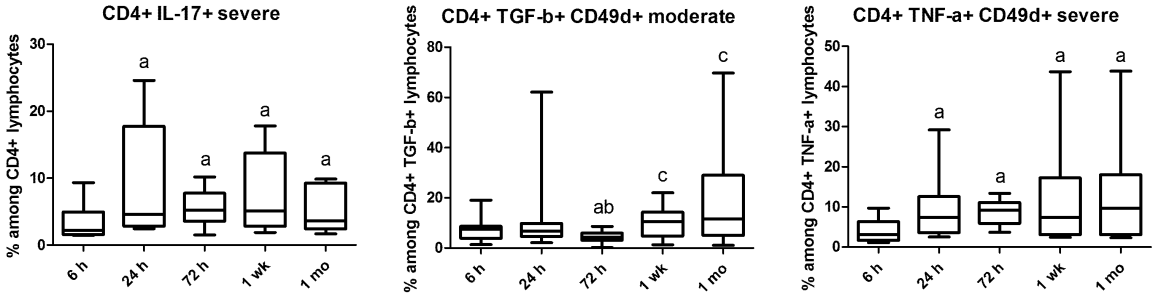

Figure 21. Cell prevalence data alterations in time in moderate and severe asphyxia. Horizontal line: median, box: interquartile range, whisker: range. $p < 0.05$ a vs 6 h, b vs 24 h, c vs 72 h, d vs 1 wk.

On the contrary, MFI of TNF-α in CD4 cells was increased at all time points compared to 6 h in both groups. At 1 mo, MFI of TNF-α was higher in the severe group, suggesting that it might play a role in the development of long term consequences of asphyxia. The prevalence of CD49d-expressing CD4+ TNF-α+ cells is lower in severe asphyxia at 6 h compared to later time points, indicating that in a severe insult it might also contribute to early tissue destruction through increased extravasation. This is further supported by the fact that the prevalence of CD49d-expressing CD4+ TNF-α+ cells is lower at 6 h and higher at 72 h in severe asphyxia compared to a moderate insult. No difference was observed in plasma levels of TNF-α (**Figures 19&21** and **Table 7**).

MFI of CD4+ IFN-γ+ cells was higher in the severe than in the moderate group at 72 h. Plasma MCP-1 levels were higher at 24 and 72 h as well as 1 wk than at 6 h in the moderate group. Plasma G-CSF levels were higher at 24 h and 1 wk in the severe compared with the moderate group. G-CSF levels decreased by 1 wk and remained low at 1 mo following the initial insult in the moderate group (**Figure 20** and **Table 7**).

5.6.2. Anti-inflammatory factors in perinatal asphyxia

The prevalence of CD49d-expressing CD4+ TGF-β+ cells was increased at 1 wk and 1 mo compared to 72 h in the moderate group potentially indicating that TGF-β plays an anti-inflammatory role in tissue regeneration in the early stage of the insult. MFI of CD4+ TGF-β+ cells was increased from 24 h onwards in the moderate but not in the severe group, which is probably also part of a compensatory phenomenon (**Figures 19&21**).

Plasma IL-10 levels were lower at 1 mo than at 6 and 24 h in the moderate group. Plasma IL-13 and IL-5 levels were higher in the moderate than in the severe group at 72 h. Plasma IL-13 levels were higher at 6 and 24 h than the following time points in the severe group (**Figure 20** and **Table 7**).

The prevalence of Tregs is somewhat higher in severe asphyxia at 24 h, which might be part of a compensatory mechanism, however, the biological significance of this increase is questionable (**Table 7**).

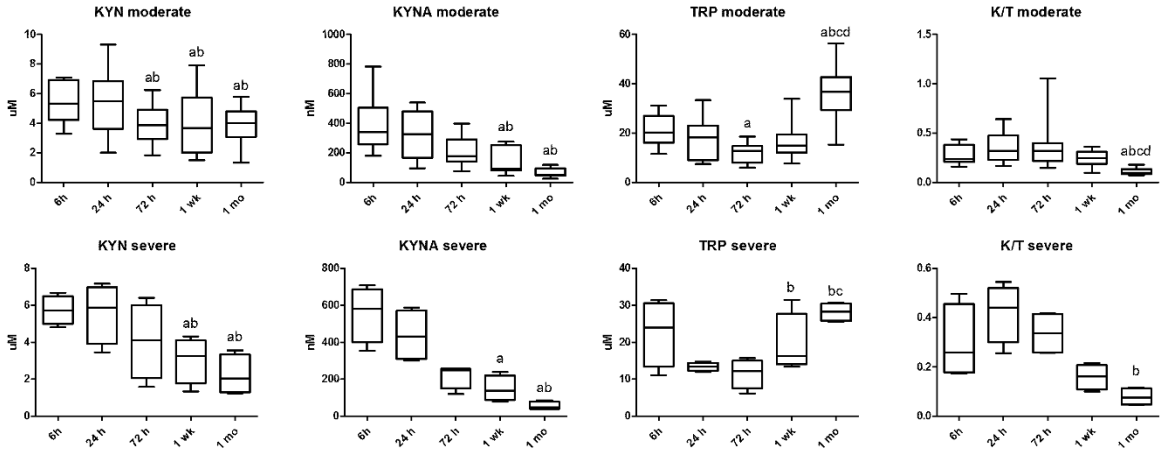

Figure 22. Alterations in the components of the kynurenine pathway in time in moderate and severe asphyxia. Horizontal line: median, box: interquartile range, whisker: range. KYN –

kynurenine, KYNA – kynurenic acid, TRP – tryptophan, K/T – kynurenine/tryptophan ratio. p < 0.05 a vs 6 h, b vs 24 h, c vs 72 h, d vs 1 wk.

Plasma KYN levels were higher at 1 mo in the moderate group compared to the severe group. KYN levels showed a decline in both groups by 1 wk and 1 mo following the insult. Similar results were observed for KYNA, while TRP levels increased significantly by 1 mo in both groups. In line with the above, the K/T ratio, corresponding to the enzymatic activity of IDO, plummeted by 1 mo in both groups (**Figure 22** and **Table 7**).

5.6.3. Receiver operating characteristic analysis in perinatal asphyxia

We performed ROC analyses to assess which parameters have the potential to discriminate between a moderate and a severe insult at an early stage. The only significant results of the ROC analyses were related to intracellular IL-1β. The prevalence of CD4+ IL-1β+ cells at 6 h (p = 0.018, ROC AUC = 0.784) and that of CD4+ IL-1β+ CD49d+ cells at 6 h (p = 0.027, ROC AUC = 0.767) was able to differentiate severity with a reasonable sensitivity and specificity (**Figure 23**).

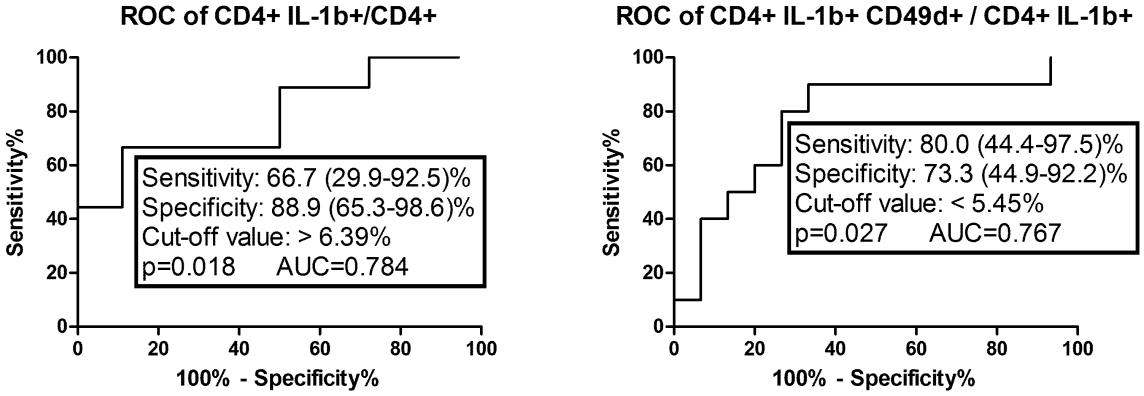

Figure 23. Receiver operating characteristic (ROC) analysis of the prevalence of CD4+ IL-1β+ and CD4+ IL-1β+ CD49d+ cell subsets in moderate and severe neonatal asphyxia. AUC – area under the curve.

5.6.4. Intracellular cytokine data in neonatal arterial ischaemic stroke

At 6 h and 72 h of age the prevalence of CD8+ IL-10+ lymphocytes remained lower in NAIS than in the severe HIE group. Although the prevalence of CD8+ IL-10+ lymphocytes remained consistently lower in NAIS, the difference did not reach significant level at the 24 h time point. On the contrary, the prevalence of CD4+ IL-10+ was higher at 24 h in NAIS compared to moderate HIE. The prevalence of CD4+ IFN-γ+ cells showed an elevated tendency from 24 h in NAIS, however this value did not reach significance, which could be due to the small population. At 1 wk the prevalence of TGF-β+ lymphocytes prone to enter the CNS (CD4+ TGF-β+ CD49d+ lymphocytes) was elevated in NAIS compared to both HIE groups, and also compared to all other time points within the NAIS group (**Figure 24**). On the other hand, at 1 mo of age, the prevalence of CD4+ TGF-β+ lymphocytes decreased in NAIS compared to HIE. Data are summarized in **Table 8**.

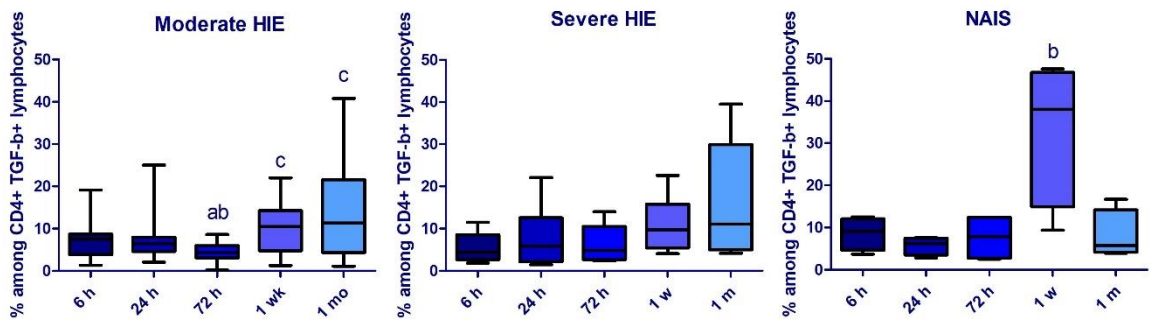

Figure 24. Alterations of the prevalence of CD4+ TGF-β+ CD49d+ cells within the CD4+ population in the first month of life in moderate (n = 17) and severe (n = 11) hypoxic-ischemic

encephalopathy (HIE) and in NAIS (n = 4). Horizontal line: median, box: interquartile range, whisker: range. $p < 0.05$ a vs 6 h, b vs 24 h, c vs 72 h.

% of parent population		**Moderate HIE** (n = 17)	**Severe HIE** (n = 11)	**NAIS** (n = 4)
IL-10+ CD8+ / CD8+	6 h	2.75 (1.19-4.12)	4.19 (1.94-6.91)	1.10 (0.40-1.36)[b]
IL-10+ CD4+ / CD4+	24 h	2.88 (1.56-7.03)	4.52 (3.02-6.59)	9.47 (5.10-20.68)[a]
IL-10+ CD8+ / CD8+	72 h	3.51 (1.85-5.12)	5.30 (2.41-6.08)	1.39 (0.52-2.99)[b]
TGF-β+ CD49d+ CD4+ / CD4+	1w	10.54 (4.77-14.28)	10.0 (5.46-15.20)	38.00 (14.93-46.78)[ab]
TGF-β+ CD4+ / CD4+	1 mo	3.51 (1.46-4.47)	3.54 (2.47-6.27)	1.30 (0.54-2.49)[b]
IL-17+ CD8+ / CD8+	6 h	3.89 (5.26-14.40)	2.30 (1.73-4.49)[a]	5.04 (4.62-7.68)[b]
IFN-γ+ CD4+ / CD4+	72 h	6.40 (3.70-11.80)	6.17 (4.75 -13.01)	17.50 (2.74-30.20)
IL-6+ CD8+ / CD8+	72 h	4.37 (3.26-6.29)	5.63 (2.68-8.80)	8.87 (4.75-10.52)
IL-6+ CD8+ / CD8+	1 mo	4.02 (2.40-10.74)	3.70 (2.31-6.16)	4.47 (2.88-8.33)

Table 8. Intracellular cytokines – cell prevalence data in NAIS. The prevalence of T cells expressing various cytokines are shown as the percentage of the parent population. Data are expressed as median and interquartile range. $p < 0.05$ a vs moderate HIE, b vs severe HIE.

At 6 h the prevalence of CD8+ IL-17+ lymphocytes was higher in NAIS than in severe HIE and CD8 cells expressed higher levels of IL-17 in NAIS than moderate HIE. The level of IL-1β in CD4+ cells was highest at 6 h and decreased significantly by 72 h within the NAIS group. MFI of IFN-γ in CD4+ lymphocytes in NAIS was the highest at 24 h and decreased significantly by 72 h, by when it reached a lower level in NAIS than in either of the HIE groups. The MFI of IL-6 in CD8+ cells was higher at 72 h in severe HIE than in NAIS. Interestingly,

by 1 mo the MFI of IL-6 in CD8+ decreased in both HIE groups and rose in NAIS. Data are shown in **Table 9**.

We found no differences between NAIS and HIE in the intracellular production of IL-1β and TNF-α in CD4 or CD8 cells, however these cytokines appear to be important in differentiating between the mild and severe form of HIE, as presented above.

arbitrary unit		**Moderate HIE** (n = 17)	**Severe HIE** (n = 11)	**NAIS** (n = 4)
MFI IL-17 / CD8	6 h	1427 (661.5-2402)	1591 (1157-7047)	4855 (2618-8706)[a]
MFI IFN-γ / CD4	72 h	455 (149.5-770)	887 (495.5-1427)	42.25 (28.13-438.5)[ab]
MFI IL-6 /CD8	72 h	701 (364.8-1441)	1073 (795-2017)	646.5 (188.7-736.3)[b]
MFI IL-6 / CD8	1 mo	429 (101.7-617.0)	347 (83-491)	918.5 (638.3-1347)[ab]
MFI IL-10 / CD8	6 h	1883 (512.5-5817)	1874 (1157-3415)	705 (280-3313)
MFI IL-10 / CD4	24 h	674.5 (177.8-2608)	1084 (203-1892)	666 (242.5-1063)
MFI IL-10 / CD8	72 h	2167 (1462-5964)	1505 (1055-3819)	443.5 (371-5977)
MFI TGF-β / CD4	1wk	4620 (2654-6647)	3129 (1238-5621)	3260 (1452-3680)
MFI TGF-β / CD4	1mo	811.5 (253-1740)	634 (259-1789)	330.5 (123-2283)

Table 9. Intracellular cytokines – mean fluorescence intensity (MFI) data in NAIS. The intracellular level of certain cytokines in T cells is shown by the MFI of each cytokine. Data are expressed as median and interquartile range. $p < 0.05$ a vs moderate HIE, b vs severe HIE.

5.6.5. Plasma cytokine data in neonatal arterial ischaemic stroke

At 72 h we found a marked inflammatory response in NAIS, characterised by elevated plasma levels of IL-5, IL-17 and MCP-1 compared to HIE. Plasma MCP-1 level was the highest at 72 h in NAIS. By 1 mo however, inflammatory response appears to be decreased in NAIS

compared with HIE, indicated by decreased plasma levels of IL-4, IL-12 and IL-17 (**Figure 25**). The level of IL-4 was lower at 1 mo than 72 h in NAIS.

We found no alterations in NAIS in the plasma level of IL-1β, IL-2, IL-6, IL-7, IL8, IL-10, IL-13, IFN-γ, TNF-α, TGF-β, G-CSF, GM-CSF, MIP-1b and VCAM when compared with HIE. Data are shown in **Table 10**.

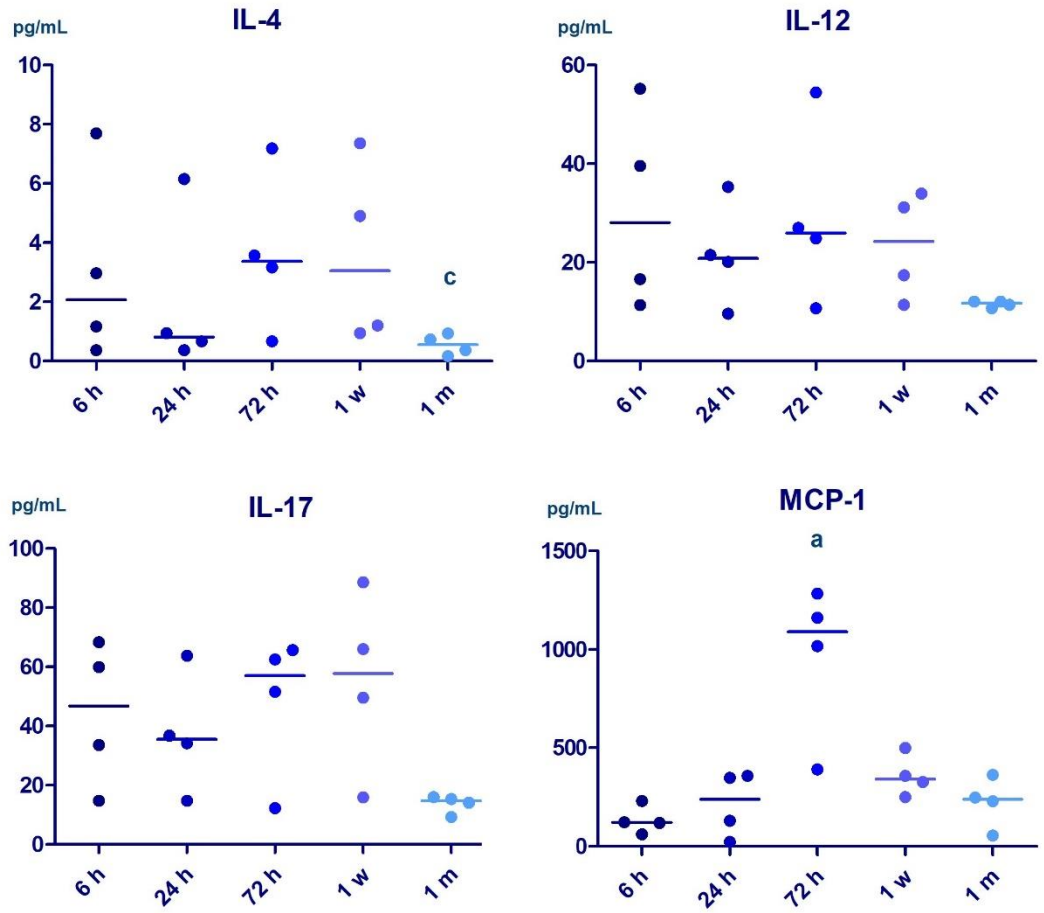

Figure 25. Alterations of plasma cytokine levels in the first month of life in neonatal arterial ischemic stroke (n = 4). Horizontal line: median. $p < 0.05$ a vs 6 h, b vs 24 h, c vs 72 h.

pg/mL		**Moderate HIE** (n = 17)	**Severe HIE** (n = 11)	**NAIS** (n = 4)
IL-5	72 h	1.37 (0.00-4.69)	0.20 (0.00-0.46)	3.42 (1.42-6.35)[b]
IL-17	72 h	30.44 (26.65-51.62)	33.91 (29.16-48.02)	62.52 (51.62-645.7)[ab]
MCP-1	72 h	251.9 (87.12-595.6)	678 (214-2311)	1090 (547.2-1254)[a]
IL-4	1 mo	1.68 (0.84-2.54)	1.52 (0.84-2.44)	0.55 (0.22-0.89)[ab]
IL-12	1 mo	18.11 (13.34-39.53)	21.52 (15.96-36.46)	11.74 (10.90-12.06)[ab]
IL-17	1 mo	32.58 (22.02-51.92)	31.11 (19.50-74.08)	14.75 (10.49-15.85)[ab]

Table 10. Plasma cytokine data in NAIS. Data are expressed as median and interquartile range. $p < 0.05$ a vs moderate HIE, b vs severe HIE.

6. DISCUSSION

6.1. B7 costimulation in the neonate

Lower reactivity of UCB T cells in comparison to APB T lymphocytes was a widely recognised phenomenon [141]. However, details behind this difference are not fully understood. Therefore, we aimed to characterise the prevalence of B7 costimulatory molecules on monocytes and their corresponding receptors on T lymphocytes in UCB compared to APB, as well as the intracellular expression of IDO and plasma levels of TRP, KYN and KYNA, important molecules with immunoregulatory properties, in order to describe their potential contribution to altered immunological reactivity of UCB T cells.

The higher prevalence of CTLA-4 expressing cells within this subset indicates that the possibility of costimulation via CD28 may be decreased in UCB compared to APB. While CD28 is constitutively expressed on T cells, CTLA-4 is directed at the cell surface upon the stimulation of CD28 in order to provide negative regulation for CD28 signalling. CTLA-4 shows a high sequence homology with CD28, and competes with CD28 for B7 molecules on the APC. Upon binding, it provides a negative signal to T lymphocytes, which terminates the proliferative phase. B7-1 and B7-2 have a higher affinity for the inhibitory receptor CTLA-4 in comparison with CD28 [11]. Since the level of CTLA-4 expression on CD4 cells is higher in UCB, and at the same time that of B7-2 is also elevated, this inhibitory relation may function to a higher extent in UCB in comparison with APB. Further functional analyses are needed to confirm or refute this hypothesis. On the other hand, the higher expression of CTLA-4 on UCB T cells might be the consequence of the higher level of antigen presentation which is a characteristic feature of immune response at this early stage of life. In a study by Han et al., UCB monocytes were characterized by low baseline expression of the costimulatory molecules B7-2 and CD40 compared to adults. Expression of these molecules was not up-regulated by

potent activators, such as the combination of IFN-γ and CD40 ligand (CD40L) [142]. The difference between this finding and ours might be due to the fact that we investigated CD11b+ activated monocytes, exhibiting elevated B7-2 levels. This notion is reinforced by our analysis of B7-2 expression on CD11b- monocytes, indicating a decrease in UCB compared to APB in line with the results of Han et al. (53.1 (34.3-65.3) % vs. 31.3 (26.6-44.7) %, p = 0.004). CD11b is an integrin-type transmembrane glycoprotein. Following a non-covalent association with CD18, it plays a crucial role in the adhesion, transendothelial migration, and thus the activation of monocytes [143]. In other investigations, UCB dendritic cells (DCs) also appeared to be immature as they exhibited low or no basal expression of CD40, B7-1 or B7-2 [144,145].

With regard to CD28 and CTLA-4, the findings of Elliott et al. are contradicting ours. In their study, a higher percentage of resting T cells expressed CD28 in UCB and young children compared to adults. CD28 expression was similar on APB and UCB T cells activated with PMA and ionomycin. Interestingly, surface CTLA-4 expression was lower on UCB than on APB T cells stimulated with PMA and ionomycin. In contrast, intracellular CTLA-4 expression was equivalent, suggesting that trafficking of CTLA-4 to the cell surface may be differentially regulated in UCB T cells [146].

In our study, the prevalence of CD3+ CD278+ lymphocytes was higher in UCB than in APB. The frequency of the corresponding costimulatory molecule, B7-H2 on CD11b+ monocytes was comparable in the two groups. In contrast, that of B7-H1 expressing CD11b+ monocytes, providing inhibitory signal via CD279, was lower in UCB compared to APB. These findings indicate that there is a shift towards the stimulatory from the inhibitory direction in UCB at the level of B7-H1 and B7-H2 proteins, the significance of which necessitates further investigations. Darmochwal-Kolarz et al. determined the expression of B7-H1, B7-H4, CD200, and CD200R on myeloid BDCA-1+ and lymphoid BDCA-2+ DCs as well as on monocytes and B lymphocytes in UCB compared to APB [147]. They revealed that the expression of these

molecules was significantly lower on UCB DCs compared to adults. The lower expression of B7-H1 on UCB APCs is in line with our findings.

IDO is a key enzyme in the catabolism of tryptophan and initiates the production of kynurenines. These metabolites have several immunological and non-immunological regulatory functions. By locally depleting TRP and increasing the levels of KYN and its metabolites, IDO provides a suppression of T cell mediated immune response via inhibiting the proliferation and inducing the apoptosis of activated T cells, as well as promoting the development of regulatory T cells and tolerogenic DCs [148]. In our study, we found that the plasma K/T ratio, a formula generally used as an estimated representation of the enzymatic activity of IDO, is two-fold higher in UCB compared to APB. Unlike cellular components, both KYN and TRP may readily cross the placenta, similarly to other biological barriers, such as the blood brain barrier [149] and enter the fetal circulation from the maternal circulation. Therefore, the observed increase in K/T ratio in UCB may well reflect the previously reported increased placental IDO activity, contributing to the feto-maternal immunological tolerance [9,150]. This elevation in K/T ratio might be an important regulatory factor that contributes to lower reactivity of UCB T lymphocytes. These results suggested that the neonatal immune system, similarly to the maternal immune system during pregnancy, may be under active suppression rather than in a state of inherently reduced functionality. This hypothesis was an important consideration in the design of our subsequent set of experiments studying immune tolerance of neonatal T lymphocytes in response to maternal antigens and vice versa in mixed lymphocyte reactions.

Furthermore, we found that the transformation of KYN to KYNA is also elevated in UCB compared to APB, resulting in a 10-fold elevation of the plasma level of the anti-inflammatory KYNA [22], which may indicate the presence and high activity of organic acid transporters in

the placental barrier; however, the increased activity of kynurenine aminotransferase enzyme in the competent cells cannot be fully excluded either.

The engagement of B7-1 and B7-2 by CTLA-4 induces back signalling into the monocyte and promotes the production of IFN-gamma, which acts in an autocrine or paracrine manner to induce IDO expression, thereby initiating the degradation of TRP and resulting in an immunosuppressive effect as described above. Thus, the interaction between CTLA-4 and B7 proteins plays two different roles: first, at the level of T cells where CTLA-4 as a negative receptor regulates TCR signal transduction; second, at the level of APCs where CTLA-4 as a ligand signals to the APC to induce IDO expression [17]. Based on the higher frequency of CTLA-4 expressing CD4+ CD28+ lymphocytes in UCB, we hypothesized that reverse signalling may be increased in UCB. However, detailed analyses did not support this notion. Indeed, the frequency of IDO-expressing CD11b+ monocytes was comparable in UCB and APB. Furthermore, MFI values for IDO were lower in UCB than in APB in CD11b+ monocytes. This might indicate a lower capacity of UCB cells to produce IDO and that reverse signalling in CD11b+ cells may not be mature in UCB. This finding strengthens our hypothesis that the elevated K/T ratio observed in UCB may reflect placental (or maternal) IDO activation rather than the effect of IDO-competent APCs in UCB. The presence of a negative correlation between IDO and B7-2 expression in activated monocytes in UCB might also reflect that reverse signalling via B7-2 is immature in UCB.

In our investigations, we identified three factors that may contribute to the previously observed reduced reactivity of UCB compared to APB lymphocytes. First, the level of CTLA-4 expression on CD4 cells was higher in UCB compared to APB, indicating that the possibility of CD28-mediated costimulation may be decreased. At the same time, we found that the level of the corresponding costimulatory molecule, B7-2 is also elevated. Therefore, this inhibitory relation may function to a higher extent in UCB in comparison with APB. Second, plasma K/T

ratio is two-fold higher in UCB compared to APB, which corresponds to earlier findings of increased placental IDO activity in favour of an immunosuppressive milieu providing feto-maternal tolerance, and may contribute to the decreased reactivity of T cells in UCB. Interestingly, the level of anti-inflammatory KYNA is also considerably, almost ten-fold higher in UCB, which may indicate the presence and high activity of organic acid transporters in the placental barrier. Finally, to our knowledge, this is the first report describing a lower capacity of UCB compared to APB monocytes to produce IDO, and that reverse signalling in UCB monocytes may not be mature, which findings suggest that the observed increase in K/T ratio may be due to placental rather than fetal overexpression of IDO in competent cells. Our study also detected a shift towards the stimulatory from the inhibitory direction in UCB at the level of B7-H1 and B7-H2 proteins, the biological significance of which is yet to be established. Further investigations aimed at the above target molecules and mechanisms are needed to provide more details on the functional importance and clinical relevance of our findings.

6.2. B7 costimulation in healthy pregnancy and preeclampsia

We aimed to characterize the prevalence of B7 costimulatory molecules on monocytes and their corresponding receptors on T lymphocytes in HP compared to NP women, as well as the intracellular expression of IDO. Pregnancy is an immunosuppressive state, with well-known alterations in the prevalence and function of T lymphocytes. We assumed that alterations in costimulation mechanisms via B7 proteins might contribute to the lower level of T lymphocyte activation compared to NP women.

However, surprisingly, the expression of CD28 was increased, while that of CTLA-4 was decreased on T lymphocytes isolated from HP women. This finding indicates that costimulation via CD28 is of great importance also during pregnancy in T cells, and it may not contribute to the immunosuppressive environment characteristic for gestation. At the same time, the

expression of B7-1 was decreased on HP monocytes, while that of B7-2 was unaltered, which might reduce the intensity of costimulation via CD28.

In cases of miscarriage, the expression of B7-2 was found to be highly upregulated at the fetomaternal interface and this was associated with high levels of Th1 cytokines (IL-2 and IFN-gamma) and low levels of Th2 cytokines (IL-4 and IL-10) [150]. Furthermore, it was reported that in vivo blockade of B7-2 costimulation shifted the cytokine balance from a Th1 to a Th2 predominance at the fetomaternal interface, and expanded peripheral CD4+ CD25+ regulatory T cells. Thus, reduction in the level or function of B7-2 appears to be advantageous to HP in the first half of pregnancy. We could not, however, demonstrate this reduction in third trimester peripheral blood HP samples.

The expression of ICOS, a stimulator of T cell activation was strongly elevated in HP, while that of its corresponding costimulatory molecule, B7-H2 was strongly decreased on HP monocytes. Since ICOS most effectively induces IL-10 instead of IL-2 production [15], its higher level may contribute to the Th2 shift observed in the third trimester of HP. The frequency of PD-1 expressing T lymphocytes was also elevated in HP. The inhibitory effect of this receptor may play a role in inhibiting the activation of T cells during gestation. Interestingly, Taglauer et al. demonstrated that the expression of PD-1 expression on CD3 cells was low in non-pregnant endometrium but increased in first-trimester decidua and remained elevated in term decidua. Additionally, higher relative proportions of term decidual CD8bright, CD4, and Treg cells expressed PD-1 in comparison to autologous peripheral blood, further strengthening the role of this molecule in the development of maternal immune tolerance [151].

The prevalence of IDO-producing T cells and monocytes was elevated in HP compared to NP samples. The well-known immunosuppressive activity of this enzyme may play an important role in the development of pregnancy-specific immune tolerance towards the developing fetus. IDO is a key enzyme in the catabolism of tryptophan and initiates the production of

kynurenines. These metabolites have several immunological and non-immunological regulatory functions. By locally depleting TRP and increasing the levels of KYN and its metabolites, IDO provides a suppression of T cell-mediated immune response via inhibiting the proliferation and inducing the apoptosis of activated T cells, as well as promoting the development of regulatory T cells and tolerogenic DCs [148]. Furthermore, we found that not only the prevalence of IDO-producing cells, but also the intracellular amount of IDO is elevated in HP (represented by the higher MFI values compared to NP women).

The engagement of B7-1 and B7-2 by CTLA-4 induces back signalling into the monocyte and promotes the production of IFN-gamma, which acts in an autocrine or paracrine manner to upregulate IDO expression, thereby initiating the degradation of TRP and resulting in an immunosuppressive effect as described above. Thus, the interaction between CTLA-4 and B7 proteins plays two different roles: first, at the level of T cells where CTLA-4 as a negative receptor regulates TCR signal transduction; second, at the level of APCs where CTLA-4 as a ligand signals to the APC to induce IDO expression [17]. We hypothesized that reverse signalling may play a role in the higher IDO activity and expression observed in HP. However, correlation analyses with B7-1 and B7-2 expression did not support this notion.

No difference was observed in the frequency of CD28 expressing T lymphocytes between HP and PE women. Therefore, PE may not be related to increased costimulation of T cells via CD28, at least in this stage of pregnancy. While CD28 is constitutively expressed on T cells, CTLA-4 is directed at the cell surface upon the stimulation of CD28 in order to provide negative regulation for CD28 signalling. CTLA-4 shows a high sequence homology with CD28, and competes with CD28 for B7 molecules on the APC. Upon binding, it provides a negative signal to T lymphocytes, which terminates the proliferative phase [11]. Therefore, we investigated the frequency of CTLA-4 expressing CD28+ T cells in both groups, but found no

difference. These results indicate that this negative regulatory receptor does not contribute to the increased level of peripheral lymphocyte activation in PE.

In contrast to non-Treg T cells, CTLA-4 is constitutively expressed on CD4+ CD25+ Tregs. Paeschke et al. previously reported comparable number of CD4+CD25+CTLA-4+ cells in HP and PE, suggesting that Tregs during pregnancy are already stimulated upon TCR, probably by fetal antigens, in both groups [152]. On the contrary, in an investigation by Miko et al., the percentage of CTLA-4 expressing cells among CD4+CD25bright T cells of PE patients was significantly higher than that in HP or in non-pregnant women. Based on these findings, the authors argue that CD4+CD25bright T cells are more activated in PE patients than in healthy individuals [153]. In another study, Sasaki et al. reported that both the number of Tregs and the level of CTLA-4 on Tregs are lower in the decidua in cases of spontaneous abortion [154]. This finding supports the protective role of CTLA-4 in early pregnancy.

As described earlier, B7-1 and B7-2 have a higher affinity for the inhibitory receptor CTLA-4 in comparison with CD28 [11]. Since the level of CTLA-4 expression is not altered in PE, but at the same time B7-1 and B7-2 levels are decreased, this inhibitory relation may function to a lower extent in PE in comparison with HP. Further functional analyses are needed to confirm or refute this hypothesis.

Based on our results, costimulation via PD-1 and ICOS does not seem to be affected in PE, since no alteration was found in the frequency of these receptors and their corresponding ligands (B7-H1 and B7-H2, respectively) in comparison to HP. As in CD3+ T cells, we found no difference in the frequency of the investigated markers in CD4+ T helper cells. This result indicates that signal transduction via B7 costimulatory molecules might not be related to the alterations of T helper cell functions in pregnancy.

Similarly to the activation of T lymphocytes [35], the activation level of monocytes is also higher in PE compared to HP, as indicated by increased expression of CD11b [155]. In line

with these earlier results, we also found a higher frequency of CD11b+ monocytes in PE samples. The engagement of B7-1 and B7-2 by the soluble form of CTLA-4 induces back signalling into the monocyte and promotes the production of IFN-gamma, which acts in an autocrine or paracrine manner to induce IDO expression in monocytes, thereby initiating the degradation of tryptophan. This results in an immunosuppressive effect via the reduction of T cell function. This mechanism could be of special importance in Tregs through which these cells, at least in part, may mediate their immunosuppressive effect [18]. Thus, the interaction between CTLA-4 and B7 proteins plays two different roles: first, at the level of T cells where CTLA-4 as a negative receptor regulates TCR signal transduction; second, at the level of APCs where CTLA-4 as a ligand signals to the APC to induce IDO expression [17]. IDO production following reverse signaling may also occur in placental macrophages [156]. Our results of lower B7-1 and B7-2 levels on PE monocytes indicates that this back signalling phenomenon may be decreased in PE, which might result in decreased immunosuppression exerted by IDO. Therefore, we measured intracellular IDO expression of monocytes and T cells in PE and HP. Although the immunosuppressive effect of IDO was first identified in pregnancy, intracellular IDO expression has not been investigated in PE before. IDO is a key enzyme in the catabolism of tryptophan and initiates the production of kynurenines. These metabolites have several immunological and non-immunological regulatory functions. By locally depleting tryptophan and increasing kynurenine levels, IDO both inhibits T cell proliferation and induces the apoptosis of T cells, respectively [148]. In our study, the frequency of IDO expressing T cells was lower in PE than in HP. Furthermore, these cells produced a lower amount of IDO based on MFI values of the antibody directed against IDO. Lower IDO levels in T cells may contribute to increased T cell reactivity in PE and may also affect decreased Treg function in PE, based on the relation between IDO and Treg cells described by Liu et al. This group demonstrated that reduced placental IDO levels may influence maternal immune tolerance by

directly reducing Tregs in PE [157]. However, lower IDO levels in T cells are probably not related to B7 costimulation signals in PE, since the expression of B7 receptors in not altered, as described earlier. In contrast to T cells, the frequency of monocytes expressing IDO and intracellular IDO levels are comparable in PE and HP.

A previous study demonstrated that higher B7-2 expression on decidual monocytes correlates with IDO production in the deciduas.29 Levels of both IDO and B7-2 in that investigation correlated with pregnancy success, since both were found to be decreased in cases of spontaneous abortion. The positive correlation between B7-2 and IDO was reinforced by our findings in peripheral blood of the investigated groups. This correlation might be related to the above described back-signalling mechanism by CTLA-4 via B7-1 and B7-2 into the monocytes. Of note, no correlation was detected between gestational age and the investigated markers, suggesting that the progression of pregnancy does not influence their expression in the third trimester. The decrease of B7-1 and B7-2 expression in PE might be a secondary regulatory mechanism in response to the ongoing systemic maternal inflammation in PE.

6.3. Regulatory T cell subtypes in preeclampsia

In this study, we analyzed the prevalence of recently described regulatory T cell subsets in PE compared to HP. As many studies have noted before [35-37], the percentage of Tregs, identified as CD4+ CD25hi FoxP3+ cells, was lower in PE than in HP, contributing to the compromised maternal immune tolerance towards the semiallogenic fetus characteristic for PE, and to the loss of control over activated T cells. Indeed, the proportion of CD4+ CD25+ FoxP3+ CD45RA- activated T cells was higher among CD4+ T cells in PE compared to HP. This might in turn contribute to the increased Th1 type response and imbalance of Th1/Th2 ratio [30].

Nevertheless, our results indicate that the decrease in the prevalence of Treg cells is specific for certain Treg subtypes, while other subsets of these regulatory cells remain unaffected in

PE. Interestingly, of all investigated subsets, the prevalence of the functionally most active effector Tregs (CD4+ FoxP3++ CD45RA-) is decreased to the highest extent, while naive Treg cells appear to be unaffected. A further factor that may contribute to the decreased functionality of Tregs in PE is that the prevalence of exhausted, functionally less active Tregs (CD4+ CD25hi FoxP3+ CD279+) is higher compared to HP. In line with these findings in pregnancy, an exhausted and dysfunctional phenotype of Tregs has been reported before in chronic disease and infection [49].

The combination of lower effector Treg and higher exhausted Treg prevalence may account not only for the lower Treg proportion, but also for the observed decrease in the functionality of Tregs in PE [158].

The Helios transcription factor belongs to the Ikaros family and is expressed by thymic-derived Treg cells [42]. Interestingly, the origin of Tregs in the periphery does not seem to play an important role in their activity in PE, since no alteration was detected in the proportion of thymic and extrathymic Tregs (CD4+ CD25hi FoxP3+ Helios+ and CD4+ CD25hi FoxP3+ Helios-, respectively) between the two study groups. Furthermore, Helios+ effector and naive Tregs are also of comparable prevalence in HP and PE. These findings are not fully in line with recent results of Hsu et al, who demonstrated that the expansion of CD4+ Helios- Foxp3+ iTreg cells, rather than CD4+ Helios+ Foxp3+ nTreg cells, accounts for Treg expansion in HP. This expansion was found to be even more pronounced in the decidua, where an overrepresentation of iTreg cells was found. In PE, however, impaired systemic iTreg cell expansion was described, associated with a lack of iTreg cell overrepresentation in the decidua [159].

Earlier studies demonstrated that the prevalence of Tregs is decreased not only on the systemic level in peripheral blood of PE patients, but also locally, within the decidual tissue [39-41]. A limitation of our study is that our findings represent circumstances in peripheral blood only. Therefore, further studies on the expression of the investigated Treg cell subtypes in the

decidua are required to identify their role played in mediating tolerance at the fetomaternal interface.

6.4. Breastfeeding and immune development

The influence of early life nutrition on the development of the immune response has not previously been studied in the first few weeks of life. This is an important question as epidemiological data suggest that breastfeeding is associated with long-term health benefits, such as a lower incidence of childhood infections, asthma, obesity and autoimmune disorders [160-162], although it may not reduce the risk of food allergy [163]. This mechanism may be imprinted early after birth when the immune system faces the dual challenge of establishing inflammatory capacity against pathogens whilst developing tolerance towards harmless antigens.

A striking finding was that Tregs expand substantially in the first 3 weeks of life and this expansion was more profound in breastfed babies in contrast to those receiving formula feed. Tregs of breastfed neonates also display an activated phenotype with increased expression of HLA-DR, a marker of increased suppressive activity [164]. A recent mouse study on the role of maternal milk in setting the frequency of Tregs in the offspring reported the importance of a double-negative feedback loop, vertically transmitted via the entero-mammary axis that governs a setpoint for Tregs in the gut [165]. On the other hand, changes in the profile of pro-inflammatory cytokine production were also observed at this early stage of life. IL-8 production, a major phenotypic attribute within cord blood, was largely maintained but a striking feature was the increase in intensity of IL-17 production by both CD4+ and CD8+ cells by 3 weeks of age. This is likely to reflect recognition of bacterial antigen during establishment of the microbiome and may be balanced by the coordinated Treg expansion during this period. An increase in serum IL-17 has been shown at 4 weeks and is likely explained by these

observations [7]. Most of these features were independent of nutrition although IFN-γ production by T cells was lower in exclusively breastfed neonates. However, in the whole study population, we did not observe any difference in the proportion of Th1 and Th2 cells between birth and 3 weeks of age. Earlier studies indicated that Th1 development may be guided by environmental exposure via epigenetic changes, and would therefore be expected to occur at later stages (first months to years) of development. Low microbial exposure during early life was reported to increase the risk of allergic disease by reducing demethylation induced activation of the IFN-γ gene of naive T cells [166]. Our observation that CD8+ cells are less abundant and have reduced cytotoxic capacity in neonates compared to adults confirms previous results [167,168].

One of the most interesting findings was that T cells from breastfed neonates display reduced proliferative responses and produce substantially lower levels of Th1 cytokines when challenged with maternal cells. This was specific to maternal antigens and was not present against unrelated PBMC and did not result from an intrinsic reduction of cytokine producing capacity. As such this reflects the development of immunological tolerance towards NIMA in exclusively breastfed neonates. Importantly, we were also able to show that NIMA-specific tolerance was mediated by Tregs, and is therefore linked to the expansion of this population in breastfed neonates.

An additional observation was that neonatal PBMC at 3 weeks of age triggered stronger immune responses from maternal PBMC compared to cord blood cells. This may reflect maturation of antigen presentation function by 3 weeks of age, although this was not assessed in this study. This also indicates that the fetal immune system may contribute to suppression of maternal immune recognition during pregnancy by maintaining a tolerogenic phenotype prior to parturition.

It is interesting to speculate on potential mechanisms by which breastfeeding can promote NIMA-specific tolerance in neonates. Our observations likely reflect immune tolerance to gastrointestinal presentation of maternal cells within breastmilk [169]. Transplacental passage of cells during pregnancy leads to reciprocal microchimerism that can persist for many years. Furthermore, this “microchiome” of maternal cells supports fertility in female offspring by promoting immune tolerance to NIMA during next-generation pregnancies [170]. Beneficial effects are also seen when NIMA are shared between donors and recipients of allogeneic renal or hemopoietic stem cell transplantation. Importantly, the establishment of NIMA-specific tolerance has been shown to be dependent on breastfeeding and nutritional history is also a determinant of NIMA-associated transplant outcome [171,172]. Our findings show that breastfeeding promotes the development of Tregs that suppress recognition of NIMA, thus potentially supporting maternal microchimerism and conferring lifelong benefits in relation to fertility and immune protection against infectious agents and cancer [170,173].

Additionally, recent studies highlighted the possible immune modulating effects of microplastics released from feeding bottles, which may be of relevance in the context of our study [174,175]. However, the possible contribution of the above mechanism to the differences observed between our study groups was not assessed.

A further recent observation is that breastfeeding, through the transfer of human milk oligosaccharides, exerts important prebiotic and immunomodulatory effects including the development of tolerogenic dendritic cells which prime Tregs [176,177].

We were also interested to assess how nutrition could impact on the formation of the early microbiome and how this might correlate with immune function. Microbial composition was broadly comparable in breastfed and formula-fed neonates and this is likely to reflect the fact that all babies in our cohort were delivered by caesarean section. Dysbiosis of the microbiota has been found to occur following delivery by caesarean section and in infants who are not

breastfed [178,179]. Nevertheless, although it may take several months for nutrition to markedly influence microbiome composition [180] subtle differences in microbial diversity were already apparent at 3 weeks of life. In line with previously published results [181], we observed that the gut microbiome of breastfed neonates is more abundant in short chain fatty acid (SCFA) producing bacterial genera, such as *Gemella* and *Veillonella*. SCFAs, in particular propionate and butyrate, play an important role in promoting Treg differentiation and proliferation via the inhibition of histone deacetylases [58]. This notion is supported by a link between the presence of *Veillonella* and the proportion of Tregs at 3 weeks of age in our network modelling analysis. Furthermore, a recent study demonstrated paucity of Veillonella and other anaerobic taxa in the microbiome of extremely preterm infants with postnatal growth failure compared to appropriate postnatal growth, indicating its role in early metabolic programming [182]. The relative abundance of Veillonella further increases by 2 months of age [183].

We selected elective caesarean deliveries for our study as labour is known to promote pro-inflammatory changes [184,185], which could have introduced unwanted variation in the study immune parameters in our population depending on the length and characteristics of labour and parturition. Further studies will therefore be needed to establish the relative contribution of mode of delivery and nutritional history on the development of NIMA-specific tolerance in the neonate. The applied method of collecting stool samples from nappies is limited by possible contamination with environmental and skin bacteria, which was taken into account during the analysis of microbiome data. A further limitation of this work is the relatively low number of neonates in the examined feeding groups. Nevertheless, we established a unique and homogenous cohort of healthy neonates who were sampled at 3 weeks of age exclusively for the purposes of this study.

In summary, we demonstrate that the neonatal immune system undergoes substantial maturation in the first 3 weeks of life with an increase in IL-17 production in T cells and a simultaneous increase in the Treg population. Moreover, breastfed neonates show a specific and Treg dependent reduction in proliferative T cell responses to NIMA, associated with a reduction in inflammatory cytokine production. These findings add to our understanding of mechanisms by which early life nutrition can determine long term health outcomes [186].

6.5. The impact of phosphodiesterase inhibitors on T cells

In this study, we investigated the effects of caffeine, milrinone and sildenafil on activation kinetics and intracellular cytokine production of adult and cord blood T cells.

Baseline calcium influx upon PHA stimulation was known to be lower in UCB than in APB samples from our earlier results [135]. In the current study, a significant difference was observed in the sensitivity of calcium influx of APB and UCB CD4 cells for the tested PDE inhibitors.

The inhibition of A2A receptors increased calcium influx in APB. This is in line with earlier findings of Linnemann et al. In their study, adenosine prevented rapid tyrosine phosphorylation of ZAP-70 as well as Akt and ERK1/2 in naïve CD3/CD28-stimulated adult CD8 cells. Consequently, CD3/CD28-induced calcium influx into CD8 cells was reduced by exposure to adenosine. These results demonstrated that extracellular adenosine influences membrane-proximal T cell receptor signalling of naïve CD8 T cells [187].

In contrast with ABP, all applied compounds (caffeine, dbcAMP, milrinone, sildenafil, ZM241385) increased calcium influx in UCB samples. However, the increase evoked by caffeine and dbcAMP was larger than that evoked by milrinone, sildenafil and ZM241385.

Therefore, this effect of caffeine on calcium influx appears to be more related to an increase in cAMP levels rather than the inhibition of A2A receptors. The activation of ER RyRs by

caffeine might also be a contributing factor. This is in line with the findings of Thakur et al. who demonstrated that caffeine evoked calcium release from the ER in activated T cells but not in resting T cells, indicating that RyRs are functionally upregulated in activated T cells compared with resting T cells [188].

As for the differences noted between caffeine and the selective PDE inhibitors, their selectivity of cGMP over cAMP may be a responsible factor. While caffeine, as a non-selective PDE inhibitor, may have a higher affinity to prevent the hydrolysis of cAMP over cGMP by blocking various subtypes of PDE, PDE3 is known to hydrolize cAMP and cGMP to a similar extent, while PDE5 specifically hydrolizes cGMP only [189]. Furthermore, cGMP is known to diminish cytoplasmic calcium and to inhibit IP3 [190], potentially contributing to a lower increase of calcium influx upon stimulation in milrinone and sildenafil treated samples.

It is interesting to note that the density of CD203c, an ectoenzyme responsible for the extracellular hydrolysis of cAMP (among other substrates) [191] is decreased on UCB Th1 and CD8 cells compared to their APB counterparts. This decrease may also contribute to the higher sensitivity of calcium influx to cAMP in UCB T lymphocytes due to reduced hydrolysis of cAMP, and in turn its increased concentration in the microenvironment of T lymphocytes.

The baseline concentration of intracellular IFN-γ in CD4 cells was lower in UCB compared to APB. The lower capability of UCB T cells to mount a Th1 response compared to APB is well known from literature [192] and is in line with our current findings.

Intracellular levels of the NFAT transcription factor, which is a key player in cytokine production, were also lower in UCB Th1 and CD8 cells compared to their APB counterparts. NFAT levels were relatively higher in Th2 cells compared to Th1 cells in both UCB and APB samples which is in line with earlier findings [193] and may contribute to the notion that UCB T cells are characterized by a Th2 bias compared to their adult counterparts.

Caffeine, milrinone and sildenafil seemed to have no effect on intracellular cytokine production of APB CD4 cells in our study. This is contradictory to the results of Yoshimura et al. who studied the cytokine production of PHA-stimulated adult PBMCs in the presence of PDE inhibitors or dbcAMP. Non-selective and selective PDE inhibitors for PDE3 and PDE4 were effective at inhibiting the production of IFN-γ and IL-2 in a dose-dependent manner. Their results indicate that PDE inhibitors or dbcAMP modulate Th1 cytokines more effectively than Th2 cytokine production [194]. A potential explanation of the differences between these findings and our current results might be that we studied intracellular cytokine levels by flow cytometry rather than cytokine concentrations measured by ELISA in culture supernatants.

Nonetheless, intracellular production of IL-2 was increased by sildenafil in our study in UCB samples. This effect was confirmed earlier in mice. Kniotek et al. showed that sildenafil diminished serum levels of IL-6 in mice and demonstrated a tendency to increase IL-2 [195]. The clinical significance of this finding remains elusive.

A limitation of this study is the small sample size. Although the populations of neonates and adult controls were homogenous and a large number of cells was analysed in each experiment, the distribution of some of the studied variables was wide which is most probably attributed to this limitation.

Our results demonstrate that caffeine increases short-term activation in neonatal lymphocytes to a larger extent than milrinone or sildenafil. This effect appears to be mediated primarily via increased cAMP levels rather than A2A receptor inhibition and is not present in adult T cells. However, cytokine production of neonatal CD4 cells remains relatively unaffected. Sildenafil may contribute to an increase in the number of IL-2-producing neonatal CD4 cells. Overall, the application of caffeine, sildenafil or milrinone does not appear to have immunosuppressive effects on neonatal T cells based on our findings.

6.6. Perinatal asphyxia and neonatal arterial ischaemic stroke

6.6.1. Perinatal asphyxia

Several studies have described the importance of cytokines in normal neuronal differentiation and survival [196-198]. The perinatal brain might be particularly susceptible to alterations in cytokine concentrations and experimental data suggest that cytokines play a pivotal role in the regulatory network orchestrating neuroinflammation [199]. Cytokines have been in the limelight of research focusing on asphyxia. The inflammatory response following hypoxic brain injury has been shown to have dual effects. A certain level of inflammation appears to be necessary for the adequate regeneration of the brain tissue [86], while extensive neuroinflammation might contribute to further CNS injury and be an important factor in worse functional outcome. Therefore, we aimed to determine factors that might differentiate between infants who have an adequate level of inflammatory response which is necessary for neuroregeneration from infants in whom the uncompensated inflammatory response contributes to brain injury. Previous studies have focused on determining the level of cytokines from plasma. However, plasma cytokine levels have been shown to have a great variability compared with intracellular cytokine levels, which closely reflect cytokine production at a cellular level and show more stable kinetics in time, and thus open new possibilities for more precise characterisation of the cytokine network in immune disorders. The relationship between cellular cytokine production and serum cytokine levels is undefined, cytokines in the serum originate from various different sources and show less stable kinetics. The advantage of intracellular cytokine analysis by flow cytometry is that with this method the cytokine production of each cell type can be accurately described. This method opens up the opportunity for precise characterisation of the function of each cell type in a physiological setting (ie. maintaining autocrine and cell-cell interactions), which could be of great value in identifying

key cellular players of various inflammatory conditions [200,201]. We therefore primarily aimed to describe intracellular cytokine values, however we also measured cytokine levels from plasma to gain a more comprehensive picture of the immunologic alterations following the hypoxic insult. Furthermore, contrary to previous studies, we expanded sampling of infants to one month of age to obtain data on longer term changes in inflammatory parameters evoked by asphyxia.

IL-1β is an important mediator of pro-inflammatory responses [202] and has been reported to have neurotoxic properties leading to BBB breakdown and apoptotic neuronal death [203,204]. Aly et al. found that the cerebrospinal fluid (CSF) level of IL-1β in term neonates had the highest predictive value of poor neurologic outcome in asphyxia after 6 and 12 months, and suggested the central role of IL-1β in the ongoing neuronal injury that occurs in the latent phase following the original hypoxic insult [96]. They also found a high CSF to plasma ratio of IL-1β, indicating elevated local production of the cytokine in the CNS. Several animal models also suggest that IL-1β contributes to the brain injury [205,206]. The exacerbation of ischemic brain injury has also been observed following exogenous administration of IL-1β. Other studies demonstrated that the deficiency of IL-1β converting enzyme or treatment with IL-1 receptor antagonists (IL-1ra) resulted in the moderation of hypoxic brain injury [207,208], decreased post-ischemic oedema [204], and improved neurological outcome [209].

The primary sources of IL-1β are APCs and monocytes [210,211], although microglia and endothelial cells are also capable of producing IL-1β [212,213]. The fact that T lymphocytes are able to produce physiologically relevant amounts of IL-1β and that it plays an important role in their functionality has only recently been revealed [214]. In this study we observed significant IL-1β production in T lymphocytes in neonatal asphyxia, which was more pronounced in a severe insult. In line with previous findings [96], our current results suggest that CD4+ IL-1β+ cells might play an important role in initiating tissue damage in the brain

following the hypoxic insult. However, intracellular concentrations of IL-1β gradually decreased in both patient groups, suggesting that a certain level of initial increase may be necessary for the regenerative processes as well. Based on our ROC analysis, the prevalence of IL-1β-producing CD4+ T cells may be useful in the differentiation of the severity of the insult at an early stage, up to 6 h after birth (**Figure 23**). The notable amount of data showing the therapeutic benefits of peripheral administration of IL-1ra following ischemic brain injury [215] and the fact that IL-1 receptor antagonistic agents are already available in clinical use in autoimmune disorders prompts further research to explore whether IL-1β levels above a certain threshold may be a potential future therapeutic target in neonatal asphyxia.

Several previous studies have associated elevated IL-6 CSF levels with poor neurological outcome, cerebral palsy and death in asphyxia [199,216]. However, Aly et al. suggested that IL-6 might have neurotrophic as well as neuroprotective, anti-inflammatory effects via inhibiting the synthesis of TNF-α and IL-1β [96,217]. They found highly elevated IL-6 CSF to plasma ratios and Martin-Ancel et al. also concluded that IL-6 appears to be primarily produced intrathecally following the ischaemic brain injury while diffusion from the plasma is secondary [199]. In this study, we found that plasma IL-6 levels were elevated in severe compared to moderate asphyxia at one week, and decreased in moderate, but not in severe asphyxia by one month. Intracellular levels of IL-6 in CD4+ cells peaked at 24 hours in both patient groups and declined later. However, we found no alterations in intracellular cytokine levels or cellular prevalence data between the two study groups, suggesting that CSF levels of IL-6 might be of more importance with regards to its deleterious effects.

IL-17 is a pro-inflammatory cytokine produced primarily by Th17 cells upon IL-23 stimulation [218]. IL-17 has been shown to play a pivotal role in the delayed progression of brain infarction following hypoxic injury in a mouse brain ischemia model. This is further supported by the fact that IL-17 KO mice show significant reduction in the infarcted area and apoptotic neuronal

death from the 4th post-stroke day onwards [219]. Yang et al. reported significant influx of Th17 cells into the brain tissue in hypoxic ischaemic encephalopathy following LPS sensitization both in neonates and in newborn rats [220]. In line with previous findings in mouse models, we observed a delayed increase in the prevalence and cytokine production of IL-17 producing T cells, which remained elevated in the severe group during the whole observation period. The prevalence of Th17 lymphocytes was higher in the severe group than in the moderate group at one week. IL-17 could play an important role in maintaining the chronic neuroinflammation leading to detrimental consequences.

TNF-α is a pro-inflammatory cytokine which stimulates the production of IL-1β and among other cytokines regulates the apoptosis of CNS cells, promotes leukocyte differentiation, proliferation and subsequent CNS infiltration [221,222]. There is an extensive amount of data supporting the role of TNF-α in ischemic brain damage [207,223-226]. The level of TNF-α in the CNS has been shown to peak 6-12 hours following the hypoxic ischemic injury in newborn rats [216]. Increased TNF-α and IL-1β plasma and CSF levels in term infants with asphyxia have been associated with neuroradiological alterations, poor neurological status at 12 months of age and cerebral palsy [227,228]. Blocking TNF-α, for example by the administration of pentoxiphylline, a competitive inhibitor of TNF-α, improved neurological outcome by attenuating ICAM-1 expression, reducing the disruption of the BBB and protecting neurons from delayed cell death in animal models of head trauma [229].

In line with previous findings, we found that the MFI of TNF-α in CD4 cells was increased in both groups at all time points compared to 6 h, suggesting a delayed increase in production of TNF-α by T cells following the insult. In severe asphyxia, we observed higher MFI of TNF-α at 1 mo than in moderate asphyxia, which might indicate that TNF-α plays a role in maintaining a chronic inflammatory response in severe asphyxia, thus contributing to long term consequences. We found increased extravasation of TNF-α producing cells at the 6 h (indicated

by decreased prevalence of CD49d-expressing CD4+ TNF-α+ cells), which may indicate the role of TNF-α in determining the extent of the initial tissue injury as well. At later time points we found that the expression of CD49d increased on TNF-α-producing CD4 cells in severe asphyxia, which might further indicate the increased potential of these cells to enter the CNS. Rothhammer et al. were able to demonstrate that under Th1 differentiation promoting circumstances, naive T cells (CD4+ CD44- FoxP3-) differentiate into encephalitogenic T cells in approximately 3 days, expressing high amounts of CD49d in mice [230]. It is therefore possible that an initial decrease in the prevalence of CD49d+ lymphocytes due to extravasation is followed by differentiation of CD4+ CD49d+ lymphocytes from the naïve T lymphocyte pool, leading to an increased prevalence of circulating CD49d+ cells as part of an ongoing inflammatory response.

In order to comprehensively assess the immunosuppressive components of the adaptive immune system in neonatal asphyxia, we examined TGF-β levels, along with the prevalence of Treg cells and the involvement of the KYN pathway. TGF-β plays a critical role in immunosuppression both by inhibiting inflammatory cells and promoting the function of Treg cells via inducing their FoxP3 expression [231-237]. Activated Tregs then produce large amounts of TGF-β, which acts as an important autocrine signal in their activation [238]. TGF-β specifically limits Th1 differentiation and expansion [239,240] without affecting Th2 effector function and suppresses the production of pro-inflammatory cytokines, while promoting the production of anti-inflammatory IL-10 [241]. Besides direct inhibition, Tregs also inhibit T cell function by affecting the APC – T cell interactions, for example via the CTLA-4 engagement-induced TRP catabolism by IDO [242,243].

TGF-β is associated with the reparation of the infarcted tissue and thus is expressed later than pro-inflammatory cytokines [93]. Interestingly, we observed an elevation after 24 h in the intracellular level of TGF-β in moderate asphyxia that was not present following a severe insult,

where the level of TGF-β remained comparable to the 6 h level throughout the whole observation period. We found increased CD49d-expression, which indicates a higher potential of TGF-β producing cells to enter the CNS at one week and one month compared to 72 h in the moderate group. These findings suggest that TGF-β plays an important role in attenuating the inflammatory response and in tissue regeneration following the hypoxic insult in moderate asphyxia. The lack of this effect may contribute to a more severe outcome. We found a moderately elevated prevalence of Tregs in severe compared to moderate asphyxia at 24 h, which might be part of a compensatory mechanism, however, the biological significance of this increase is unremarkable.

Plasma KYN levels were higher at 1 mo in the moderate than in the severe group, which might contribute to an immunosuppressive effect. KYN levels showed a decline in both groups by 1 wk following the insult (**Figure 22**). Similar results were observed for KYNA, while TRP levels increased significantly by one month in both groups. In line with the above, the K/T ratio, indicating IDO enzymatic activity plummeted by one month in both groups. This increased activation of IDO and TRP catabolism in the postnatal period (up to one week) appears to be part of a regulatory mechanism that might play an important role in attenuating the inflammatory response following the hypoxic insult. This effect was comparable in moderate and severe asphyxia, which could mean that this early activation of the KYN pathway is part of the physiological process that accompanies the neuroinflammatory response. However, it appears, that the importance of this regulatory mechanism decreases by one month.

A limitation of our study is that we did not investigate cell prevalence or cytokine levels in CSF samples. Although this would have provided further data on the local inflammatory response in the CNS, collection of CSF samples was not possible due to ethical considerations in the lack of clinical indication. A further limitation of this study is the fact that five neonates in each study group received hydrocortisone during intensive care which might have influenced

their cytokine balance. Further studies are needed to establish the immunologic effects of hydrocortisone therapy in HIE infants undergoing intensive care. Finally, the relatively low number of participants limits the direct clinical utility of the assessment of the prevalence of CD4+ IL-1β+ and CD4+ IL-1β+ CD49d+ cells at 6 h as a predictive marker for the severity of the insult at an early stage in asphyxia.

In conclusion, the need for more specific prognostic markers, other than clinical assessment in neonatal asphyxia is clear, since clinical signs often do not correlate with neurological outcome and do not enable differentiation between moderate and severe hypoxic-ischemic encephalopathy. The role of various cytokines in neuroinflammation following hypoxic-ischemic injury is supported by a rapidly expanding body of evidence. IL-1β and IL-6 appear to play a key role in the early events of the inflammatory response, while TNF-α seems to be responsible for triggering a prolonged inflammation, potentially contributing to a worse outcome. On the other hand, TGF-β has a compensatory role in decreasing the level of inflammation from an early stage following the insult (**Table 11**). Based on ROC analysis, the assessment of the prevalence of CD4+ IL-1β+ and CD4+ IL-1β+ CD49d+ cells at 6 h appears to be able to predict severity at an early stage in asphyxia. Our current results open a potentially fruitful area of research as well as diagnostic and therapeutic development in neonatal asphyxia.

	Pro-inflammatory	Anti-inflammatory
Contribution to better outcome	**IL-1β:** rapid decrease, higher initial prevalence and extravasation in severe insult **G-CSF:** rapid decrease in moderate insult, higher plasma levels in severe insult	**TGF-β:** increased production and extravasation in moderate insult **IDO:** early compensation up to 1 wk
Contribution to worse outcome	**TNF-α:** elevated intracellular levels up to 1 mo **IL-17:** high prevalence in severe insult up to 1 mo **IL-6:** higher plasma levels in severe insult at 1 wk, decrease in moderate insult by 1 mo	**Treg:** unremarkable difference at 24 h, not upregulated

Table 11. Summary of the proposed effects of distinct cytokines on the severity of perinatal asphyxia

6.6.2. Neonatal arterial ischaemic stroke

The contribution of T lymphocytes to ischemic brain injury now appears to be clear, with CD8+ and CD4+ T cells appearing in the CNS already a few hours after an ischemic insult. The accumulation of T cells peaks around 3-4 days following injury and the inhibition of T cell trafficking to the CNS decreases the deleterious consequences of neuroinflammation [107,244]. Data from murine stroke models showed persisting presence of T cells up to 7 weeks after the ischemic attack [245]. In our NAIS patients, CD8 lymphocytes appear to show a different cytokine production pattern than HIE with a more prominent pro-inflammatory response in NAIS. At 6 h CD8 cells from NAIS patients produce higher levels of pro-inflammatory IL-17 than those from neonates with moderate HIE and CD8+ IL17+ cells are more prevalent in NAIS than in severe HIE. At 72 h CD8 cells of neonates with severe HIE

produce higher level of pro-inflammatory IL-6 than CD8 cells of NAIS patients. IL-6 is known to be an important factor in the early phase of HIE and this difference could reflect an aggravated neuroinflammation in severe HIE. On the other hand, IL-6 has also been described to have neurotrophic, neuroregenerative, and anti-inflammatory properties within the brain [225,246-248]. The alteration in intracellular levels of IL-6 in CD8 cells becomes reversed by 1 mo, when it remains elevated in NAIS, whereas it decreases in both HIE groups, indicating that a sustained level of IL-6 might be present for a longer time in NAIS, which is in line with literary data [121]. Therefore, IL-6 may exert its neuroprotective effects over a longer period of time in NAIS.

Plasma cytokine levels also indicate a difference between NAIS and HIE, with a higher level of pro-inflammatory response at 72 h in NAIS than in HIE. We found elevated IL-5, IL-17 and MCP-1 levels at 72 in NAIS. MCP-1 was found to be elevated following ischemic insult after in-utero LPS exposure in a chorioamnionitis associated perinatal stroke murine model [86]. We found an elevation in the level of MCP-1 at 72 h compared to 6 h value in NAIS and to moderate HIE, which supports previous data emphasizing the role of in-utero inflammation. Both the plasma levels of IL-17 and the prevalence of pro-inflammatory Th17 and γδ T cells is known to increase one week after adult acute ischemic stroke [249] and decrease by one month. In line with these findings, we found a higher level of IL-17 in the second phase (at 72 h) of neuroinflammation in NAIS compared with HIE. By one month however, the level of IL-17 decreased in NAIS, while it remained elevated in HIE. We observed the same phenomenon with other cytokines such as IL-4 and IL-12. Overall, the plasma levels of several cytokines appear to decrease by one month of age in NAIS and appears to remain at a higher level in HIE.

We also found alterations in the anti-inflammatory pathways. IL-10 was thought to be primarily produced by CD4+ lymphocytes, however Trandem et al. demonstrated in a murine model of

virus encephalitis, that the most highly activated and cytotoxic CD8+ T cells are also an important source of IL-10 at the peak of the inflammatory response. Their data suggests that CD8+ cells autoregulate their activation by IL-10 production when the inflammatory response reaches a certain level and that CD8 derived IL-10 has a primarily local effect to prevent tissue damage. IL-10 expression by CD8 cells rapidly decreased after 7 days, while CD4+ cells continued to express IL-10 for at least 42 days [250]. Our data showed a significantly higher prevalence of IL-10+ CD8+ lymphocytes in severe HIE than NAIS in the first 72 hours of life. IL10 producing CD8 cells were also more prevalent in mild HIE than in NAIS, however the difference was not significant. A lower prevalence of IL-10 producing CD8 cells, which at the same time produce more of pro-inflammatory cytokines such as IL-17 could lead to a more prominent pro-inflammatory and cytolytic response with decreased auto-regulatory IL-10 production in CD8 cells in NAIS in the first 72 hours. Another interpretation could be that the decreased level of IL-10 production by CD8+ cells reflects an in-utero inflammatory response that decreases by the time of birth. Supporting this hypothesis, in NAIS we found elevated prevalence of CD4+ IL10+ lymphocytes, which are known to produce IL-10 for over a month following the insult. Altogether, it appears that IL-10 production is different in T cell subpopulations in NAIS and HIE and the manipulation of the IL-10 pathway could be interesting to explore from a neuroprotective point of view.

The prevalence of TGF-β producing CD4+ cells, the majority of which are Treg cells was also different in NAIS and HIE. TGF-β is one of the most important cytokines regulating CNS repair. We found increased CD49d expression in this population in NAIS at one week compared to 24 h and both HIE groups, reflecting a higher capacity of these cells to enter the CNS. Meanwhile the prevalence of the entire population decreased by one month in NAIS compared to HIE. This appears to be in line with plasma cytokine data, which showed an increased inflammatory response in NAIS in the second phase of neuroinflammation which

could be followed by an earlier reparative phase and a decreasing inflammatory response by one month of age.

Therapeutic hypothermia is currently the standard of care for term neonates with HIE. There is substantial evidence supporting the role of hypothermia in reducing mortality and improving neurological outcome [251] in infants with hypoxic ischemic encephalopathy. There is notable evidence in animal focal cerebral ischemia models supporting the role of hypothermia in the reduction of infarct size [252] and data suggesting that hypothermia might reduce the risk of seizures after perinatal stroke and thus improve outcome [253]. Therefore, there is intense discussion in the scientific community about extending guidelines to include new categories for therapeutic hypothermia such as preterm HIE and perinatal stroke, however many issues remain to be addressed. Based on results from our previous study, one of the mechanism behind the neuroprotective effect of hypothermia may be the reduction of systemic inflammatory response, seen in the reduced level of cytokines such as IL-6 and IL-4 in HIE patients treated with hypothermia compared to the normothermia group [100]. Therefore, it is likely that hypothermia may similarly reduce cytokine levels following NAIS.

The main limitation of these data is the small number of cases, however, they could provide a hypothesis for future, larger case-control studies. Another limitation is the lack of healthy control population, however, due to ethical considerations and the large number of blood sampling, enrolling healthy neonates was not possible. We also saw a notable variation in certain plasma cytokine levels, which is likely a result of the relative instability of these molecules in plasma. This formed the basis of primarily focusing on intracellular cytokine production in our study. The value of the data from our observations in NAIS could lie in providing incentive for further clinical research on factors enabling differentiation between NAIS and HIE which often present with similar symptoms at birth. Gaining a better

understanding of the underlying pathophysiological factors is a main aim at the current stage of research in NAIS.

CD8 lymphocytes appear to show a shift in the pro-inflammatory direction in NAIS compared with HIE, with elevated production of pro-inflammatory IL-17 at 6 h, decreased auto-regulatory IL-10 production in the first 3 days and elevated production of IL-6 at one month. Altogether the inflammatory response appears to be higher at 72 h in NAIS than in HIE, but appears to decrease faster, indicated by lower levels of inflammatory markers at one month in NAIS than in HIE. Our data indicate similarities to observations in adult acute ischaemic stroke and also support the hypothesis of an ongoing in-utero inflammation prior to NAIS. Further clinical research in this area is pivotal and a better understanding of the pathophysiology could lead to identifying specific factors to distinguish HIE from NAIS early and could open up new pathways for prevention and individualized care.

7. SUMMARY OF NOVEL SCIENTIFIC FINDINGS

7.1. B7 costimulation in the neonate

1. The level of CTLA-4 expression on CD4 cells is higher in umbilical cord blood compared with adult samples, indicating that the possibility of CD28-mediated costimulation may be decreased. The level of the corresponding costimulatory molecule, B7-2, is also elevated. Therefore, this inhibitory relation may function to a higher extent in neonates than in adults.

2. Plasma IDO activity is two-fold higher in umbilical cord blood compared with adult samples. However, the capacity of umbilical cord blood monocytes and T lymphocytes to produce IDO is lower in comparison with adults, and reverse signalling via B7-2 in umbilical cord blood monocytes is immature, suggesting that the observed increase in IDO activity may be due to placental, rather than fetal overexpression of IDO in competent cells.

7.2. B7 costimulation in healthy pregnancy and preeclampsia

3. A significant increase in the prevalence of CD28+ T cells was observed in HP compared to NP women. At the same time a decrease was shown in the expression of CD152 on these cells. The prevalence of both CD278+ and CD279+ T cells was higher in HP than in NP women. The frequency of both CD80+ and CD275+ monocytes was lower in HP women. The frequency of CD80 and CD86 expressing activated monocytes was lower in PE than in HP.

4. The prevalence of IDO-expressing T cells and monocytes was higher in HP compared to NP or PE women. At the same time, MFI values for IDO were also significantly higher in T cells in HP compared to NP or PE women.

7.3. Regulatory T cell subtypes in preeclampsia

5. The earlier described decrease in the prevalence of Tregs in PE is specific for certain Treg subtypes. The prevalence of the functionally most active effector Tregs is decreased to the highest extent, while naive Tregs appear to be unaffected. The combination of lower effector Treg and higher exhausted Treg prevalence may account for the decrease in the functionality of Tregs in PE.

7.4. Breastfeeding and immune development

6. The proportion of regulatory T cells increases in the first three weeks of life and is nearly two-fold higher in exclusively breastfed neonates compared to those who received formula milk only. The proportion of Th17 cells also increases in this period, while that of Th1 cells does not change significantly.

7. Breastfed neonates show a specific and regulatory T cell dependent reduction in proliferative T cell responses to non-inherited maternal antigens, associated with a reduction in inflammatory cytokine production. These data indicate that exposure of the neonate to maternal cells through breastfeeding acts to drive the maturation of regulatory T cells and “tolerizes” the neonate towards non-inherited maternal antigens.

8. We observed the enrichment of short chain fatty acid producing taxa (*Veillonella* and *Gemella*) in stool samples of exclusively breastfed neonates compared to those

receiving formula milk only. Our network modelling analysis links Veillonella to regulatory T cell expansion whilst skin-associated bacteria enhance T cell proliferation in breastfed neonates.

7.5. The impact of phosphodiesterase inhibitors on T cells

9. In adult T lymphocytes, only ZM241385, a specific A2A receptor antagonist causes a 1.14-fold increase in calcium influx, while caffeine, milrinone, sildenafil, ZM241385, and dbcAMP, a synthetic cAMP analogue, all increase calcium influx in T cells derived from umbilical cord blood. Caffeine increases calcium influx in neonatal T lymphocytes to a larger extent than milrinone or sildenafil. This effect appears to be mediated primarily via increased cAMP levels rather than A2A receptor inhibition.

10. Intracellular levels of IFN-γ, IL-2, IL-4, IL-6, IL-17 are unaffected by caffeine, milrinone, sildenafil, ZM241385 or dbcAMP treatment in both adult and umbilical cord blood T cells. Overall, the application of caffeine, sildenafil or milrinone does not appear to have immunosuppressive effects on neonatal T cells.

11. The density of CD203c, an ectoenzyme responsible for the extracellular hydrolysis of cAMP, is decreased on umbilical Th1 and CD8 cells compared to their adult counterparts. This decrease may contribute to the higher sensitivity of calcium influx mediated by cAMP in umbilical T lymphocytes due to an increased cAMP concentration in the microenvironment of T lymphocytes.

12. Intracellular levels of NFAT are lower in umbilical Th1 and CD8 cells compared to their adult counterparts and this may contribute to the notion that umbilical T cells are characterized by a Th2 cytokine bias.

7.6. Perinatal asphyxia and neonatal arterial ischaemic stroke

13. The prevalence and extravasation of CD4+ IL-1β+ cells are higher in severe than in moderate HIE at 6 h. Based on ROC analysis, the assessment of the prevalence of CD4+ IL-1β+ and CD4+ IL-1β+ CD49d+ cells at 6 h appears to be able to predict the severity of the insult at an early stage in HIE.

14. Plasma IL-6 levels were higher at one week in severe HIE and decreased by one month in the moderate group. Intracellular levels of IL-6 peaked at 24 h in both groups. Intracellular levels of TNF-α in CD4 cells were increased at all time points compared to 6 h in both moderate and severe HIE. At one month, intracellular levels of TNF-α were higher in the severe group. Therefore, IL-1β and IL-6 appear to play a key role in the early events of the inflammatory response, while TNF-α seems to be responsible for prolonged neuroinflammation, potentially contributing to a worse outcome.

15. KYN levels showed a decline in both HIE groups by one week following the insult but were higher at one month in the moderate group. Similar results were observed for KYNA, while TRP levels increased significantly by one month in both groups. The increased activation of IDO and TRP catabolism in the immediate postnatal period

appears to be part of a regulatory mechanism that might play an important role in attenuating the inflammatory response following the hypoxic insult.

16. At 6 and 72 h, the prevalence of CD8+ IL-10+ lymphocytes remained lower in NAIS compared to severe HIE. At 6 h, CD8+ lymphocytes in NAIS produced more IL-17 compared to HIE. At 72 h, CD8+ cells produced more IL-6 in severe HIE than in NAIS, but IL-6 production remained elevated in CD8 cells at one month in NAIS, while it decreased in HIE. Overall, CD8 lymphocytes appear to shift towards the pro-inflammatory direction in NAIS compared to HIE.

17. By one month of age, the prevalence of CD4+ TGF-β+ lymphocytes decreased in NAIS compared to HIE. By one month, plasma levels of IL-4, IL-12, and IL-17 also decreased in NAIS but remained elevated in HIE. As a consequence, the inflammatory response appears to be more pronounced at 72 h in NAIS but decreases faster than in HIE.

8. REFERENCES

References to the applicant's publications are marked with bold.

1. Shane AL, Sánchez PJ, Stoll BJ. Neonatal sepsis. Lancet 2017; 390: 1770-80.
2. Hug L, Alexander M, You D, et al. National, regional, and global levels and trends in neonatal mortality between 1990 and 2017, with scenario-based projections to 2030: a systematic analysis. Lancet Glob Health 2019; 7: e710-20.
3. Fleischmann-Struzek C, Goldfarb DM, Schlattmann P, et al. The global burden of paediatric and neonatal sepsis: a systematic review. Lancet Respir Med 2018; 6: 223-30.
4. Zhang X, Zhivaki D, Lo-Man R. Unique aspects of the perinatal immune system. Nat Rev Immunol 2017; 17: 495-507.
5. Kollmann TR, Kampmann B, Mazmanian SK, et al. Protecting the newborn and young infant from infectious diseases: lessons from immune ontogeny. Immunity 2017; 46: 350-63.
6. Gibbons D, Fleming P, Virasami A, et al. Interleukin-8 (CXCL8) production is a signatory T cell effector function of human newborn infants. Nat Med 2014; 20: 1206-10.
7. Olin A, Henckel E, Chen Y, et al. Stereotypic immune system development in newborn children. Cell 2018; 174: 1277-92.
8. Lee AH, Shannon CP, Amenyogbe N, et al. Dynamic molecular changes during the first week of human life follow a robust developmental trajectory. Nat Commun 2019; 10: 1092.

9. Petroff MG, Perchellet A. B7 family molecules as regulators of the maternal immune system in pregnancy. Am J Reprod Immunol 2010; 63: 506-19.

10. Gimmi CD, Freeman GJ, Gribben JG, et al. Human T-cell clonal anergy is induced by antigen presentation in the absence of B7 costimulation. Proc Natl Acad Sci USA 1993; 90: 6586-90.

11. Chambers CA, Kuhns MS, Egen JG, et al. CTLA-4-mediated inhibition in regulation of T cell responses: mechanisms and manipulation in tumor immunotherapy. Annu Rev Immunol 2001; 19: 565-94.

12. Wang S, Bajorath J, Flies DB, et al. Molecular modeling and functional mapping of B7-H1 and B7-DC uncouple costimulatory function from PD-1 interaction. J Exp Med 2003; 197: 1083-91.

13. Nishimura H, Nose M, Hiai H, et al. Development of lupus-like autoimmune diseases by disruption of the PD-1 gene encoding an ITIM motif- carrying immunoreceptor. Immunity 1999; 11: 141-51.

14. Coyle AJ, Lehar S, Lloyd C, et al. The CD28-related molecule ICOS is required for effective T cell-dependent immune responses. Immunity 2000; 13: 95-105.

15. Hutloff A, Dittrich AM, Beier KC, et al. ICOS is an inducible T-cell co-stimulator structurally and functionally related to CD28. Nature 1999; 397: 263-6.

16. Tuettenberg A, Huter E, Hubo M, et al. The role of ICOS in directing T cell responses: ICOS-dependent induction of T cell anergy by tolerogenic dendritic cells. J Immunol 2009; 182: 3349-56.

17. Wang S, Chen L. T lymphocyte co-signaling pathways of the B7-CD28 family. Cell Mol Immunol 2004; 1: 37-42.

18. Grohmann U, Orabona C, Fallarino F, et al. CTLA-4-Ig regulates tryptophan catabolism in vivo. Nat Immunol 2002; 3: 1097-101.

19. Munn DH, Zhou M, Attwood JT, et al. Prevention of allogeneic fetal rejection by tryptophan catabolism. Science 1998; 281: 1191-3.

20. Swartz KJ, During MJ, Freese A, et al. Cerebral synthesis and release of kynurenic acid: an endogenous antagonist of excitatory amino acid receptors. J Neurosci 1990; 10: 2965-73.

21. Vécsei L, Miller J, MacGarvey U, et al. Kynurenine and probenecid inhibit pentylenetetrazol-induced and NMDA-induced seizures and increase kynurenic acid concentrations in the brain. Brain Res Bull 1992; 28: 233-8.

22. Mándi Y, Vécsei L. The kynurenine system and immunoregulation. J Neural Transm 2012; 119: 197-209.

23. Vécsei L, Szalárdy L, Fülöp F, et al. Kynurenines in the CNS: recent advances and new questions. Nat Rev Drug Discov 2013; 12: 64-82.

24. Stone TW. Kynurenines in the CNS: from endogenous obscurity to therapeutic importance. Prog Neurobiol 2001; 64: 185-218.

25. Schwarcz R, Pellicciari R. Manipulation of brain kynurenines: glial targets, neuronal effects, and clinical opportunities. J Pharmacol Exp Ther 2002; 303: 1-10.

26. Marchi M, Risso F, Viola C, et al. Direct evidence that release-stimulating alpha7* nicotinic cholinergic receptors are localized on human and rat brain glutamatergic axon terminals. J Neurochem 2002; 80: 1071-8.

27. Lugo-Huitron R, Blanco-Ayala T, Ugalde-Muniz P, et al. On the antioxidant properties of kynurenic acid: free radical scavenging activity and inhibition of oxidative stress. Neurotoxicol Teratol 2011; 33: 538-47.

28. Redman CW, Sacks GP, Sargent IL. Preeclampsia: an excessive maternal inflammatory response to pregnancy. Am J Obstet Gynecol 1999; 180: 499-506.

29. Saito S, Shiozaki A, Nakashima A, et al. The role of the immune system in preeclampsia. Mol Aspects Med 2007; 28: 192-209.

30. Saito S, Sakai M. Th1/Th2 balance in preeclampsia. J Reprod Immunol 2003; 59: 161-73.

31. Saito S, Nakashima A, Shima T, et al. Th1/Th2/Th17 and regulatory T-cell paradigm in pregnancy. Am J Reprod Immunol 2010; 63: 601-10.

32. Sakaguchi S, Yamaguchi T, Nomura T, et al. Regulatory T cells and immune tolerance. Cell 2008; 133: 775-87.

33. Quinn KH, Parast MM. Decidual regulatory T cells in placental pathology and pregnancy complications. Am J Reprod Immunol 2013; 69: 533-8.

34. Samstein R, Josefowicz S, Arvey A, et al. Extrathymic generation of regulatory T cells in placental mammals mitigates maternal-fetal conflict. Cell 2012; 150: 29-38.

35. Darmochwal-Kolarz D, Saito S, Rolinski J, et al. Activated T lymphocytes in pre-eclampsia. Am J Reprod Immunol 2007; 58: 39-45.

36. Prins JR, Boelens HM, Heimweg J, et al. Preeclampsia is associated with lower percentages of regulatory T cells in maternal blood. Hypertens Pregnancy 2009; 28: 300-11.

37. Steinborn A, Haensch GM, Mahnke K, et al. Distinct subsets of regulatory T cells during pregnancy: is the imbalance of these subsets involved in the pathogenesis of preeclampsia? Clin Immunol 2008; 129: 401-12.

38. Toldi G, Svec P, Vásárhelyi B, et al. Decreased number of FoxP3+ regulatory T cells in preeclampsia. Acta Obstet Gynecol Scand 2008; 87: 1229-33.

39. Tilburgs T, Roelen DL, Van der Mast BJ, et al. Differential distribution of CD4+CD25bright and CD8+CD28- T-cells in decidua and maternal blood during human pregnancy. Placenta 2006; 27 Suppl. A: S47-53.

40. Tilburgs T, Roelen D, van der Mast B, et al. Evidence for a selective migration of fetus-specific CD4+CD25bright regulatory T cells from the peripheral blood to the decidua in human pregnancy. J Immunol 2008; 180: 5737-45.

41. Sasaki Y, Darmochwal-Kolarz D, Suzuki D, et al. Proportion of peripheral blood and decidual CD4+ CD25bright regulatory T cells in pre-eclampsia. Clin Exp Immunol 2007; 149: 139-45.

42. Thornton AM, Korty PE, Tran DQ, et al. Expression of Helios, an Ikaros transcription factor family member, differentiates thymic-derived from peripherally induced Foxp3+ T regulatory cells. J Immunol 2010; 184: 3433-41.

43. Zabransky DJ, Nirschl CJ, Durham NM, et al. Phenotypic and functional properties of Helios+ regulatory T cells. PLoS One 2012; 7: e34547.

44. Cai Q, Dierich A, Oulad-Abdelghani M, et al. Helios deficiency has minimal impact on T cell development and function. J Immunol 2009; 183: 2303-11.

45. Miyara M, Yoshioka Y, Kitoh A, et al. Functional delineation and differentiation dynamics of human CD4+ T cells expressing the FoxP3 transcription factor. Immunity 2009; 30: 899-911.

46. Pan X, Yuan X, Zheng Y, et al. Increased CD45RA+ FoxP3(low) regulatory T cells with impaired suppressive function in patients with systemic lupus erythematosus. PLoS One 2012; 7: e34662.

47. Steinborn A, Schmitt E, Kisielewicz A, et al. Pregnancy-associated diseases are characterized by the composition of the systemic regulatory T cell (Treg) pool with distinct subsets of Tregs. Clin Exp Immunol 2012; 167: 84-98.

48. Saito S, Shima T, Inada K, et al. Which types of regulatory T cells play important roles in implantation and pregnancy maintenance? Am J Reprod Immunol 2013; 69: 340-45.

49. Shen T, Zheng J, Liang H, et al. Characteristics and PD-1 expression of peripheral CD4+CD127loCD25hiFoxp3+ Treg cells in chronic HCV infected-patients. Virol J 2011; 88: 279.

50. Franceschini D, Paroli M, Francavilla V, et al. PD-L1 negatively regulates CD4+CD25+Foxp3+ Tregs by limiting STAT-5 phosphorylation in patients chronically infected with HCV. J Clin Invest 2009; 119: 551-64.

51. Barber DL, Wherry EJ, Masopust D, et al. Restoring function in exhausted CD8 T cells during chronic viral infection. Nature 2006; 439: 682-7.

52. Day CL, Kaufmann DE, Kiepiela P, et al. PD-1 expression on HIV-specific T cells is associated with T-cell exhaustion and disease progression. Nature 2006; 443: 350-4.

53. Brown JA, Dorfman DM, Ma FR, et al. Blockade of programmed death-1 ligands on dendritic cells enhances T cell activation and cytokine production. J Immunol 2003; 170: 1257-66.

54. Sharpe AH, Wherry EJ, Ahmed R, et al. The function of programmed cell death 1 and its ligands in regulating autoimmunity and infection. Nat Immunol 2007; 8: 239-45.

55. Aluvihare VR, Kallikourdis M, Betz AG. Regulatory T cells mediate maternal tolerance to the fetus. Nat Immunol 2004; 5: 266-71.

56. Mold JE, Michaelsson J, Burt TD, et al. Maternal alloantigens promote the development of tolerogenic fetal regulatory T cells in utero. Science 2008; 322:1562-5.

57. McGovern N, Shin A, Low G, et al. Human fetal dendritic cells promote prenatal T-cell immune suppression through arginase-2. Nature 2017; 546: 662-6.

58. Arpaia N, Campbell C, Fan X, et al. Metabolites produced by commensal bacteria promote peripheral regulatory T-cell generation. Nature 2013; 504: 451-5.

59. Salminen S, Gibson GR, McCartney AL, et al. Influence of mode of delivery on gut microbiota composition in seven year old children. Gut 2004; 53: 1388-9.

60. Gritz EC, Bhandari V. The human neonatal gut microbiome: a brief review. Front Pediatr 2017; 3: 17.

61. Walker WA, Iyengar RS. Breast milk, microbiota, and intestinal immune homeostasis. Pediatr Res 2015; 77: 220-8.

62. Verhasselt V. Breastfeeding, a personalized medicine with influence on short- and long-term immune health. Nestle Nutr Inst Workshop Ser 2020; 94: 48-58.

63. Witkowska-Zimny M, Kaminska-El-Hassan E. Cells of human breast milk. Cell Mol Biol Lett 2017; 22: 11.

64. Schmidt B, Roberts RS, Davis P, et al. Caffeine therapy for apnea of prematurity. N Engl J Med 2006; 354: 2112-21.

65. Herlenius E, Lagercrantz H, Yamamoto Y. Adenosine modulates inspiratory neurons and the respiratory pattern in the brainstem of neonatal rats. Pediatr Res 1997; 42: 46-53.

66. Schmidt B, Roberts RS, Davis P, et al. Long-term effects of caffeine therapy for apnea of prematurity. N Engl J Med 2007; 357: 1893-1902.

67. Sei Y, Gallagher KL, Daly JW. Multiple effects of caffeine on Ca2+ release and influx in human B lymphocytes. Cell Calcium 2001; 29: 149-60.

68. De Leon J, Diaz FJ, Rogers T, et al. A pilot study of plasma caffeine concentrations in a US sample of smoker and nonsmoke volunteers. Prog Neuropsychopharmacol Biol Psych 2003; 27: 165-71.

69. Lelo A, Miners JO, Robson R, et al. Assessment of caffeine exposure: caffeine content of beverages, caffeine intake, and plasma concentrations of methylxanthines. Clin Pharmacol Ther 1986; 39: 54-9.

70. Horrigan LA, Kelly JP, Connor TJ. Immunomodulatory effects of caffeine: friend or foe? Pharmacol Ther. 2006; 111: 877-92.

71. Haskó G, Németh ZH, Vizi S, et al. An agonist of adenosine A3 receptors decreases interleukin-12 and interferon-α production and prevents lethality in endotoxemic mice. Eur J Pharmacol 1998; 358: 261-8.

72. Zhang JG, Hepburn L, Cruz G, et al. The role of adenosine A2A and A2B receptors in the regulation of TNF-alpha production by human monocytes. Biochem Pharmacol 2005; 69: 883-9.

73. Szczypka M, Obmińska-Mrukowicz B. Modulating effects of nonselective and selective phosphodiesterase inhibitors on lymphocyte subsets and humoral immune response in mice. Pharmacol Rep 2010; 62: 1148-58.

74. Lawn JE, Cousens S, Zupan J. 4 million neonatal deaths: when? Where? Why? Lancet 2005; 365: 891-900.

75. Beckstrom AC, Humston EM, Snyder LR, et al. Application of comprehensive two-dimensional gas chromatography with time-of-flight mass spectrometry method to identify potential biomarkers of perinatal asphyxia in a non-human primate model. J Chromatogr A 2011; 1218: 1899-1906.

76. Martinez Biarge M, Diez Sebastian J, Wusthoff CJ, et al. Antepartum and intrapartum factors preceding neonatal hypoxic ischemic encephalopathy. Pediatrics 2013; 132: e952-9.

77. Azzopardi DV, Strohm B, Edwards AD, et al. Moderate hypothermia to treat perinatal asphyxial encephalopathy. N Engl J Med 2009; 361: 1349-58.

78. Groenendaal F, van Bel F. Clinical Aspects and Treatment of the Hypoxic Ischemic Syndrome. In: Buonocore G, Bracci R, Weindling M (ed). Neonatology. Springer International Publishing, Cham, 2016.

79. Perlman JM, Tack ED, Martin T, et al. Acute systemic organ injury in term infants after asphyxia. Am J Dis Child 1989; 143: 617-20.

80. Ferriero DM. Neonatal brain injury. N Engl J Med 2004; 351: 1985-95.

81. Van Bel F, Walther FJ. Myocardial dysfunction and cerebral blood flow velocity following birth asphyxia. Acta Paediatr Scand 1990; 79: 756-62.

82. Alderliesten T, Nikkels PG, Benders MJ, et al. Antemortem cranial MRI compared with postmortem histopathologic examination of the brain in term infants with neonatal encephalopathy following perinatal asphyxia. Arch Dis Child Fetal Neonatal Ed 2013; 98: F304-9.

83. Okazaki K, Nishida A, Kato M, et al. Elevation of cytokine concentrations in asphyxiated neonates. Biol Neonate 2006; 89:183-9.

84. Medana I, Li Z, Flugel A, et al. Fas ligand (CD95L) protects neurons against perforin-mediated T lymphocyte cytotoxicity. J Immunol 2001; 167: 674-81.

85. Giuliani F, Goodyer CG, Antel JP, et al. Vulnerability of human neurons to T cell-mediated cytotoxicity. J Immunol 2003; 171: 368-79.

86. Schwartz M, Moalem G, Leibowitz-Amit R, et al. Innate and adaptive immune responses can be beneficial for CNS repair. Trends Neurosci 1999; 22: 295-9.

87. Kerschensteiner M, Meinl E, Hohlfeld R. Neuro-immune crosstalk in CNS diseases. Neuroscience 2009, 158: 1122-32.

88. D'Souza S, Alinauskas K, McCrea E, et al. Differential susceptibility of human CNS-derived cell populations to TNF-dependent and independent immune-mediated injury. J Neurosci 1995; 15: 7293-300.

89. Torres C, Aranguez I, Rubio N. Expression of interferon-gamma receptors on murine oligodendrocytes and its regulation by cytokines and mitogens. Immunology 1995; 86: 250-5.

90. Hisahara S, Shoji S, Okano H, et al. ICE/CED-3 family executes oligodendrocyte apoptosis by tumor necrosis factor. J Neurochem 1997; 69: 10-20.

91. Gehrmann J, Banati RB, Wiessner C, et al. Reactive microglia in cerebral ischaemia: an early mediator of tissue damage? Neuropathol Appl Neurobiol 1995; 21: 277-89.

92. Stoll G, Jander S, Schroeter M. Inflammation and glial responses in ischemic brain lesions. Prog Neurobiol 1998; 56: 149-71.

93. Saliba E, Henrot A. Inflammatory mediators and neonatal brain damage. Biol Neonate 2001; 79: 224-7.

94. Merrill JE. Tumor necrosis factor alpha, interleukin 1 and related cytokines in brain development: normal and pathological. Dev Neurosci 1992; 14: 1-10.

95. Woiciechowsky C, Schoning B, Stoltenburg-Didinger G, et al. Brain-IL-1 beta triggers astrogliosis through induction of IL-6: inhibition by propranolol and IL-10. Med Sci Monit 2004; 10: 325-30.

96. Aly H, Khashaba MT, El-Ayouty M, et al. IL-1beta, IL-6 and TNF-alpha and outcomes of neonatal hypoxic ischemic encephalopathy. Brain Dev 2006; 28: 178-82.

97. Savman K, Blennow M, Gustafson K, et al. Cytokine response in cerebrospinal fluid after birth asphyxia. Pediatr Res 1998; 43: 746-51.

98. Alvarez-Diaz A, Hilario E, de Cerio FG, et al. Hypoxic-ischemic injury in the immature brain--key vascular and cellular players. Neonatology 2007; 92: 227-35.

99. Pongor V, Toldi G, Szabo M, et al. [Systemic and immunomodulatory effects of whole body therapeutic hypothermia]. Orv Hetil 2011; 152: 575-80.

100. Roka A, Beko G, Halasz J, et al. Changes in serum cytokine and cortisol levels in normothermic and hypothermic term neonates after perinatal asphyxia. Inflamm Res 2013; 62: 81-7.

101. Abbott NJ. Inflammatory mediators and modulation of blood-brain barrier permeability. Cell Mol Neurobiol 2000; 20: 131-47.

102. de Vries HE, Blom-Roosemalen MC, van Oosten M, et al. The influence of cytokines on the integrity of the blood-brain barrier in vitro. J Neuroimmunol 1996; 64: 37-43.

103. Issekutz TB. Inhibition of in vivo lymphocyte migration to inflammation and homing to lymphoid tissues by the TA-2 monoclonal antibody. A likely role for VLA-4 in vivo. J Immunol 1991; 147: 4178-84.

104. Baron JL, Madri JA, Ruddle NH, et al. Surface expression of alpha 4 integrin by CD4 T cells is required for their entry into brain parenchyma. J Exp Med 1993; 177: 57-68.

105. Yednock TA, Cannon C, Fritz LC, et al. Prevention of experimental autoimmune encephalomyelitis by antibodies against alpha 4 beta 1 integrin. Nature 1992; 356: 63-6.

106. Polman CH, O'Connor PW, Havrdova E, et al. A randomized, placebo-controlled trial of natalizumab for relapsing multiple sclerosis. N Engl J Med 2006; 354: 899-910.

107. Liesz A, Zhou W, Mracsko E, et al. Inhibition of lymphocyte trafficking shields the brain against deleterious neuroinflammation after stroke. Brain 2011; 134: 704-20.

108. Lee SJ, Benveniste EN. Adhesion molecule expression and regulation on cells of the central nervous system. J Neuroimmunol 1999; 98: 77-88.

109. Raju TN, Nelson KB, Ferriero D, et al. Ischemic perinatal stroke: summary of a workshop sponsored by the National Institute of Child Health and Human Development and the National Institute of Neurological Disorders and Stroke. Pediatrics 2007; 120: 609-16.

110. Kirton A, Deveber G. Life after perinatal stroke. Stroke 2013; 44: 3265-71.

111. Giraud A, Guiraut C, Chevin M, et al. Role of perinatal inflammation in neonatal arterial ischemic stroke. Front Neurol 2017; 8: 612.

112. Nelson KB, Lynch JK. Stroke in newborn infants. Lancet Neurol 2004; 3: 150-8.

113. Guiraut C, Cauchon N, Lepage M, et al. Perinatal arterial ischemic stroke is associated to materno-fetal immune activation and intracranial arteritis. Int J Mol Sci 2016; 17: 1980.

114. Osborn AG. Diagnostic cerebral angiography. Am J Neuroradiol 1999; 20: 1767-9.

115. Kirton A, deVeber G. Paediatric stroke: pressing issues and promising directions. Lancet Neurol 2015; 14: 92-102.

116. Ramaswamy V, Miller SP, Barkovich AJ, et al. Perinatal stroke in term infants with neonatal encephalopathy. Neurology 2004; 62: 2088-91.

117. Kirton A, Armstrong-Wells J, Chang T, et al. Symptomatic neonatal arterial ischemic stroke: the International Pediatric Stroke Study. Pediatrics 2011; 128: e1402-10.

118. Chalmers EA. Perinatal stroke--risk factors and management. Br J Haematol 2005; 130: 333-43.

119. Bernson-Leung ME, Rivkin MJ. Stroke in neonates and children. Pediatr Rev 2016; 37: 463-77.

120. Husson B, Hertz-Pannier L, Adamsbaum C, et al. MR angiography findings in infants with neonatal arterial ischemic stroke in the middle cerebral artery territory: A prospective study using circle of Willis MR angiography. Eur J Radiol 2016; 85: 1329-35.

121. Yururer D, Teber S, Deda G, et al. The relation between cytokines, soluble endothelial protein C receptor, and factor VIII levels in Turkish pediatric stroke patients. Clin Appl Thromb Hemost 2009; 15: 545-51.

122. Yilmaz G, Arumugam TV, Stokes KY, et al. Role of T lymphocytes and interferon-gamma in ischemic stroke. Circulation 2006; 113: 2105-12.

123. Vogelgesang A, Becker KJ, Dressel A. Immunological consequences of ischemic stroke. Acta Neurol Scand 2014; 129: 1-12.

124. Siniscalchi A, Gallelli L, Malferrari G, et al. Cerebral stroke injury: the role of cytokines and brain inflammation. J Basic Clin Physiol Pharmacol 2014; 25: 131-37.

125. Zhu Y, Yang GY, Ahlemeyer B, et al. Transforming growth factor-beta 1 increases bad phosphorylation and protects neurons against damage. J Neurosci 2002; 22: 3898-909.

126. Spera PA, Ellison JA, Feuerstein GZ, et al. IL-10 reduces rat brain injury following focal stroke. Neurosci Lett 1998; 251: 189-92.

127. Herve C, Beyne P, Jamault H, et al. Determination of tryptophan and its kynurenine pathway metabolites in human serum by high-performance liquid chromatography with simultaneous ultraviolet and fluorimetric detection. J Chromatogr B 1996; 675: 157-61.

128. Betts MR, Brenchley JM, Price DA, et al. Sensitive and viable identification of antigen-specific CD8+ T cells by a flow cytometric assay for degranulation. J Immunol Methods 2003; 281: 65-78.

129. Powell RM, Lissauer D, Tamblyn J, et al. Decidual T cells exhibit a highly differentiated phenotype and demonstrate potential fetal specificity and a strong transcriptional response to IFN. J Immunol 2017; 199: 3406-17.

130. Caporaso JG, Lauber CL, Walters WA, et al. Ultra-high-throughput microbial community analysis on the Illumina HiSeq and MiSeq platforms. ISME J 2012; 6: 1621-4.

131. Quraishi MN, Acharjee A, Beggs AD, et al. A pilot integrative analysis of colonic gene expression, gut microbiota and immune infiltration in primary sclerosing

cholangitis-inflammatory bowel disease: association of disease with bile acid pathways. J Crohns Colitis 2020; 14: 935-47.

132. Hall M, Beiko RG. 16S rRNA gene analysis with QIIME2. Methods Mol Biol 2018; 1849: 113-29.

133. Breiman L. Random Forests. Machine Learning 2001; 45: 5-32.

134. Orbán C, Bajnok A, Vásárhelyi B, et al. Different calcium influx characteristics upon Kv1.3 and IKCa1 potassium channel inhibition in T helper subsets. Cytometry A 2014; 85: 636-41.

135. Toldi G, Treszl A, Pongor V, et al. T-lymphocyte calcium influx characteristics and their modulation by Kv1.3 and IKCa1 channel inhibitors in the neonate. Int Immunol 2010; 22: 769-74.

136. Kaposi AS, Veress G, Vásárhelyi B, et al. Cytometry-acquired calcium-flux data analysis in activated lymphocytes. Cytometry A 2008; 73: 246-53.

137. Azzopardi D, Brocklehurst P, Edwards D, et al. The TOBY Study. Whole body hypothermia for the treatment of perinatal asphyxial encephalopathy: a randomised controlled trial. BMC Pediatr 2008; 8: 17.

138. Cseko AJ, Bango M, Lakatos P, et al. Accuracy of amplitude-integrated electroencephalography in the prediction of neurodevelopmental outcome in asphyxiated infants receiving hypothermia treatment. Acta Paediatr 2013; 102: 707-11.

139. Rutherford M, Malamateniou C, McGuinness A, et al. Magnetic resonance imaging in hypoxic-ischaemic encephalopathy. Early Hum Dev 2010; 86: 351-60.

140. Cossarizza A, Chang HD, Radbruch A, et al. Guidelines for the use of flow cytometry and cell sorting in immunological studies. Eur J Immunol. 2017; 47: 1584-797.

141. Adkins B. T-cell function in newborn mice and humans. Immunol Today 1999; 220: 330-5.

142. Han P, McDonald T, Hodge G. Potential immaturity of the T-cell and antigen-presenting cell interaction in cord blood with particular emphasis on the CD40-CD40 ligand costimulatory pathway. Immunology 2004; 113: 26-34.

143. Stewart M, Thiel M, Hogg N. Leukocyte integrins. Curr Opin Cell Biol 1995; 7: 690-6.

144. Sorg RV, Kogler G, Wernet P. Identification of cord blood dendritic cells as an immature CD11c-population. Blood 1999; 93: 2302-7.

145. Borras FE, Matthews NC, Lowdell MW, et al. Identification of both myeloid CD11c+ and lymphoid CD11c- dendritic cell subsets in cord blood. Br J Haematol 2001; 113: 925-31.

146. Elliott SR, Macardle PJ, Roberton DM, et al. Expression of the costimulator molecules, CD80, CD86, CD28, and CD152 on lymphocytes from neonates and young children. Hum Immunol 1999; 60: 1039-48.

147. Darmochwal-Kolarz D, Serafin A, Tabarkiewicz J, et al. The expressions of co-stimulatory molecules are altered on putative antigen-presenting cells in cord blood. Am J Reprod Immunol 2013; 69: 180-7.

148. Grohmann U, Fallarino F, Puccetti P. Tolerance, DCs and tryptophan: much ado about IDO. Trends Immunol 2003; 24: 242-8.

149. Fukui S, Schwarcz R, Rapoport SI, et al. Blood-brain barrier transport of kynurenines: implications for brain synthesis and metabolism. J Neurochem. 1991; 56: 2007-17.

150. Jin LP, Fan DX, Zhang T, et al. The costimulatory signal upregulation is associated with Th1 bias at the maternal-fetal interface in human miscarriage. Am J Reprod Immunol 2011; 66: 270-8.

151. Taglauer ES, Trikhacheva AS, Slusser JG, et al. Expression and function of PDCD1 at the human maternal-fetal interface. Biol Reprod 2008; 79: 562-9.

152. Paeschke S, Chen F, Horn N, et al. Pre-eclampsia is not associated with changes in the levels of regulatory T cells in peripheral blood. Am J Reprod Immunol 2005; 54: 384-9.

153. Miko E, Szereday L, Barakonyi A, et al. Immunoactivation in preeclampsia: Vdelta2+ and regulatory T cells during the inflammatory stage of disease. J Reprod Immunol 2009; 80: 100-8.

154. Sasaki Y, Sakai M, Miyazaki S, et al. Decidual and peripheral blood CD4+ CD25+ regulatory T cells in early pregnancy subjects and spontaneous abortion cases. Mol Hum Reprod 2004; 10: 347-53.

155. Holthe MR, Staff AC, Berge LN, et al. Leukocyte adhesion molecules and reactive oxygen species in preeclampsia. Obstet Gynecol 2004; 103: 913-22.

156. Miwa N, Hayakawa S, Miyazaki S, et al. IDO expression on decidual and peripheral blood dendritic cells and monocytes/macrophages after treatment with CTLA-4 or interferon-c increase in normal pregnancybut decrease in spontaneous abortion. Mol Hum Reprod 2005; 11: 865-70.

157. Liu X, Liu Y, Ding M, et al. Reduced expression of indoleamine 2,3-dioxygenase participates in pathogenesis of preeclampsia via regulatory T cells. Mol Med Report 2011; 4: 53-8.

158. Darmochwal-Kolarz D, Kludka-Sternik M, Tabarkiewicz J, et al. The predominance of Th17 lymphocytes and decreased number and function of Treg cells in preeclampsia. J Reprod Immunol 2012; 93: 75-81.

159. Hsu P, Santner-Nanan B, Dahlstrom JE, et al. Altered decidual DC-SIGN+ antigen-presenting cells and impaired regulatory T-cell induction in preeclampsia. Am J Pathol 2012; 181: 2149-60.

160. Vieira Borba V, Sharif K, Shoenfeld Y. Breastfeeding and autoimmunity: Programing health from the beginning. Am J Reprod Immunol 2018; 79: e12778.

161. Oddy WH. Breastfeeding, childhood asthma, and allergic disease. Ann Nutr Metab 2017; 70 Suppl 2: 26-36.

162. Victoria CG, Bahl R, Barros AJD, et al. Breastfeeding in the 21st century: epidemiology, mechanisms, and lifelong effect. Lancet 2016; 387: 475-90.

163. de Silva D, Halken S, Singh C, et al. Preventing food allergy in infancy and childhood: Systematic review of randomised controlled trials. Pediatr Allergy Immunol 2020; 31: 813-26.

164. Schaier M, Seissler M, Schmitt E, et al. DR(high+)CD45RA(-)-Tregs potentially affect the suppressive activity of the total Treg pool in renal transplant patients. PLoS One 2012; 7: e34208.

165. Ramanan D, Sefik E, Galvan-Pena S, et al. An immunologic mode of multigenerational transmission governs a gut Treg setpoint. Cell 2020; 181: 1276-90.

166. Vuillermin PJ, Ponsonby AL, Saffery R, et al. Microbial exposure, interferon gamma gene demethylation in naive T-cells, and the risk of allergic disease. Allergy 2009; 64: 348-53.

167. Fike AJ, Kumova OK, Carey AJ. Dissecting the defects in the neonatal CD8+ T-cell response. J Leukoc Biol 2019; 106: 1051-61.

168. Galindo-Albarrán AO, López-Portales OH, Gutiérrez-Reyna DY, et al. CD8+ T cells from human neonates are biased toward an innate immune response. Cell Rep 2016; 17: 2151-60.

169. Moles JP, Tuaillon E, Kankasa C, et al. Breastmilk cell trafficking induces microchimerism-mediated immune system maturation in the infant. Pediatr Allergy Immunol 2018; 29: 133-43.

170. Kinder JM, Stelzer IA, Arck PC, et al. Immunological implications of pregnancy-induced microchimerism. Nat Rev Immunol 2017; 17: 483-94.

171. Aoyama K, Matsuoka KI, Teshima T. Breast milk and transplantation tolerance. Chimerism 2010; 1: 19-20.

172. Aoyama K, Koyama M, Matsuoka K, et al. Improved outcome of allogeneic bone marrow transplantation due to breastfeeding-induced tolerance to maternal antigens. Blood 2009; 113: 1829-33.

173. Darby MG, Chetty A, Mrjden D, et al. Pre-conception maternal helminth infection transfers via nursing long-lasting cellular immunity against helminths to offspring. Sci Adv 2019; 5: eaav3058.

174. Li D, Shi Y, Yang L, et al. Microplastic release from the degradation of polypropylene feeding bottles during infant formula preparation. Nat Food 2020; 1: 746-54.

175. Banerjee A, Shelver WL. Micro- and nanoplastic induced cellular toxicity in mammals: A review. Sci Total Environ 2020; 755: 142518.

176. Xiao L, Van't Land B, Engen PA, et al. Human milk oligosaccharides protect against the development of autoimmune diabetes in NOD-mice. Sci Rep 2018; 8: 3829.

177. Xiao L, van De Worp W, Stassen R, et al. Human milk oligosaccharides promote immune tolerance via direct interactions with human dendritic cells. Eur J Immunol 2019; 49: 1001-14.

178. Logan AC, Jacka FN, Prescott SL. Immune-microbiota interactions: dysbiosis as a global health issue. Curr Allergy Asthma Rep 2016; 16: 13.

179. Shao Y, Forster SC, Tsaliki E, et al. Stunted microbiota and opportunistic pathogen colonization in caesarean-section birth. Nature 2019; 574: 117-21.

180. Davis EC, Wang M, Donovan SM. The role of early life nutrition in the establishment of gastrointestinal microbial composition and function. Gut Microbes 2017; 8: 143-71.

181. Timmerman HM, Rutten NBMM, Boekhorst J, et al. Intestinal colonisation patterns in breastfed and formula-fed infants during the first 12 weeks of life reveal sequential microbiota signatures. Sci Rep 2017; 7: 8327.

182. Younge NE, Newgard CB, Cotten CM, et al. Disrupted maturation of the microbiota and metabolome among extremely preterm infants with postnatal growth failure. Sci Rep 2019; 9: 8167.

183. Kuang YS, Li SH, Guo Y, et al. Composition of gut microbiota in infants in China and global comparison. Sci Rep 2016; 6: 36666.

184. Norman JE, Bollapragada S, Yuan M, et al. Inflammatory pathways in the mechanism of parturition. BMC Pregnancy Childbirth 2007; 7 Suppl 1: S7.

185. Shah NM, Edey LF, Imami N, et al. Human labour is associated with altered regulatory T cell function and maternal immune activation. Clin Exp Immunol 2020; 199: 182-200.

186. Binns C, Lee M, Low WY. The long-term public health benefits of breastfeeding. Asia Pac J Public Health 2016; 28: 7-14.

187. Linnemann C, Schildberg FA, Schurich A, et al. Adenosine regulates CD8 T-cell priming by inhibition of membrane-proximal T-cell receptor signalling. Immunology. 2009; 128: e728-37.

188. Thakur P, Dadsetan S, Fomina AF. Bidirectional coupling between ryanodine receptors and Ca2+ release-activated Ca2+ (CRAC) channel machinery sustains store-operated Ca2+ entry in human T lymphocytes. J Biol Chem 2012; 287: 37233-44.

189. Weiss B. Differential activation and inhibition of the multiple forms of cyclic nucleotide phosphodiesterase. Adv Cyclic Nucleotide Res 1975; 5: 195-211.

190. Guerrero A, Singer JJ, Fay FS. Simultaneous measurement of Ca2+ release and influx into smooth muscle cells in response to caffeine. A novel approach for calculating the fraction of current carried by calcium. J Gen Physiol 1994; 104: 395-442.

191. Bühring HJ, Seiffert M, Giesert C, et al. The basophil activation marker defined by antibody 97A6 is identical to the ectonucleotide pyrophosphatase/phosphodiesterase 3. Blood 2001; 97: 3303-5.

192. Zaghouani H, Hoeman CM, Adkins B. Neonatal immunity: faulty T-helpers and the shortcomings of dendritic cells. Trends Immunol 2009; 30: 585-91.

193. Hermann-Kleiter N, Baier G. NFAT pulls the strings during CD4+ T helper cell effector functions. Blood 2010; 115: 2989-97.

194. Yoshimura T, Nagao T, Nakao T, et al. Modulation of Th1- and Th2-like cytokine production from mitogen-stimulated human peripheral blood mononuclear cells by phosphodiesterase inhibitors. Gen Pharmacol 1998; 30: 175-80.

195. Kniotek M, Boguska A. Sildenafil can affect innate and adaptive immune system in both experimental animals and patients. J Immunol Res. 2017; 2017: 4541958.

196. Satoh T, Nakamura S, Taga T, et al. Induction of neuronal differentiation in PC12 cells by B-cell stimulatory factor 2/interleukin 6. Mol Cell Biol 1988; 8: 3546-9.

197. Hama T, Miyamoto M, Tsukui H, et al. Interleukin-6 as a neurotrophic factor for promoting the survival of cultured basal forebrain cholinergic neurons from postnatal rats. Neurosci Lett 1989; 104: 340-4.

198. Mehler MF, Marmur R, Gross R, et al. Cytokines regulate the cellular phenotype of developing neural lineage species. Int J Dev Neurosci 1995; 13: 213-40.

199. Martin-Ancel A, Garcia-Alix A, Pascual-Salcedo D, et al. Interleukin-6 in the cerebrospinal fluid after perinatal asphyxia is related to early and late neurological manifestations. Pediatrics 1997; 100: 789-94.

200. Buck RH, Cordle CT, Thomas DJ, et al. Longitudinal study of intracellular T cell cytokine production in infants compared to adults. Clin Exp Immunol 2002; 128: 490-7.

201. Jason J, Archibald LK, Nwanyanwu OC, et al. Comparison of serum and cell-specific cytokines in humans. Clin Diagn Lab Immunol 2001; 8: 1097-103.

202. Ren K, Torres R. Role of interleukin-1beta during pain and inflammation. Brain Res Rev 2009; 60: 57-64.

203. Friedlander RM, Gagliardini V, Hara H, et al. Expression of a dominant negative mutant of interleukin-1 beta converting enzyme in transgenic mice prevents neuronal cell death induced by trophic factor withdrawal and ischemic brain injury. J Exp Med 1997; 185: 933-40.

204. Yamasaki Y, Matsuura N, Shozuhara H, et al. Interleukin-1 as a pathogenetic mediator of ischemic brain damage in rats. Stroke 1995; 26: 676-80.

205. Buttini M, Boddeke H. Peripheral lipopolysaccharide stimulation induces interleukin-1 beta messenger RNA in rat brain microglial cells. Neuroscience 1995; 65: 523-30.

206. Yabuuchi K, Minami M, Katsumata S, et al. An in situ hybridization study on interleukin-1 beta mRNA induced by transient forebrain ischemia in the rat brain. Brain Res Mol Brain Res 1994; 26: 135-42.

207. Hagberg H, Gilland E, Bona E, et al. Enhanced expression of interleukin (IL)-1 and IL-6 messenger RNA and bioactive protein after hypoxia-ischemia in neonatal rats. Pediatr Res 1996; 40: 603-9.

208. Liu F, Ooi VE, Fung MC. Analysis of immunomodulating cytokine mRNAs in the mouse induced by mushroom polysaccharides. Life Sci 1999; 64: 1005-11.

209. Garcia JH, Liu KF, Relton JK. Interleukin-1 receptor antagonist decreases the number of necrotic neurons in rats with middle cerebral artery occlusion. Am J Pathol 1995; 147: 1477-86.

210. Dinarello CA. Biologic basis for interleukin-1 in disease. Blood 1996; 87: 2095-147.

211. Rao DA, Tracey KJ, Pober JS. IL-1alpha and IL-1beta are endogenous mediators linking cell injury to the adaptive alloimmune response. J Immunol 2007; 179: 6536-46.

212. Heneka MT, Kummer MP, Stutz A, et al. NLRP3 is activated in Alzheimer's disease and contributes to pathology in APP/PS1 mice. Nature 2013; 493: 674-8.

213. Shahzad K, Bock F, Dong W, et al. Nlrp3-inflammasome activation in non-myeloid-derived cells aggravates diabetic nephropathy. Kidney Int 2015; 87: 74-84.

214. Doitsh G, Galloway NL, Geng X, et al. Cell death by pyroptosis drives CD4 T-cell depletion in HIV-1 infection. Nature 2014; 505: 509-14.

215. Relton JK, Martin D, Thompson RC, et al. Peripheral administration of Interleukin-1 Receptor antagonist inhibits brain damage after focal cerebral ischemia in the rat. Exp Neurol 1996; 138: 206-13.

216. Silveira RC, Procianoy RS. Interleukin-6 and tumor necrosis factor-alpha levels in plasma and cerebrospinal fluid of term newborn infants with hypoxic-ischemic encephalopathy. J Pediatr 2003; 143: 625-9.

217. Chiesa C, Pellegrini G, Panero A, et al. Umbilical cord interleukin-6 levels are elevated in term neonates with perinatal asphyxia. Eur J Clin Invest 2003; 33: 352-8.

218. Langrish CL, Chen Y, Blumenschein WM, et al. IL-23 drives a pathogenic T cell population that induces autoimmune inflammation. J Exp Med 2005; 201: 233-40.

219. Shichita T, Sugiyama Y, Ooboshi H, et al. Pivotal role of cerebral interleukin-17-producing gammadeltaT cells in the delayed phase of ischemic brain injury. Nat Med 2009; 15: 946-50.

220. Yang D, Sun YY, Bhaumik SK, et al. Blocking lymphocyte trafficking with FTY720 prevents inflammation-sensitized hypoxic-ischemic brain injury in newborns. J Neurosci 2014; 34: 16467-81.

221. Pulera MR, Adams LM, Liu H, et al. Apoptosis in a neonatal rat model of cerebral hypoxia-ischemia. Stroke 1998; 29: 2622-30.

222. Tarkowski E, Rosengren L, Blomstrand C, et al. Intrathecal expression of proteins regulating apoptosis in acute stroke. Stroke 1999; 30: 321-7.

223. Szaflarski J, Burtrum D, Silverstein FS. Cerebral hypoxia-ischemia stimulates cytokine gene expression in perinatal rats. Stroke 1995; 26: 1093-100.

224. Stroemer RP, Rothwell NJ. Exacerbation of ischemic brain damage by localized striatal injection of interleukin-1beta in the rat. J Cereb Blood Flow Metab 1998; 18: 833-9.

225. Loddick SA, Turnbull AV, Rothwell NJ. Cerebral interleukin-6 is neuroprotective during permanent focal cerebral ischemia in the rat. J Cereb Blood Flow Metab 1998; 18: 176-9.

226. Dihne M, Block F. Focal ischemia induces transient expression of IL-6 in the substantia nigra pars reticulata. Brain Res 2001; 889: 165-73.

227. Oygur N, Sonmez O, Saka O, et al. Predictive value of plasma and cerebrospinal fluid tumour necrosis factor-alpha and interleukin-1 beta concentrations on outcome of full term infants with hypoxic-ischaemic encephalopathy. Arch Dis Child Fetal Neonatal Ed 1998; 79: F190-3.

228. Foster-Barber A, Dickens B, Ferriero DM. Human perinatal asphyxia: correlation of neonatal cytokines with MRI and outcome. Dev Neurosci 2001; 23: 213-8.

229. Shohami E, Bass R, Wallach D, et al. Inhibition of tumor necrosis factor alpha (TNFalpha) activity in rat brain is associated with cerebroprotection after closed head injury. J Cereb Blood Flow Metab 1996; 16: 378-84.

230. Rothhammer V, Heink S, Petermann F, et al. Th17 lymphocytes traffic to the central nervous system independently of alpha4 integrin expression during EAE. J Exp Med 2011; 208: 2465-76.

231. Kehrl JH, Wakefield LM, Roberts AB, et al. Production of transforming growth factor beta by human T lymphocytes and its potential role in the regulation of T cell growth. J Exp Med 1986; 163: 1037-50.

232. Kulkarni AB, Huh CG, Becker D, et al. Transforming growth factor beta 1 null mutation in mice causes excessive inflammatory response and early death. Proc Natl Acad Sci U S A 1993; 90: 770-4.

233. Gorelik L, Flavell RA. Abrogation of TGFbeta signaling in T cells leads to spontaneous T cell differentiation and autoimmune disease. Immunity 2000; 12: 171-81.

234. Laouar Y, Sutterwala FS, Gorelik L, et al. Transforming growth factor-beta controls T helper type 1 cell development through regulation of natural killer cell interferon-gamma. Nat Immunol 2005; 6: 600-7.

235. Lucas PJ, Kim SJ, Melby SJ, et al. Disruption of T cell homeostasis in mice expressing a T cell-specific dominant negative transforming growth factor beta II receptor. J Exp Med 2000; 191: 1187-96.

236. Yang X, Letterio JJ, Lechleider RJ, et al. Targeted disruption of SMAD3 results in impaired mucosal immunity and diminished T cell responsiveness to TGF-beta. EMBO J 1999; 18: 1280-91.

237. Wan YY, Flavell RA. 'Yin-Yang' functions of transforming growth factor-beta and T regulatory cells in immune regulation. Immunol Rev 2007; 220: 199-213.

238. Li MO, Wan YY, Flavell RA. T cell-produced transforming growth factor-beta1 controls T cell tolerance and regulates Th1- and Th17-cell differentiation. Immunity 2007; 26: 579-91.

239. Gorelik L, Flavell RA. Transforming growth factor-beta in T-cell biology. Nat Rev Immunol 2002; 2: 46-53.

240. Sad S, Mosmann TR. Single IL-2-secreting precursor CD4 T cell can develop into either Th1 or Th2 cytokine secretion phenotype. J Immunol 1994; 153: 3514-22.

241. Kitani A, Fuss I, Nakamura K, et al. Transforming growth factor (TGF)-beta1-producing regulatory T cells induce Smad-mediated interleukin 10 secretion that facilitates coordinated immunoregulatory activity and amelioration of TGF-beta1-mediated fibrosis. J Exp Med 2003; 198: 1179-88.

242. Fallarino F, Grohmann U, Hwang KW, et al. Modulation of tryptophan catabolism by regulatory T cells. Nat Immunol 2003; 4: 1206-12.

243. Tadokoro CE, Shakhar G, Shen S, et al. Regulatory T cells inhibit stable contacts between CD4+ T cells and dendritic cells in vivo. J Exp Med 2006; 203: 505-11.

244. Gelderblom M, Leypoldt F, Steinbach K, et al. Temporal and spatial dynamics of cerebral immune cell accumulation in stroke. Stroke 2009; 40: 1849-57.

245. Selvaraj UM, Stowe AM. Long-term T cell responses in the brain after an ischemic stroke. Discov Med 2017; 24: 323-33.

246. Sun L, Li Y, Jia X, et al. Neuroprotection by IFN-γ via astrocyte-secreted IL-6 in acute neuroinflammation. Oncotarget 2017; 8: 40065-78.

247. Hirota H, Kiyama H, Kishimoto T, et al. Accelerated Nerve Regeneration in Mice by upregulated expression of interleukin (IL) 6 and IL-6 receptor after trauma. J Exp Med 1996; 183: 2627-34.

248. Sébire G, Emilie D, Wallon C, et al. In vitro production of IL-6, IL-1 beta, and tumor necrosis factor-alpha by human embryonic microglial and neural cells. J Immunol 1993; 150: 1517-23.

249. Hu Y, Zheng Y, Wu Y, et al. Imbalance between IL-17A-producing cells and regulatory T cells during ischemic stroke. Mediators Inflamm 2014; 2014: 813045.

250. Trandem K, Zhao J, Fleming E, et al. Highly activated cytotoxic CD8 T cells express protective IL-10 at the peak of coronavirus-induced encephalitis. J Immunol 2011; 186: 3642-52.

251. Azzopardi D, Strohm B, Marlow N, et al. Effects of hypothermia for perinatal asphyxia on childhood outcomes. N Engl J Med 2014; 371: 140-9.

252. Gancia P, Pomero G. Therapeutic hypothermia in the prevention of hypoxic-ischaemic encephalopathy: new categories to be enrolled. J Matern Fetal Neonatal Med 2012; 25 Suppl 4: 94-6.

253. Harbert MJ, Tam EW, Glass HC, et al. Hypothermia is correlated with seizure absence in perinatal stroke. J Child Neurol 2011; 26: 1126-30.

9. LIST OF PUBLICATIONS OF THE APPLICANT

9.1. International publications presented in detail in this thesis

1. Grozdics E, Berta L, Gyarmati B, Veres G, Zádori D, Szalárdy L, Vécsei L, Tulassay T, **Toldi G.** B7 costimulation and intracellular indoleamine 2,3-dioxygenase (IDO) expression in umbilical cord blood and adult peripheral blood. Biol Blood Marrow Transplant. 2014;20:1659-65. IF: 3.404
2. Grozdics E, Berta L, Bajnok A, Veres G, Ilisz I, Klivényi P, Rigó J Jr, Vécsei L, Tulassay T, **Toldi G.** B7 costimulation and intracellular indoleamine-2,3-dioxygenase (IDO) expression in peripheral blood of healthy pregnant and non-pregnant women. BMC Pregnancy Childbirth. 2014;14:306. IF: 2.190
3. **Toldi G,** Vásárhelyi B, Biró E, Fügedi G, Rigó J Jr, Molvarec A. B7 costimulation and intracellular indoleamine-2,3-dioxygenase (IDO) expression in peripheral blood of healthy pregnant and preeclamptic women. Am J Reprod Immunol. 2013;69:264-71. IF: 2.668
4. **Toldi G,** Vásárhelyi ZE, Rigó J Jr, Orbán C, Tamássy Z, Bajnok A, Shima T, Saito S, Molvarec A. Prevalence of regulatory T cell (Treg) subtypes in preeclampsia. Am J Reprod Immunol. 2015;74:110-5. IF: 2.916
5. Wood HL, Acharjee A, Pearce H, Quraishi MN, Powell RM, Rossiter AE, Beggs AD, Ewer AK, Moss P, **Toldi G.** Breastfeeding promotes early neonatal regulatory T cell expansion and immune tolerance of non-inherited maternal antigens. Allergy. 2020, in press. *IF: 8.706*
6. Orbán C, Vásárhelyi Z, Bajnok A, Sava F, **Toldi G.** Effects of caffeine and phosphodiesterase inhibitors on activation of neonatal T lymphocytes. Immunobiology. 2018;223:627-633. IF: 2.798

7. Bajnok A, Berta L, Orbán C, Veres G, Zádori D, Barta H, Méder Ü, Vécsei L, Tulassay T, Szabó M, **Toldi G**. Distinct cytokine patterns may regulate the severity of neonatal asphyxia – an observational study. J Neuroinflammation. 2017;14:244. IF: 5.193
8. Bajnok A, Berta L, Orbán C, Tulassay T, **Toldi G.** Cytokine production pattern of T lymphocytes in neonatal arterial ischemic stroke during the first month of life - a case study. J Neuroinflammation. 2018;15:191. IF: 5.700

Number of citations to the above papers: 88.

9.2. Hungarian publication related to the present thesis

1. Pongor V, **Toldi G,** Szabó M, Vásárhelyi B. Systemic and immunomodulatory effects of whole body therapeutic hypothermia. Orv Hetil. 2011;152:575-580.

9.3. International publications not related to the present thesis published after obtaining the PhD degree

1. Williamson SL, Gadd E, Pillay T, **Toldi G.** Non-specific effects of BCG vaccination on neutrophil and lymphocyte counts of healthy neonates from a developed country. Vaccine. 2021, in press. *IF: 3.143*
2. Folyovich A, Mátis R, Al-Muhanna N, Jarecsny T, Dudás E, Jánoska D, Pálosi M, Béres-Molnár AK, **Toldi G.** Christmas, acute ischemic stroke and stroke-related mortality in Hungary. Brain Behav. 2021, in press. *IF: 2.091*
3. Balog A, Varga B, Fülöp F, Lantos I, **Toldi G,** Vécsei L, Mándi Y. Kynurenic Acid analogue attenuates the production of Tumor Necrosis Factor-α (TNF-α), calgranulins (S100A 8/9 and S100A 12), and the secretion of HNP1–3 and stimulates the

production of Tumor Necrosis Factor-Stimulated Gene-6 (TSG-6) in whole blood cultures of patients with rheumatoid arthritis. Front Immunol. 2021, in press. *IF: 5.085*

4. Burcsár S, **Toldi G,** Kovács L, Szalay B, Vásárhelyi B, Balog A. Urine soluble urokinase plasminogen activator receptor as a potential biomarker of lupus nephritis activity. Biomarkers. 2020, in press. *IF: 2.070*
5. Folyovich A, Majoros A, Jarecsny T, Pánczél G, Pápai Z, Rudas G, Kozák L, Barna G Béres-Molnár KA, Vadasdi K, Liszkay G, Horváth E, **Toldi G.** Epileptic seizure provoked by bone metastasis of chronic lymphoid leukemia and Merkel cell carcinoma. Case Rep Med. 2020;2020:4318638.
6. **Toldi G,** Legany N, Ocsovszki I, Balog A. Calcium influx kinetics and the characteristics of potassium channels in peripheral T lymphocytes in systemic sclerosis. Pathobiology. 2020, in press. *IF: 1.985*
7. Balogh E, Chandler JC, Varga M, Tahoun M, Menyhárd DK, Schay G, Goncalves T, Hamar R, Légrádi R, Szekeres Á, Gribouval O, Kleta R, Stanescu H, Bockenhauer D, Kerti A, Williams H, Kinsler V, Di WL, Curtis D, Kolatsi-Joannou M, Hammid H, Szőcs A, Perczel K, Maka E, **Toldi G,** Sava F, Arrondel C, Kardos M, Fintha A, Hossain A, D'Arco F, Kaliakatsos M, Koeglmeier J, Mifsud W, Moosajee M, Faro A, Jávorszky E, Rudas G, Saied MH, Marzouk S, Kelen K, Götze J, Reusz G, Tulassay T, Dragon F, Mollet G, Motameny S, Thiele H, Dorval G, Nürnberg P, Perczel A, Szabó AJ, Long DA, Tomita K, Antignac C, Waters AM, Tory K. Pseudouridylation defect due to DKC1 and NOP10 mutations cause nephrotic syndrome with cataracts, hearing impairment and enterocolitis. Proc Natl Acad Sci U S A. 2020;117:15137-15147. *IF: 9.412*

8. Dulic S, **Toldi G,** Sava F, Kovács L, Molnár T, Milassin Á, Farkas K, Rutka M, Balog A. Specific T-cell subsets can predict the efficacy of anti-TNF treatment in inflammatory bowel diseases. Arch Immunol Ther Exp (Warsz). 2020;68:12. *IF: 3.200*
9. Cossarizza A, Chang HD, Radbruch A, …, **Toldi G,** …, Zychlinsky A. Guidelines for the use of flow cytometry and cell sorting in immunological studies (second edition). Eur J Immunol. 2019;49:1457-1973. IF: 4.404
10. Folyovich A, Biczó D, Jarecsny T, Al-Muhanna N, Jánoska D, Béres-Molnár KA, Dudás E, **Toldi G.** Daylight Saving Time and the incidence of thrombolysis to treat acute ischemic stroke. Rev Neurol. 2020;176:361-365. *IF: 1.911*
11. Hargitai B, **Toldi G,** Marton T, Ramalingam V, Ewer AK, Bedford Russell AR. Pathophysiological mechanism of extravasation via umbilical venous catheters. Pediatr Dev Pathol. 2019;22:340-343. IF: 0.885
12. Ward J, Motwani J, Baker N, Nash M, Ewer AK, **Toldi G.** Congenital methemoglobinaemia identified by pulse oximetry screening. Pediatrics. 2019;143:e20182814. IF: 5.359
13. **Toldi G,** Batel P, Baráth S, Szerémy P, Apjok A, Filkor K, Szántó S, Szűcs G, Szamosi S, Häupl T, Grützkau A, Szekanecz Z. Peripheral lymphocyte multidrug resistance activity as a predictive tool of biological therapeutic response in rheumatoid arthritis. J Rheumatol. 2019;46:572-578. IF: 3.350
14. Szerémy P, Tauberné Jakab K, Baráth S, Apjok A, Filkor K, Holló Z, Márki-Zay J, Kappelmayer J, Sipka S, Krajcsi P, **Toldi G.** Determination of reference values of MDR-ABC transporter activities in CD3+ lymphocytes of healthy volunteers using a flow cytometry based method. Cytometry B Clin Cytom. 2019;96:469-474. IF: 2.070

15. Folyovich A, Biczó D, Béres-Molnár AK, **Toldi G.** Assessment of the efficiency of stroke awareness campaigns in Hungary. J Stroke Cerebrovasc Dis. 2018;27:1770-1774. IF: 1.646
16. Dulic S, Vásárhelyi Z, Bajnok A, Szalay B, **Toldi G,** Kovács L, Balog A. The impact of anti-TNF therapy on CD4+ and CD8+ cell subsets in ankylosing spondylitis. Pathobiology. 2018;85:201-210. IF: 1.831
17. Cossarizza A, Chang HD, Radbruch A, …, **Toldi G,** …, Zimmermann J. Guidelines for the use of flow cytometry and cell sorting in immunological studies. Eur J Immunol. 2017;47:1584-1797. IF: 4.248
18. Stanciu AE, Sava F, **Toldi G.** A rare case of polyglandular autoimmune syndrome type IIIc with primary antibody failure. Gynecol Endocrinol. 2018;34:283-285. IF: 1.406
19. Dulic S, Vásárhelyi ZE, Sava F, Berta L, Szalay B, **Toldi G,** Kovács L, Balog A. T-cell subsets in rheumatoid arthritis patients on long-term anti-TNF or IL6-receptor-blocker therapy. Mediators Inflamm. 2017;2017:6894374. IF: 3.549
20. Bajnok A, Ivanova M, Rigó J Jr, **Toldi G.** The distribution of activation markers and selectins on peripheral T lymphocytes in preeclampsia. Mediators Inflamm. 2017;2017:8045161. IF: 3.549
21. Orbán C, Szabó D, Bajnok A, Vásárhelyi B, Tulassay T, Arató A, Veres G, **Toldi G.** Altered activation of peripheral CD8+ T cells in pediatric Crohn's disease. Immunol Lett. 2017;185:48-51. IF: 2.436
22. Sava F, **Toldi G,** Treszl A, Hajdú J, Harmath Á, Rigó J Jr, Tulassay T, Vásárhelyi B. Immune cell subsets, cytokine and cortisol levels during the first week of life in neonates born to preeclamptic mothers. Am J Reprod Immunol. 2017;77: e12659. IF: 2.745

23. Legány N, Berta L, Kovács L, Balog A, **Toldi G.** The role of B7 family costimulatory molecules and indoleamine 2,3-dioxygenase in primary Sjögren's syndrome and systemic sclerosis. Immunol Res. 2017;65: 622-629. IF: 2.487
24. Sava F, **Toldi G,** Treszl A, Hajdú J, Harmath Á, Tulassay T, Vásárhelyi B. Expression of lymphocyte activation markers of preterm neonates is associated with perinatal complications. BMC Immunol. 2016;17:19. IF: 2.485
25. Legány N, **Toldi G,** Orbán C, Megyes N, Bajnok A, Balog A. Calcium influx kinetics, and the features of potassium channels of peripheral lymphocytes in primary Sjögren's syndrome. Immunobiology. 2016;221:1266-72. IF: 2.720
26. Sava F, Treszl A, Hajdú J, **Toldi G,** Rigó J Jr, Tulassay T, Vásárhelyi B. Plasma vitamin D levels at birth and immune status of preterm infants. Immunobiology. 2016;221:1289-92. IF: 2.720
27. Orbán C, Szabó D, Bajnok A, Vásárhelyi B, Tulassay T, Arató A, Veres G, **Toldi G.** Altered calcium influx of peripheral Th2 cells in pediatric Crohn's disease: infliximab may normalize activation patterns. Oncotarget. 2016;7:44966-44974. IF: 5.008
28. Vásárhelyi B, **Toldi G,** Balog A. The clinical value of soluble urokinase plasminogen activator receptor (suPAR) levels in autoimmune connective tissue disorders. e-JIFCC. 2016;27:122-9.
29. Ivancsó I, Bohács A, Szalay B, **Toldi G,** Szilasi ME, Müller V, Losonczy G, Rigó J Jr, Vásárhelyi B, Tamási L. Circulating periostin level in asthmatic pregnancy. J Asthma. 2016;53:900-6. IF: 1.746
30. Orbán C, Pérez-García E, Bajnok A, McBean G, **Toldi G,** Blanco-Fernandez A. Real time kinetic flow cytometry measurements of cellular parameter changes evoked by nanosecond pulsed electric field (nsPEF). Cytometry A. 2016;82:472-9. IF: 3.222

31. Folyovich A, Biczó D, Bajnok A, Bessenyei D, Kis I, Gimesi-Országh J, Béres-Molnár AK, **Toldi G.** Higher incidence of stroke on the last day of the month in Hungary – a role for psychosocial factors and financial insecurity? J Stroke Cerebrovasc Dis. 2016;25:1192-5. IF: 1.517
32. **Toldi G,** Munoz L, Herrmann M, Schett G, Balog A. The effects of Kv1.3 and IKCa1 channel inhibition on cytokine production and calcium influx of T lymphocytes in rheumatoid arthritis and ankylosing spondylitis. Immunol Res. 2016;64:627-31. IF: 2.905
33. Mészáros G, Orbán C, Kaposi A, **Toldi G,** Gyarmati B, Tulassay T, Vásárhelyi B. Altered mitochondrial functional response to activation in T-cells of the neonate. Acta Physiol Hung. 2015;102:216-27. IF: 0.814
34. Kollár S, Berta L, Vásárhelyi ZE, Balog A, Vásárhelyi B, Rigó J Jr, **Toldi G.** Impact of aging on calcium influx and potassium channel characteristics of T lymphocytes. Oncotarget. 2015;6:13750-6. IF: 5.008
35. Legány N, **Toldi G,** Distler JHW, Beyer C, Szalay B, Kovács L, Vásárhelyi B, Balog A. Increased plasma soluble urokinase plasminogen activator receptor levels in systemic sclerosis: possible association with microvascular abnormalities and extent of fibrosis. Clin Chem Lab Med. 2015;53:1799-805. IF: 3.017
36. Huusko JM, Karjalainen MK, Mahlman M, Haataja R, Kari MA, Andersson S, **Toldi G,** Tammela O, Rämet M, Lavoie PM, Hallman M. A study of genes encoding cytokines (IL6 IL10 TNF), cytokine receptors (IL6R IL6ST) and glucocorticoid receptor (NR3C1) and susceptibility to bronchopulmonary dysplasia. BMC Medical Genetics. 2014;15:120. IF: 2.083

37. Folyovich A, Biró E, Orbán C, Bajnok A, Vásárhelyi B, **Toldi G.** Kv1.3 lymphocyte potassium channel inhibition as a potential novel therapeutic target in acute ischemic stroke. CNS Neurol Disord Drug Targets. 2014;13:801-6. IF: 2.628
38. Orbán C, Bajnok A, Vásárhelyi B, Tulassay T, **Toldi G.** Different calcium influx characteristics upon Kv1.3 and IKCa1 potassium channel inhibition in T helper subsets. Cytometry A. 2014;85:636-41. IF: 2.928
39. Eszes N, **Toldi G,** Bekő G, Bohács A, Ivancsó I, Müller V, Rigó J Jr, Losonczy G, Vásárhelyi B, Tamási L. Relationship of circulating hyaluronic acid levels to disease control in asthma and asthmatic pregnancy. PLoS One. 2014;9:e94678. IF: 3.234
40. Blois SM, Gueuvoghlanian-Silva BY, Tirado-González I, Torloni MR, Freitag N, Mattar R, Conrad ML, Unverdorben L, Barrientos G, Knabl J, **Toldi G,** Molvarec A, Rose M, Markert UR, Jeschke U, Daher S. Getting too sweet: galectin-1 dysregulation in gestational diabetes mellitus. Mol Hum Reprod. 2014;20:644-9. IF: 3.747
41. Folyovich A, Bíró E, Orbán C, Bajnok A, Varga V, Béres-Molnár AK, Vásárhelyi B, **Toldi G.** Relevance of novel inflammatory markers in stroke-induced immunosuppression. BMC Neurology. 2014;14:41. IF: 2.040
42. Huusko JM, Mahlman M, Karjalainen MK, Kaukola T, Haataja R, Marttila R, **Toldi G,** Szabó M, Kingsmore SF, Rämet M, Lavoie PM, Hallman M. Polymorphisms of the gene encoding Kit ligand are associated with bronchopulmonary dysplasia. Pediatr Pulmonol. 2014;15:120. IF: 2.704
43. Grozdics E, **Toldi G.** Antigen presentation and T cell response in umbilical cord blood and adult peripheral blood. J Hematol Res. 2014;1:16-26.
44. **Toldi G**. The regulation of calcium homeostasis in T lymphocytes. Front Immunol. 2013;4:432.

45. Orbán C, Bíró E, Grozdics E, Bajnok A, **Toldi G.** Modulation of T lymphocyte calcium influx patterns via the inhibition of Kv1.3 and IKCa1 potassium channels in autoimmune disorders. Front Immunol. 2013;4:234.

46. Marsovszky L, Németh J, Resch MD, **Toldi G,** Legány N, Kovács L, Balog A. Corneal Langerhans cell and dry eye examinations in ankylosing spondylitis. Innate Immun. 2013;20:471-477. IF: 2.459

47. Ivancsó I*, **Toldi G*,** Bohács A, Eszes N, Müller V, Rigó J Jr, Vásárhelyi B, Losonczy G, Tamási L. Relationship of circulating soluble urokinase plasminogen activator receptor (suPAR) levels to disease control in asthma and asthmatic pregnancy. PLoS One. 2013;8:e60697. IF: 3.534 * contributed equally

48. Bajnok A, Kaposi A, Kovács L, Vásárhelyi B, Balog A, **Toldi G.** Analysis by flow cytometry of calcium influx kinetics in peripheral lymphocytes of patients with rheumatoid arthritis. Cytometry A. 2013;83:287-93. IF: 3.066

49. Biró E, Vásárhelyi B, **Toldi G.** Calcium influx characteristics during T lymphocyte activation measured with flow cytometry. e-JIFCC. 2012;23:1-7.

50. **Toldi G,** Szalay B, Bekő G, Bocskai M, Deák M, Kovács L, Vásárhelyi B, Balog A. Plasma soluble urokinase plasminogen activator receptor (suPAR) levels in systemic lupus erythematosus. Biomarkers. 2012;17:758-63. IF: 1.879

51. Marsovszky L, Resch MD, Németh J, **Toldi G,** Medgyesi E, Kovács L, Balog A. In vivo confocal microscopic evaluation of corneal Langerhans cell density and distribution and evaluation of dry eye in rheumatoid arthritis. Innate Immun. 2013;19:348-54. IF: 2.459

52. **Toldi G,** Szalay B, Bekő G, Kovács L, Vásárhelyi B, Attila A. Plasma soluble urokinase plasminogen activator receptor (suPAR) levels in ankylosing spondylitis. Joint Bone Spine. 2013;80:96-8. IF: 3.218

53. **Toldi G,** Bekő G, Kádár G, Mácsai E, Kovács L, Vásárhelyi B, Balog A. Soluble urokinase plasminogen activator receptor (suPAR) in the assessment of inflammatory activity of rheumatoid arthritis patients in remission. Clin Chem Lab Med. 2013;51:327-32. IF: 2.955
54. **Toldi G,** Bajnok A, Dobi D, Kaposi A, Kovács L, Vásárhelyi B, Balog A. The effects of Kv1.3 and IKCa1 potassium channel inhibition on calcium influx of human peripheral T lymphocytes in rheumatoid arthritis. Immunobiology. 2013;218:311-6. IF: 3.180

9.4. International edited book and book chapters

1. The regulation of calcium homeostasis in T lymphocytes (Frontiers Research Topic Ebook). Frontiers Media SA, 2014. ISBN 978-2-88919-235-9.
2. Kaposi A, **Toldi G,** Mészáros G, Szalay B, Veress G, Vásárhelyi B. Experimental conditions and mathematical analysis of kinetic measurements using flow cytometry - the FacsKin method. In: Flow Cytometry – Recent Perspectives (ed: Schmid I). Intech, 2012. ISBN 979-953-307-355-1.
3. **Toldi G,** Treszl A, Vásárhelyi B. T Lymphocyte Characteristics and Immune Tolerance during Human Pregnancy. In: Autoimmune Disorders – Pathogenetic Aspects (ed: Mavragani C). Intech, 2011. ISBN 978-953-308-70-9.
4. **Toldi G,** Vásárhelyi B. The Contribution of Lymphocyte Potassium Channels to the Perinatal Regulation of the Immune Response in Mother and Newborn. In: Potassium Channels: Types, Structure and Blockers (ed: Fonseca DS). Nova Publishers, 2011. ISBN: 978-1-61324-880-5.

5. Treszl A, Mészáros G, **Toldi G**, Vásárhelyi B. Histone Deacetylases and Autoimmunity. In: The Epigenetics of Autoimmune Diseases (ed: Zoulai M). Wiley & Sons, 2009. ISBN: 978-0-470-75861-8.

9.5. Scientometric data

Total impact factors: 230.772

Impact factors of first and last author publications: 142.223

Total number of citations: 1619

Independent citations: 1271

Hirsch index: 19

Toldi Gergely tudományos és oktatási közleményeinek összefoglalása
MTA V. Orvostudományi Osztály (2021.06.02)

Tudományos és oktatási közlemények	Száma		Hivatkozások[1]	
	Összesen	Részletezve	Független	Összes
I. Folyóiratcikk[2]	91	---	---	---
szakcikk nemzetközi folyóiratban, idegen nyelvű	---	72	889	1021
szakcikk, hazai idegen nyelvű	---	2	5	6
szakcikk, magyar nyelvű	---	7	0	0
szakcikk, sokszerzős, érdemi szerzőként[3]	---	5	359	569
összefoglaló közlemény	---	2	5	6
rövid közlemény	---	3	12	15
II. Könyv	1	---	---	---
a) Szakkönyv, kézikönyv, tankönyv szerzőként	1	---	---	---
idegen nyelvű	---	1	0	0
magyar nyelvű	---	0	0	0
aa) Felsőoktatási tankönyv	---	0	0	0
b) Szakkönyv, kézikönyv, konferenciakötet, tankönyv szerkesztőként	0	---	---	---
idegen nyelvű	---	0	---	---
magyar nyelvű	---	0	---	---
bb) Felsőoktatási tankönyv	---	0	---	---
III. Könyrészlet	4	---	---	---
idegen nyelvű	---	4	0	0
magyar nyelvű	---	0	0	0
cc) Felsőoktatási tankönyvfejezet	---	0	0	0
IV. Konferenciaközlemény[4]	0	---	0	0
Oktatási közlemények összesen (II.aa,bb-III.cc)	---	0	0	0
Tudományos közlemények összesen (I-IV.)	---	96	1270	1617
Tudományos és oktatási közlemények összesen (I-IV.)	96	---	1270	1617
V. További tudományos művek	19	---	---	---
További tudományos művek, ide értve a nem teljes folyóiratcikkeket és a nem ismert lektoráltságú folyóiratokban megjelent teljes folyóiratcikkeket is	---	18	0	0
Szerkesztőségi levelezés, hozzászólások, válaszok	---	0	0	0
Oltalmak, szabadalmak	---	1	0	0
VI. Hivatkozott absztraktok[5]	2	---	1	2
Összes hivatkozás[1]	---	---	1271	1619
Hirsch index[6]	19	---	---	---
g index[6]	39	---	---	---

Speciális tudománymetriai adatok	Száma	Összes hivatkozás
Első szerzős teljes folyóiratcikkek száma[2]	23	581
Utolsó szerzős teljes folyóiratcikkek száma[2]	28	129
A tudományos fokozat (PhD) elnyerése utáni (2012) teljes tudományos folyóiratcikkek száma	65	1016
Az utolsó 10 év (2011 - 2021) tudományos, teljes, lektorált tudomáyos folyóiratcikkeinek száma	82	1436
A legmagasabb hivatkozottságú közlemény hivatkozásainak száma (az összes hivatkozás százalékában)	276	17,05%
Hivatkozások száma, amelyek nem szerepelnek a WoS/Scopus rendszerben	---	94
Jelentés, guideline	0	0
Csoportos (multicentrikus) közleményben kollaborációs közreműködő[7]	1	7

Megjegyzések:

1. a disszertáció és egyéb típusú hivatkozás nélküli, a WoS és/vagy Scopus rendszerben nyilvántartott adatok
2. lektorált, tudományos folyóiratban
3. a szerző írásban nyilatkozik, hogy érdemi szerzői hozzájárulásával készültek szerzőként jegyzett közleményei, és az érdemi hozzájárulást dokumentálni tudja
4. konferenciaközlemény folyóiratban, könyvben vagy egyéb konferenciakötetben
5. nem-hivatkozott absztrakt itt nem kerül az összesítésbe
6. a disszertáció és egyéb típusú hivatkozás nélküli összes hivakozással számolva. A Hirsch és a g index definíciója
7. közreműködés esetén a csoportos szerzőségű közlemények hivatkozottsága külön értékelendő, és nem számítható be az összesített hivatkozások közé

10.ACKNOWLEDGEMENTS

My involvement with research began at the First Department of Paediatrics, Semmelweis University under the guidance of **Professor Barna Vásárhelyi**. I thank him for all his teaching and support throughout my years as a medical student, a PhD student, and beyond. He taught me not only the basics of critical thinking and publication skills, but also gave me the opportunity and freedom to develop my own ideas. I truly appreciate his guidance. I am most grateful for the support of **Professor Tivadar Tulassay**, who always encouraged me to follow an academic clinician career path and created an environment at his department that enabled me to do so. I would also like to thank **Professor János Rigó** for providing me with the opportunity to engage with research activity besides my clinical work at the the First Department of Obstetrics and Gynecology, Semmelweis University. I am most thankful to my mentors, **Professor István Seri** and **Dr Alison Bedford Russell** who were always available to guide me with their advice.

Over the years, my research collaborations with **Dr Attila Balog** and **Dr András Folyovich** developed into bonds of friendship. I am grateful for what I learnt from both of them not only throughout our research work, but also in the clinical setting. Their professional and compassionate care served as an example in my own clinical practice.

I would like to sincerely thank all my numerous collaborators in Hungary and abroad, with a particular emphasis on colleagues from the First Department of Obstetrics and Gynecology, Semmelweis University, the University of Szeged and the University of Birmingham. Their support is truly appreciated.

My scientific work would not have been possible without my students. I have been fortunate enough to be surrounded by bright, enthusiastic and talented people who showed a genuine interest in the immunological problems that we set out to explore. I am grateful to have had the

opportunity of supervising the PhD work of **Dr Anna Bajnok**, **Dr Enikő Grozdics** and **Dr Florentina Sava**.

I would like to remember a special student and friend, **Dr Csaba Orbán** whose life and commitment to science serves as an example to all. Csaba was a truly dedicated scientist, and a hard-working, kind, gentle person with a great sense of humour. His priority until the very last minute in his fight with cancer was to complete his work with unparalleled motivation to making a difference to patients. His untimely death four years ago left an enormous gap in lives of those around him. He is truly missed and we will maintain his legacy of dedication to the advancement of science.

Finally, I am indebted to all the families and neonates who donated samples to our studies. Without their altruism and generosity our work would not have been possible.